A LOCAL RELEASE OF MICROTUBULE-STABILIZING AGENTS FROM AN ALIGNED MICROFIBER PLATFORM TO PROMOTE SPINAL CORD TISSUE REPAIR

by
José A. Román

A thesis dissertation submitted to Johns Hopkins University in conformity with the requirements for the degree of Doctor of Philosophy of Biomedical Engineering

Baltimore, Maryland
October 2016

Abstract

In the field of tissue engineering, some of the most promising therapeutic applications to promote spinal cord tissue repair have involved biomaterials. Electrospun microfibers provide an optimum platform to both promote directional guidance and release a therapeutic treatment for a long-duration. Paclitaxel administration has been shown to promote nerve tissue repair, but translation has been limited due to its incorporation in a neuropathic pain-inducing solvent. This thesis describes our work in establishing a platform that releases microtubule-stabilizing agents (paclitaxel and sunitinib) from aligned, electrospun fibers to promote tissue repair after a traumatic central nervous system injury.

Approximately 282,000 patients in the United States have a traumatic spinal cord injury (SCI), resulting in a loss of function below the site of injury, and yet there remains no clinically approved treatment for patients after an injury. Traumatic spinal cord injuries ultimately result in an inhibitory environment that prevents axonal regeneration from occurring. Previously, a low concentration administration of paclitaxel has been shown to promote axonal extension and attenuate the upregulation of inhibitory molecules after a spinal cord injury, yet requires a new incorporation method due to toxicity and potency issues with a high concentration administration. Previously, aligned, electrospun poly-lactic acid (PLA) microfibers have promoted spinal cord tissue regeneration, but had a limited effect on the inhibitory components present after a spinal cord injury. In this study we effectively incorporated paclitaxel, and other microtubule-stabilizing agents, into electrospun PLA microfibers and sustained their release for up to

twelve weeks *in vitro*. Additionally, we established that a local release of these molecules from electrospun microfibers promotes dorsal root ganglion neurite extension in a growth-conducive and inhibitory environment, as well as inhibits astrocytic activity such as proliferation and chondroitin-sulfate proteoglycan upregulation. Finally, this study tested this platform in a rat model of spinal cord injury and determined that it inhibits reactive gliosis and does not exacerbate neuropathic pain. Our findings provide a targeted approach to improve overall spinal cord tissue repair after a traumatic injury in the spinal cord.

Readers:
Hai-Quan Mao, Ph.D. (Advisor)
Lawrence Schramm, Ph.D.

Defense Committee:
Martin Oudega, Ph.D.

Acknowledgements

I wholeheartedly understand that this thesis research process has been in collaboration with multiple people and parties, and I sincerely thank each of them for their contributions throughout my adventures in Baltimore and at Johns Hopkins.

First and foremost, I would like to thank Dr. Hai-Quan Mao for all of his support throughout this entire research endeavor. For some reason, he decided to let me stay in his lab after a "rotation" with limited funding and a minimal background in materials science. Without his continued guidance, I would not have advanced my scientific knowledge, professional development, or career progression. Without his direction and leadership, I have no doubt that I would not be completing my thesis research for at least another five years, and for this and more I am exceptionally grateful.

I next want to thank my remaining thesis committee members, Drs. Lawrence Schramm and Martin Oudega. Dr. Schramm was instrumental in my decision to attend Johns Hopkins and has been a constant source of information and advice throughout my time at Hopkins and in Baltimore. Dr. Oudega willingly accepted to collaborate with Dr. Mao and me throughout these past few years, and his expertise and assistance with the *in vivo* aspects of my research have been instrumental in advancing this research and the field of spinal cord injury therapeutics as well.

Throughout my academic education and research I have also had additional influential mentors. Dr. Andres Hurtado planted the initial idea for this research and helped me learn more about spinal cord injury models. Dr. Candace Floyd took a chance on me almost 9 years ago by allowing me to join her laboratory, introduced me to scientific research, and made me into the researcher that I am today. Dr. Diane Tucker

taught me the professional aspects of research and provided me the scientific foundation to constantly question my findings as well.

As I completed my thesis research, I constantly sought the insight and assistance from collaborators and other labs in the Translational and Tissue Engineering Center at Johns Hopkins for some of my protocols and assays. At Hopkins, I would like to especially thank members of the Don Zack lab for their collaborations on the retinal ganglion cell projects and the Derek Welsbie lab for their insight and assistance with the sunitinib project. Furthermore, I would like to thank Dr. Agnes Haggerty of the University of Miami for her assistance with all of the *in vivo* data presented in this thesis dissertation.

While in Baltimore and at Hopkins, I have been surrounded by friends and colleagues that have constantly challenged me and kept me sane outside of the lab. Chris and Christie Copeland have accepted my wife and I into their life, like family, and also made the transition to Baltimore significantly easier for both of us. I have been fortunate enough to not only work with great colleagues, but also be able to call some of them my friends outside of work as well. Specifically, I would like to thank Russell Martin for introducing me to electrospinning and accommodating my constant barrage of questions. Thank you to Markus Tammia, who is one of the smartest people I know, for always having the most challenging questions for me and having the most interesting stories. Charles Hu has constantly kept me grounded and has been a blast to hang out with throughout this tenure. I would also like to thank the entire Mao lab for their constant questions and for being a great lab to work with, especially Brian Ginn, John-Michael Williford, Calvin Chang, Xiaowei Li, and Xuesong Jiang. Finally, I would like to thank

the high school and undergraduate students that helped me complete this research especially Ian Reucroft and Brittany Tsou.

My family has been a constant source of encouragement and inspiration for me throughout my life. Without a doubt, my parents instilled in me a sense of curiosity and initiated my love for science and engineering. Even though each move has pushed me farther away from them, they have always supported my education and career decisions. My brothers are undertaking similar journeys to mine and constantly remind me why I want to continue to be a scientist and mentor.

Most importantly, I would like to thank my wife for her constant love and assistance throughout the past five years. Through the constant late nights and erratic schedule, she has always supported me. For some reason, she willingly decided to help and assist me through this tedious and trying endeavor, and for this and more I am eternally grateful.

Last, but certainly not least, I would like to thank all of my funding sources. I would like to especially thank the National Science Foundation for their funding of my research and allowing me the flexibility and capability to conduct the research that I thought was the most impactful based on my background and interests. Without their support, I could not have completed any of this research.

Table of Contents

Table of Figures

Chapter 1

Tissue Engineering and Electrospun Fibers

1.1 Tissue Engineering and Regenerative Medicine

Tissue engineering as a field refers to the usage of cells, materials, and biologically active molecules to enhance or replace biological tissues [1]. Due to this broad definition and tissue engineering's promising applications for translational therapeutics, the field of tissue engineering has grown at a tremendous rate with almost 625,000 publications mentioning tissue engineering since its inception with almost 400,000 of those produced within the past 10 years alone [2]. To meet this demand for tissue engineering research, institutes and centers focused on tissue engineering, such as the Translational Tissue Engineering Center at the Johns Hopkins University, have been established across the United States.

1.1.1 Cells

The cellular based components for tissue engineering provide a platform to replace the damaged tissue, initiate a network, and upregulate growth-conducive factors. Stem cells, an undifferentiated cell type that is capable of becoming more specialized or producing additional stem cells, have been commonly researched for tissue engineering applications due to their ability to produce multiple cell types. Within the past few years, multiple varieties of stem cells have been discovered and produced such as induced pluripotent stem cells (iPSCs), which are developed without the ethical issues of other

stem cell types (i.e. embryonic stem cells) [3]. The usage of stem cells as therapeutic agents, however, has been limited due to their lack of viability after implantation, potential to differentiate into a carcinogenic lineage, and lack of FDA approval.

1.1.2 Materials

In tissue engineering, materials present a scaffold for the body to integrate onto, stabilize the surrounding area, and direct cellular growth [4]. Materials are commonly used in tissue engineering applications due to their diversity, degradability, and established FDA-approved usages. That being said, materials must also be selectively chosen for each application due the host body's immune response, toxicity of the material's degradation products, and difficulty to scale up the material's production.

1.1.3 Biologically Active Molecules

Biologically active molecules such as growth factors, hormones, and therapeutic molecules are needed to stimulate growth, activate a systematic response (e.g. immune), and even attenuate an inhibitory reaction [5]. These molecules are advantageous in tissue engineering usages due to their amenability (due to a concentration-dependent effect) and specificity; however, they can be difficult to acquire/produce and can have issues with loading for drug-delivery applications.

1.1.4 Regenerative Medicine

Regenerative medicine refers to the manipulating of tissue engineering concepts to help direct the body to repair or replace tissue [6]. Many high profile regenerative

medicine projects have been previously developed such as the stimulation of chondrocytes to form a human ear on a mouse and generating a functional heart from a decellularized heart implanted with autologous cells [7, 8]. Although these results have shown the potential direction of regenerative medicine, the field has only incrementally advanced within the past 20 years due to the fact that the host body regenerates poorly due to the activation of the immune response coupled with poor blood vessel growth and the fact that implanted cells do not survive in the body for an extended duration. Therefore, a system that either avoids or mitigates these issues could help advance the field.

1.2 Biomaterials

Biomaterials are substances that have been developed to interact with biological systems for a medical purpose – generally in a therapeutic or diagnostic capacity [9]. Biomaterials are commonly used in tissue engineering applications due to their ability to effectively mimic the native extracellular matrix (ECM), vary in size, shape, and dimension, as well as mimic the natural three-dimensional geometries present *in vivo* to stimulate growth and extension [10-12]. Certain applications require different types of biomaterials, such as using hydrogels as a drug-delivery system, functionalizing the surface to promote better cellular adhesion, or even improving the biodegradability of the material to better suit the specific therapeutic application [13-15].

Based on their composition, biomaterials can be divided into two different varieties: natural substrates such as collagen, fibrin, etc. and synthetic substrates such as polyester polymers [9]. Both material types can be modified, loaded with a therapeutic

treatment, degrade in the body, and have FDA-approved therapeutic applications. However, natural materials lack adhesion peptides and structural strength, whereas synthetic polymers induce a foreign body response and can produce toxic degradation byproducts. For synthetic polyester polymers, these issues can be minimized by changing the morphology of the surface through different production techniques, functionalizing the surface, or incorporating molecules to attenuate the immune response [16].

1.2.1 Topographical Guidance

Through topographical guidance, cells interact with their surroundings by direct adhesion to a surface, which can modulate multiple cellular activities, such as proliferation, migration, extension, and differentiation [17]. Varying the surface through variations in the porosity, functionalization of a molecule, separation distance, or fiber diameter can be done by various methods such as chemical etching, photolithography, and electrospinning [18]. *In situ*, cells have evolved to recognize various molecules and morphologies present in the ECM, such as integrins (i.e. laminin, fibrin, collagen, etc.), proteoglycans, and growth factors [19]. For instance, the effects of various collagen and laminin integrins have been extensively studied in nerve extension, regeneration, and function [20, 21]. This knowledge of integrin binding has been further manipulated to modify natural materials to mimic the natural ECM and promote cellular growth and tissue regeneration [10]. Furthermore, synthetic materials such as polyester polymers (i.e. poly-lactic acid, polycaprolactone, etc.) can regulate cellular function by functionalizing adhesion proteins to their surface or modifying their surface morphology [22]. For example, by simply varying the diameter of electrospun polymer fibers by a few hundred

nanometers, neuronal stem cell differentiation can be modified, neuronal extension can be directed and promoted, and glial cell migration speed and distance can be altered [23, 24]. Interestingly, maximum neurite extension occurred on fibers with a diameter most similar to that of the axons growing directly on them as shown in Figure 1.1 [24].

Although topographical guidance presents multiple ways to control cellular function, there are some limitations. Most importantly, cells must adhere or interact with the surface in order to be effective, which limits the ability of the guidance to direct contact. Furthermore, modifying cellular function for multiple axes and dimensions is difficult with this system due to the surface production techniques currently available. Finally, this system must currently be limited to *in vitro* studies due to surface degradation, changes in the surface morphology, or blocking due to complement activation *in vivo*.

1.3 Discussion

Fiber diameter and alignment modulates the direction and lengths of neurite extension, but the mechanism that drives this system remains poorly understood. The systems tested (as well as subsequent studies) contain a culture of mixed glial with the neurons as well. Although methods to mitigate these cells are used, these glia, specifically Schwann cells, could be modulating neuronal extension under these conditions. Therefore, their response should also be monitored and quantified in subsequent studies.

1.4 Figures

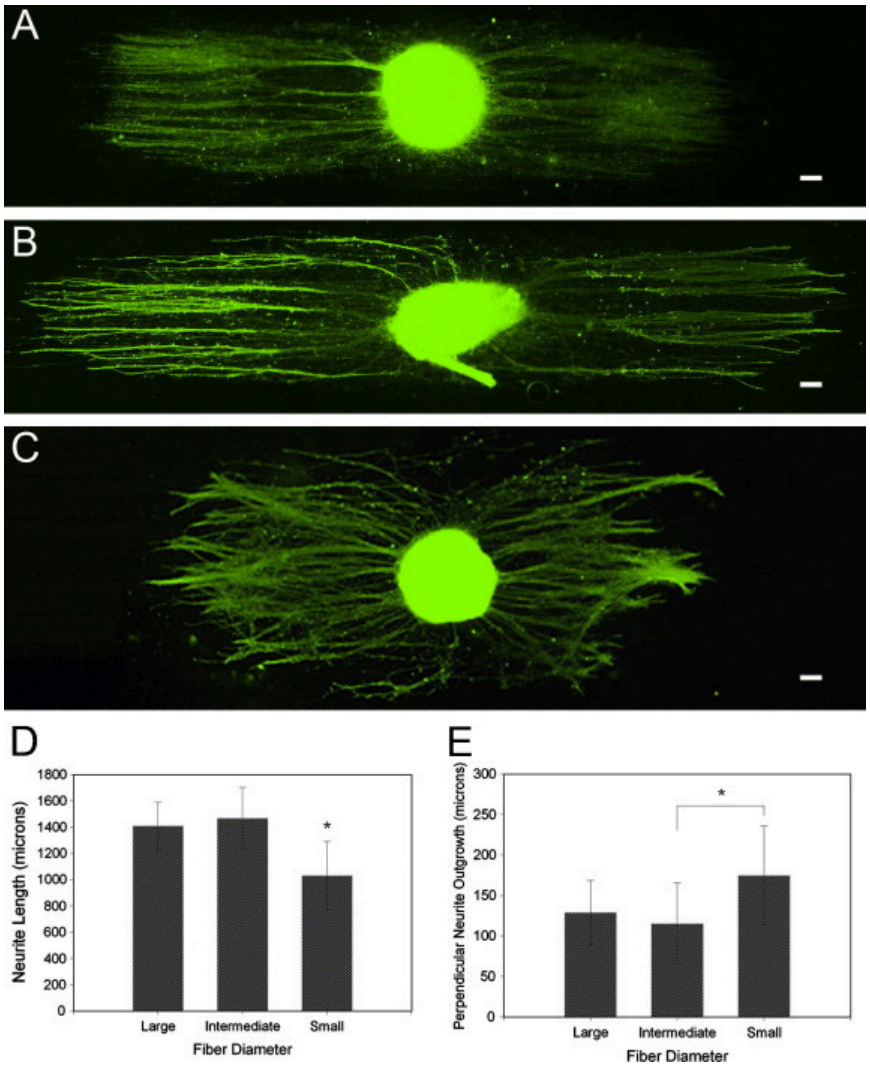

Figure 1-1: Fiber diameter and morphology modulate neurite extension

Dorsal root ganglion neurons were cultured on aligned, electrospun poly-lactic acid fibers with large (A), intermediate (B), or small (C) diameter fibers for 5 days. Neurons had longer protrusions on the large diameter fibers (D) and better aligned to their direction as well (E). Scale bar: 100 μm

1.5 References

[1] Saltzman WM. Tissue engineering : engineering principles for the design of replacement organs and tissues. Oxford ; New York: Oxford University Press; 2004.

[2] Wobma H, Vunjak-Novakovic G. Tissue Engineering and Regenerative Medicine 2015: A Year in Review. Tissue Eng Part B Rev. 2016;22:101-13.

[3] Nakagawa M, Koyanagi M, Tanabe K, Takahashi K, Ichisaka T, Aoi T, et al. Generation of induced pluripotent stem cells without Myc from mouse and human fibroblasts. Nat Biotechnol. 2008;26:101-6.

[4] Hubbell JA. Biomaterials in tissue engineering. Biotechnology (N Y). 1995;13:565-76.

[5] Chen FM, Zhang M, Wu ZF. Toward delivery of multiple growth factors in tissue engineering. Biomaterials. 2010;31:6279-308.

[6] Mason C, Dunnill P. A brief definition of regenerative medicine. Regen Med. 2008;3:1-5.

[7] Cao Y, Vacanti JP, Paige KT, Upton J, Vacanti CA. Transplantation of chondrocytes utilizing a polymer-cell construct to produce tissue-engineered cartilage in the shape of a human ear. Plast Reconstr Surg. 1997;100:297-302; discussion 3-4.

[8] Ott HC, Matthiesen TS, Goh SK, Black LD, Kren SM, Netoff TI, et al. Perfusion-decellularized matrix: using nature's platform to engineer a bioartificial heart. Nature medicine. 2008;14:213-21.

[9] Buddy D. Ratner ASH, Frederick J. Schoen, Jack E. Lemons. Biomaterials Science, Third Edition: An Introduction to Materials in Medicine: Academic Press; 2013.

[10] Ma PX. Biomimetic materials for tissue engineering. Adv Drug Deliv Rev. 2008;60:184-98.

[11] Place ES, Evans ND, Stevens MM. Complexity in biomaterials for tissue engineering. Nat Mater. 2009;8:457-70.

[12] Mahoney MJ, Anseth KS. Three-dimensional growth and function of neural tissue in degradable polyethylene glycol hydrogels. Biomaterials. 2006;27:2265-74.

[13] Perale G, Rossi F, Santoro M, Peviani M, Papa S, Llupi D, et al. Multiple drug delivery hydrogel system for spinal cord injury repair strategies. Journal of controlled release : official journal of the Controlled Release Society. 2012;159:271-80.

[14] Roman JA, Niedzielko TL, Haddon RC, Parpura V, Floyd CL. Single-walled carbon nanotubes chemically functionalized with polyethylene glycol promote tissue repair in a rat model of spinal cord injury. Journal of neurotrauma. 2011;28:2349-62.

[15] Novikov LN, Novikova LN, Mosahebi A, Wiberg M, Terenghi G, Kellerth JO. A novel biodegradable implant for neuronal rescue and regeneration after spinal cord injury. Biomaterials. 2002;23:3369-76.

[16] Franz S, Rammelt S, Scharnweber D, Simon JC. Immune responses to implants - a review of the implications for the design of immunomodulatory biomaterials. Biomaterials. 2011;32:6692-709.

[17] Curtis A, Wilkinson C. Topographical control of cells. Biomaterials. 1997;18:1573-83.

[18] Norman JJ, Desai TA. Methods for fabrication of nanoscale topography for tissue engineering scaffolds. Ann Biomed Eng. 2006;34:89-101.

[19] Kim SH, Turnbull J, Guimond S. Extracellular matrix and cell signalling: the dynamic cooperation of integrin, proteoglycan and growth factor receptor. J Endocrinol. 2011;209:139-51.

[20] Toyota B, Carbonetto S, David S. A dual laminin/collagen receptor acts in peripheral nerve regeneration. Proc Natl Acad Sci U S A. 1990;87:1319-22.

[21] Chen P, Cescon M, Bonaldo P. The Role of Collagens in Peripheral Nerve Myelination and Function. Mol Neurobiol. 2015;52:216-25.

[22] Lutolf MP, Hubbell JA. Synthetic biomaterials as instructive extracellular microenvironments for morphogenesis in tissue engineering. Nat Biotechnol. 2005;23:47-55.

[23] Christopherson GT, Song H, Mao HQ. The influence of fiber diameter of electrospun substrates on neural stem cell differentiation and proliferation. Biomaterials. 2009;30:556-64.

[24] Wang HB, Mullins ME, Cregg JM, McCarthy CW, Gilbert RJ. Varying the diameter of aligned electrospun fibers alters neurite outgrowth and Schwann cell migration. Acta biomaterialia. 2010;6:2970-8.

Chapter 2

Drug Delivery Systems and Microtubule-Stabilizing Agents

2.1 Drug Delivery

Drug delivery systems involve administering molecules to the body in order to safely achieve a desired therapeutic effect [1]. In order to deliver an efficacious concentration of a drug, the quantity released and duration of the release must be controlled. There are various ways to control the device's drug release, such as diffusion-controlled, water penetration-controlled, and chemically-controlled (controlled by the device degradation). In a diffusion-controlled system, a first-order release is more common, which can lead to an initial toxic level. Water-soluble drugs work best for water penetration-controlled systems, which limit their therapeutic applications. For chemically-controlled devices, a longer duration (months-years) can be achieved.

Among all of these drug delivery systems, non-specific targeting of treatments (resulting in toxicity or a lack of efficacy) and variations in drug release (due to variations in molecule size and uptake) can be issues.

2.1.1 Targeted Drug Delivery

A targeted drug delivery system involves administering a higher concentration of a specific treatment to certain cells or tissues relative to others, which prevents non-specific binding of the treatment and requires a lower concentration of the treatment for efficacy. There are two ways to administer a targeted drug delivery system: deliver

externally from the site of interest or locally administer the treatment to the site of injury. When the treatment is delivered externally, either the biology of the site of interest must be manipulated (i.e. via the enhanced permeability and retention effect) or the treatment/carrier must be modified to target the correct cells (i.e. functionalization) [2, 3]. However, when a local, targeted delivery is administered, there is a diminished chance of non-specific binding as well as the ability to bypass obstructive membranes, and therefore, prevent toxicity and other adverse effects [4].

2.1.2 Local Administration and Cellular Interactions

When a therapeutic molecule is administered locally at the treatment site, patient compliance increases, blood incorporation and transport is avoided, and a lower concentration of the molecule is needed, which results in a higher potency and fewer side effects. Various studies have applied this knowledge to improve the efficacy of growth factors for cardiomyocyte growth and nerve regeneration [5, 6]. Additionally, when a local release of a hydrophobic molecule occurs, the molecular uptake will vary due to the drug not easily dissolving in the surrounding volume, but rather be directly uptaken into the cell through transcellular transport or other similar techniques [7]. Furthermore, local administration of a treatment ensures that the therapeutic molecule binds to the targeted cell's extracellular receptors, which facilitates efficacy and could result in a lower effective concentration needed.

2.2 Therapeutic Molecules

In treatment applications, therapeutic molecules regulate a biological process (i.e.

regeneration, apoptosis, growth, etc.). FDA-approved molecules have a wide range of sizes (from hundreds of Daltons for vitamins to thousands for hormones), specificity, and current therapeutic applications, but are continuously being repurposed for new therapeutic indication due to the large costs associated with receiving FDA-approval for a novel molecule.

2.2.1 Paclitaxel

Paclitaxel (PTX) is a hydrophobic, mitotic inhibitor that stabilizes microtubule formation and is clinically administered as an anticancer agent (Taxol™) at a high concentration dosage (μM) for ovarian, breast, and liver cancers [8]. Mechanistically, paclitaxel stabilizes microtubule formation integral for cellular division, proliferation, and elongation through multiple signal transduction pathways such as the c-Jun N-terminal kinase/stress-activated protein kinase (JNK/SAPK) pathway [9]. Paclitaxel uptake is regulated by organic anion transporting polypeptide (OATP) family members, which control paclitaxel's transcellular transport [10]. In other therapeutic applications, such as neuronal regeneration, a low concentration administration of paclitaxel have shown promise [11]. However, these paclitaxel administrations must be delivered externally, dissolved in a toxic solvent (Kolliphor EL) due to paclitaxel's hydrophobicity, and dispensed at a higher effective concentration due to cerebral spinal fluid flow [12].

2.2.2 Sunitinib

Researchers have been investigating other potential molecules to promote neuronal tissue repair after an injury, such as sunitinib (STB) – another anti-cancer

therapeutic that blocks the dual-leucine zipper kinase (DLK) pathway and has been shown to promote neuronal survival [13]. Sunitinib binds to and targets the receptor tyrosine kinase (RTK) pathway, which regulates neuronal apoptosis and proliferation, among other functions [14]. However, sunitinib's role in neuronal regeneration remains unknown and it's smaller size than other therapeutics could lead to issues with its release from certain drug delivery systems.

2.3 Electrospun PLA Microfibers

Engineered technologies, specifically synthetic biomaterials, provide a preferred treatment mechanism for tissue engineering applications, because of their tunable design, consistent manufacturing, minimal host immune response, and ease of sterilization [15]. Electrospun fibers offer a molecule-loadable, biodegradable, and topographical guidance platform [16, 17]. Furthermore, electrospun fibers provide a flexible platform in that they range in size from nanometers to micrometers in diameter, can be manufactured from various natural and synthetic materials, and can be designed with an aligned or random-orientation. However, electrospun fibers do not provide an adequate platform for scaling to a 3-dimensional cell culture model, large-scale manufacturing, and also have a limited material library.

2.3.1 Production

Poly-lactic acid (PLA) was chosen as the standard polymer for this research for multiple reasons. To begin with, it is a biodegradable polymer that undergoes hydrolysis degradation. Its degradation properties can also be tuned by varying its chiral forms as

well as its molecular weight. Furthermore, due to its long-term FDA-approval, it has been extensively tested in medical devices, is easy to obtain/synthesize, and is available in clinical-grade varieties [18].

Electrospinning is a fiber-producing process in which a material (natural or synthetic) is incorporated in a solvent and extruded onto a grounded surface while a large voltage is applied. By applying the voltage to the solution, the liquid becomes charged, which produces an electrostatic repulsion that overcomes the original surface tension of the solution and results in the droplet stretching into a fiber. When this jet of charged particles overcomes the surface tension of the solution, it forms a conical shape, referred to as a Taylor cone. As the fibers are being produced from the solution, the fiber diameter is continually reduced as the original solvent evaporates while the fiber travels and whips around to the grounded collection plate [19]. In electrospinning applications, parameters such as the applied voltage, separation distance, and polymer concentration can be modified in order to produce fibers of various compositions, diameters, and orientations. For instance, aligned, electrospun microfibers are developed and optimized by rotating the grounded surface [17, 20, 21].

To produce electrospun PLA fibers, a modified version of the setup in Figure 2.1 was used. Paclitaxel-loaded PLA fibers were produced by electrospinning an 8% w/w polymer solution of PLA (Grade 6201D, $\overline{M_w}$ = 78 kDa, $\overline{M_n}$ = 48 kDa, NatureWorks LLC, Minnetonka, MN), in chloroform and dimethylformamide (99:1 w/w) with increasing concentrations of paclitaxel (0, 0.025, 0.05, 0.1, 0.5, 1.0% w/w in reference to fiber weight; LC Laboratories, Woburn, MA). Sunitinib-loaded fibers were produced by electrospinning an 8% w/w polymer solution of PLA in chloroform and

dimethylformamide (99:1 w/w) with increasing concentrations of sunitinib (0, 0.025, 0.05, w/w in reference to fiber weight; LC Laboratories) and polyethylene glycol (0.6% and 1.2% w/w, $\overline{M_w}$ = 200 kDa, Sigma-Aldrich, St. Louis, MO). For random-oriented fibers, this solution was administered from a syringe for 2 hours at a rate of 0.65 mL/hour with an 11 kV electrical potential applied to the needle onto a stationary, grounded surface 10 centimeters away from the needle (Figure 2.2). For aligned fibers, this solution was administered from a syringe for 2 hours at a rate of 1.1 mL/hour with a 10 kV electrical potential applied to the needle. This solution was collected on 15-millimeter coverslips (Fisher Scientific, Waltham, MA) grounded to a 45-centimeter disc collector rotating at 1450 rotations/minute (rpm) from a separation distance of 6 centimeters (Figure 2.3 and Figure 2.4). Although it seems like an increase in PEO resulted in a decrease in fiber alignment (Figure 2.4), additional modifications of this fiber production could ensure that this is optimized for future studies. To evaporate any residual organic solvent, the coverslips were placed in a fume hood overnight. Fiber morphology and alignment are maintained after 28 days in PBS and from sterilization by exposing the samples to ultraviolet radiation in a biosafety cabinet for 45 minutes as shown in Figures 2.5 and 2.6. Even though the fibers are biodegradable, these findings ensure that the fibers maintain their morphology long enough for the cells to bind and interact with them throughout *in vitro* assays and *in vivo* implantation.

For *in vivo* applications, PLA microfiber bundles were developed. Three kilovolts was applied to 1 milliliter of a 12% w/w polymer solution of PLA in chloroform and dimethylformamide (99:1 w/w) that was extruded at 2.5 milliliters/hour twenty centimeters away from a 100-rpm rotating water bath. The fibers were then removed

from the water bath and twisted together to form a microfiber bundle with a diameter of ~1 millimeter (Figure 2.7). All of these electrospun fiber production details have been summarized in Table 2.1.

2.3.2 Characterization

To determine the encapsulation efficiency of paclitaxel and sunitinib in the electrospun fibers, treatment-loaded fibers (1 mg) were dissolved in chloroform (1 mL). Then, acetonitrile/water mixture (85:15, 9 mL) was added to the solution. A nitrogen stream was added to evaporate the chloroform at room temperature. The resulting solution was then processed through an absorbance microplate reader (Molecular Devices, Sunnyvale, CA) at 227 nm and 431 nm for sunitinib, and maximum absorbance was quantified.

Fiber micrographs were acquired using a field-emission scanning electron microscope (SEM, JEOL 6700F) and fiber diameter and alignment were quantified using the Image J software (US National Institutes of Health, Bethesda, MD). These values were then averaged per sample (n = 100/group).

In order to first develop a platform that could sustain an extended treatment release, paclitaxel was incorporated into the polymer solution at an expected loading concentration, assuming a 100% loading efficiency, from 0 – 5% (mass paclitaxel/mass microfiber). Due to some of the paclitaxel binding to the vials and some not being completely incorporated in the fibers, approximately 40–65% of the paclitaxel was actually loaded in the microfibers (Table 2.2). Furthermore, the fiber diameter remained between 1.37–1.51 μm for all paclitaxel incorporation groups and median fiber alignment

was quantified between 2–8 degrees for aligned microfibers (Table 2.2). Neither paclitaxel nor sunitinib incorporation into aligned microfibers altered the diameter or alignment of these fibers.

Therapeutic molecule incorporation efficiency was determined by dissolving the electrospun microfibers into an organic solvent solution (85% acetonitrile: 15% water) and processing them through an ultraviolet detector, and maximum absorbance was quantified for each sample (Table 2.2). Paclitaxel incorporation was determined to be 39–65% for groups with an expected loading level of paclitaxel from 0.05–5.0%, respectively. For fibers incorporated with 0–5% sunitinib, the loading efficiency was determined to range from 70–30%, respectively. One caveat of this loading methodology, however, is that the consistency of the treatment in the fibers is unknown. Therefore, before preparing the fibers the polymer solution was mixed for approximately 30 seconds in order to attempt to evenly distribute the treatment throughout the solution.

The release of paclitaxel and sunitinib from the fibers was determined by placing coverslips of paclitaxel-loaded fibers (1.5 mg) in PBS (500 mL) and obtaining aliquots of the solution once every three days. These samples were analyzed by high-performance liquid chromatography (HPLC; Waters, Milford, MA) with a mixture of acetonitrile and water (85:15, v/v) as the mobile phase. Fifty microliters of the samples were passed in the mobile phase through a C-18 column (Agilent Technologies, Santa Clara, CA) at a rate of 1 mL/min. The column effluent was detected at 227 nm or 431 nm using an ultraviolet detector for detection of paclitaxel or sunitinib, respectively.

Release rate and duration of paclitaxel and sunitinib were quantified by submerging 1.5 mg of electrospun microfibers into 500 mL of phosphate buffer solution

at 37ºC for 84 days and 14 days, respectively. Biweekly aliquots of the supernatant were removed and processed by HPLC for each sample (n = 3). The cumulative release of paclitaxel from electrospun microfibers was well maintained over 84 days in the higher expected loading level groups (0.02–3.26%; Figure 2.8). Paclitaxel release from the microfibers is inversely correlated to the percent release of paclitaxel depending on the loading-level of paclitaxel in the microfibers. As such, 7–97% of the paclitaxel loaded into the fibers was released from the microfibers with a paclitaxel loading between 3.26–0.02% paclitaxel, respectively (Figure 2.8).

In order to translate this microfiber platform to an *in vivo* model of spinal cord injury, a conduit or bundle of microfibers was used. Before this bundle can be used, though, its release characteristics must be compared to that of the individual microfibers. In Figure 2.9, one-milligram of this bundle is shown to release paclitaxel at a higher rate and concentration than the previously produced individual fibers when compared to the same weight of fibers for both groups. However, a major advantage of this entire platform is its tunable capabilities, so a lower concentration of paclitaxel could instead be used for additional *in vivo* studies.

In addition, sunitinib release was characterized for 14 days in a phosphate buffer solution. Originally, sunitinib release was limited among all groups (Figure 2.10), but polyethylene glycol (PEG/PEO) was added to weaken the bond between the hydrophobic polymer (PLA) and the hydrophobic treatment (sunitinib) as well as increasing the porosity of the fibers to promote more sunitinib release [22]. Once the PEO was added to the fibers at 0.6 or 1.2% w/v, the release of sunitinib increased approximately 500 fold (Figure 2.10) to a level consistent with previous therapeutic concentrations [13].

2.4 Conclusions

We have developed a platform that controls the release of molecules from a variety of electrospun fiber types, which allows this system to be easily translated and modified for multiple therapeutic applications. Electrospun fibers provide an ideal conduit to promote tissue engineering through contact guidance and the ability to release treatments over a prolonged period of time. In this study, we have shown that we can produce electrospun fibers that can be loaded with and release paclitaxel and sunitinib from 12 weeks to a minimum of 2 weeks, respectively. Furthermore, incorporating these molecules and using our current sterilization technique do not modify the fiber diameter, alignment, or morphology.

2.5 Figures

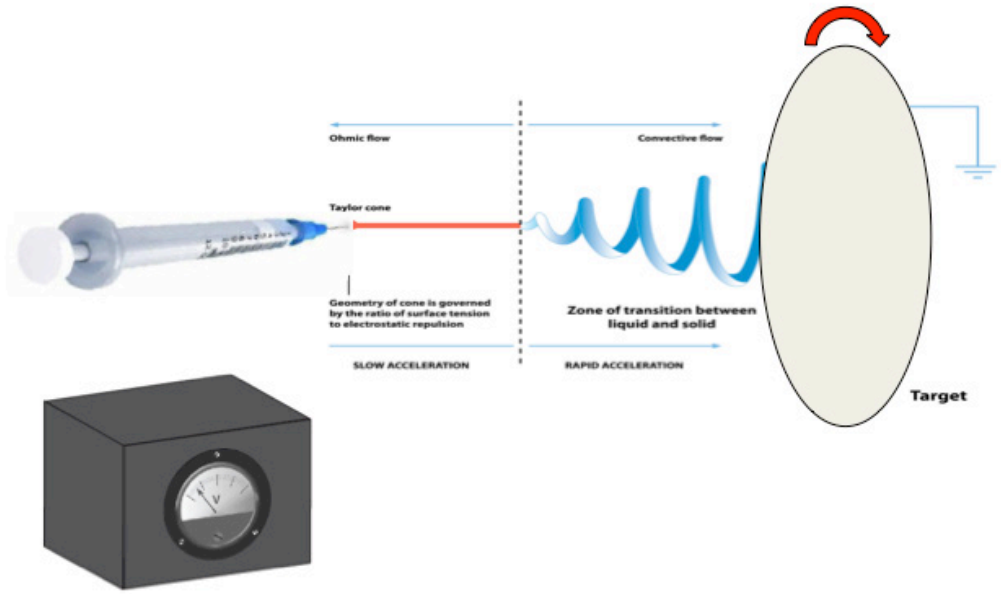

Figure 2-1: Electrospinning setup for producing aligned microfibers

In order to produce aligned, electrospun microfibers, a voltage (kV) is produced and applied to a needle as a solution is extruded and collected on a rotating, grounded disc.

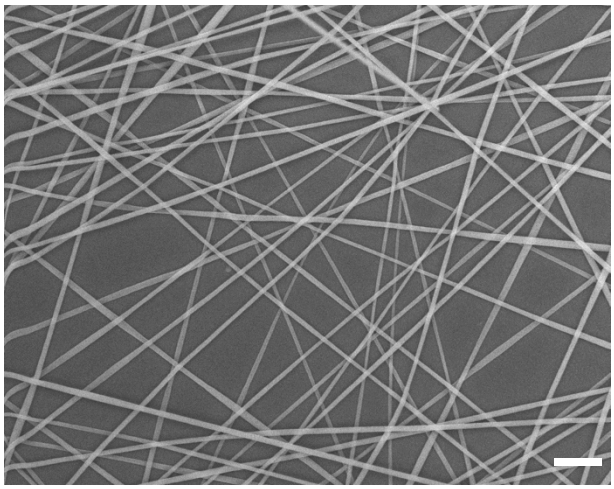

Figure 2-2: SEM micrograph of random-oriented PLA fibers.

Random-oriented PLA fibers were produced by electrospinning PLA onto a grounded, immobile surface. Scale bar: 5 μm

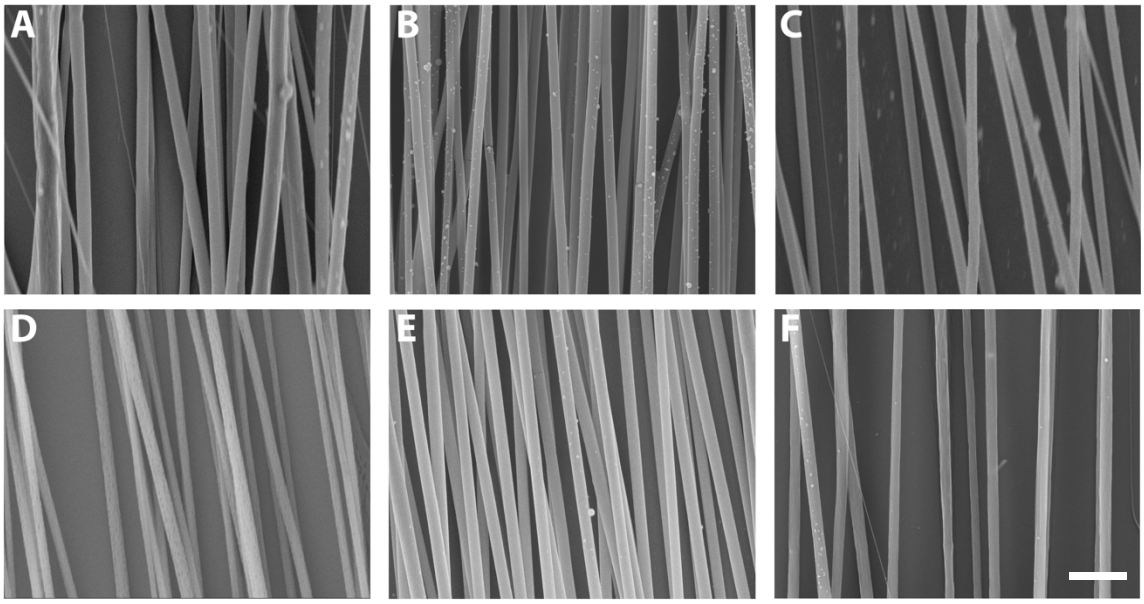

Figure 2-3: SEM micrographs of aligned, electrospun paclitaxel-loaded PLA fibers

Incorporating paclitaxel in electrospun PLA microfibers does not alter fiber morphology, diameter, or alignment. Aligned PLA microfibers were produced by electrospinning a PLA solution with increasing expected concentrations of paclitaxel 0% (A), 0.05% (B), 0.1% (C), 0.5% (D), 1.0% (E), 5.0% (F) (w/w 1 milligram of PLA) and visualized by scanning electron microscopy. Scale bar: 5 μm.

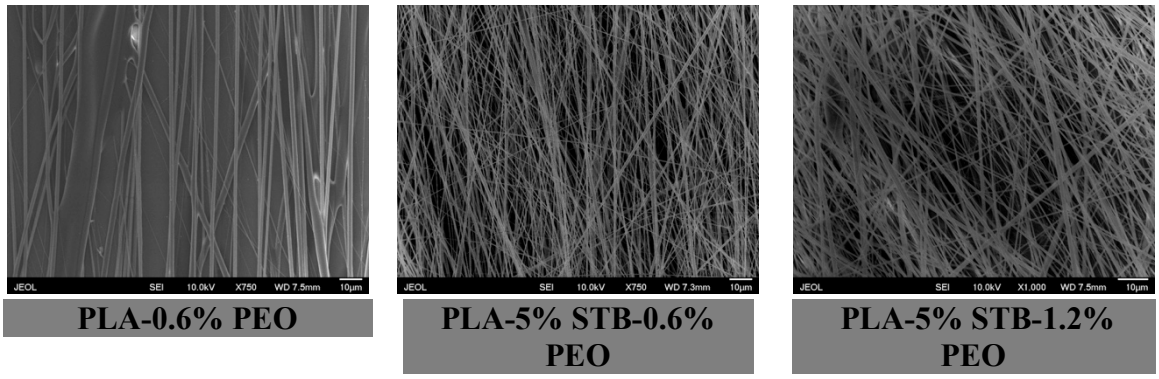

Figure 2-4: SEM micrographs of aligned, electrospun sunitinib-loaded PLA fibers

Incorporating sunitinib in electrospun PLA microfibers does not alter fiber morphology or diameter. Sunitinib was loaded in PLA fibers at increasing concentrations (0–5%) with two concentrations of PEO (0.6% and 1.2%) and visualized by scanning electron microscopy. Scale bar: 10 μm.

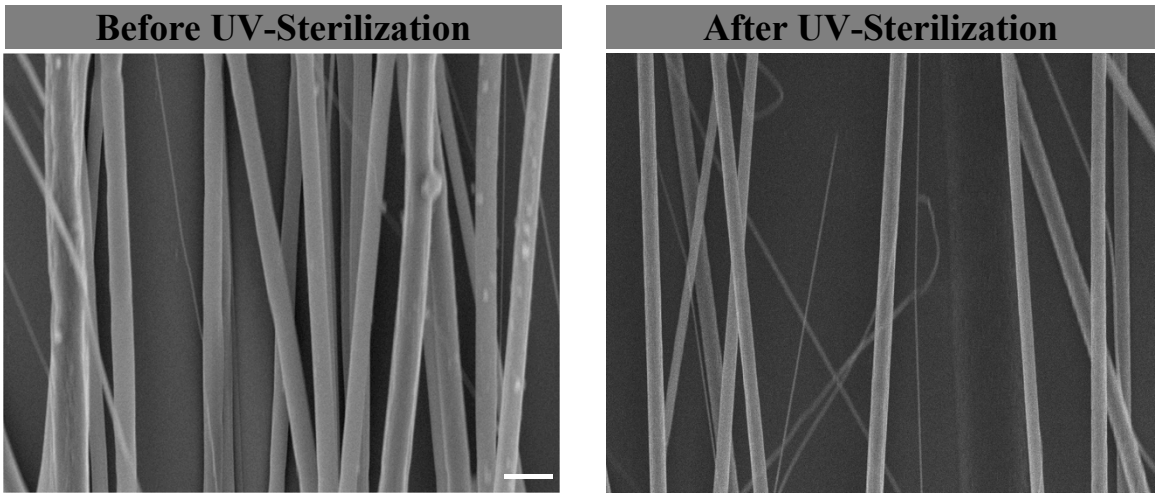

Figure 2-5: Sterilization by UV light does not affect fiber morphology

After 45 minutes of sterilization in a biosafety cabinet, electrospun microfibers did not lose their morphology or experience a significant variation in fiber diameter as shown by the micrographs taken by a scanning electron microscope. Scale bar: 5 μm

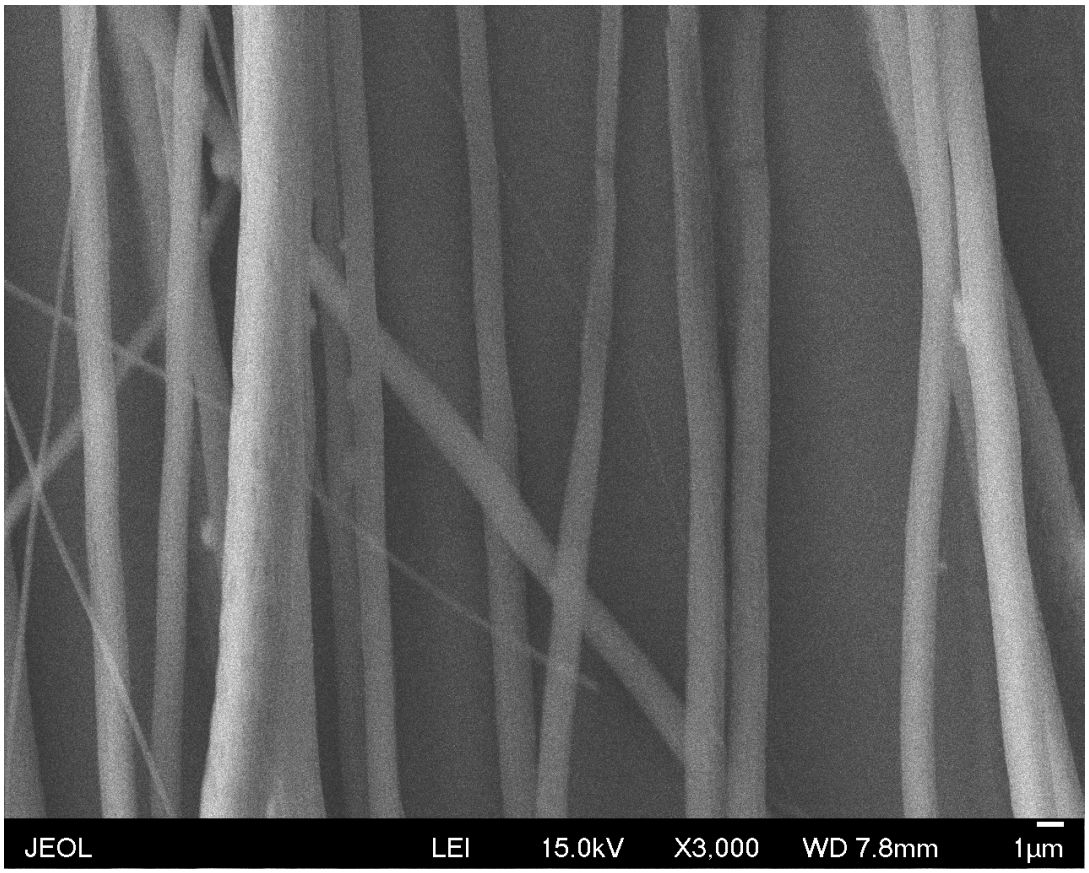

Figure 2-6: Fiber degradation observed after 28d in in PBS

Fibers retain their morphology after 28 days in PBS. Pores are beginning to enlarge in some of the fibers, but overall the fibers retain their morphology and alignment after 28 days in phosphate buffer solution (PBS). Scale bar: 1 μm.

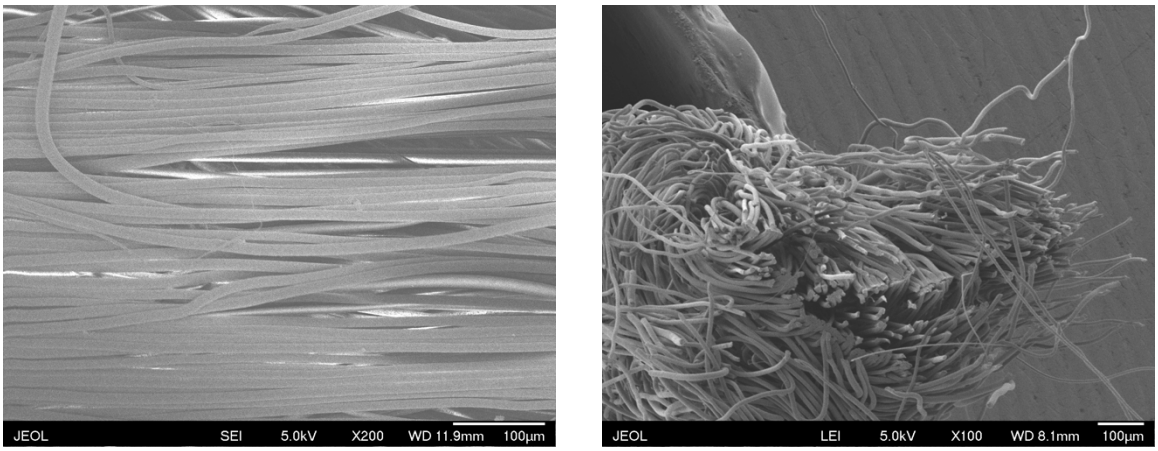

Figure 2-7: SEM micrographs of PLA microfiber bundles

Electrospun microfibers were developed using a water-based electrospinning process as shown in the longitudinal (left) and transverse cross-sectional images (right). Scale bar: 100 µm

	PLA Composition (%)	Separation Distance (cm)	Flow Rate (mL/hr)	Applied Voltage (kV)	Rotation Speed (rpm)	Needle Gauge	Fiber Diameter (µm ± STD)	Fiber Alignment (STD)
Paclitaxel -Loaded Aligned Fibers	8	6	1.1	10	1450	27	1.44 ± 0.42	4.44
Paclitaxel -Loaded Random Fibers	8	11	0.65	8	Ø	27	0.734 ± 0.37	Ø
Paclitaxel -Loaded Aligned Fiber Bundles	12	20	2.5	3	100 (in water bath)	27	9.22 ± 1.02	N/A
Sunitinib -Loaded Fibers	8 (with PEO)	6	1.1	8	1450	27	1.11 ± 0.40	3.72

Table 2-1: Parameters to produce electrospun microfibers

Expected Loading (PTX %)	Paclitaxel Encapsulation Efficiency (%)	Actual Loading (PTX %)	Fiber Diameter (μm ± STD)	Fiber Alignment (° ± STD)
0 (PLA)	N/A	0	1.41 ± 0.29	4.79 ± 4.36
0.05	39.4	0.0197	1.56 ± 0.45	3.21 ± 2.47
0.1	42.4	0.0424	1.39 ± 0.37	7.56 ± 6.84
0.5	50.7	0.254	1.50 ± 0.51	6.32 ± 3.83
1.0	58.2	0.582	1.36 ± 0.43	2.32 ± 1.99
5.0	65.2	3.261	1.44 ± 0.41	4.45 ± 4.16

Table 2-2: Characterization of paclitaxel-loaded, aligned PLA fibers

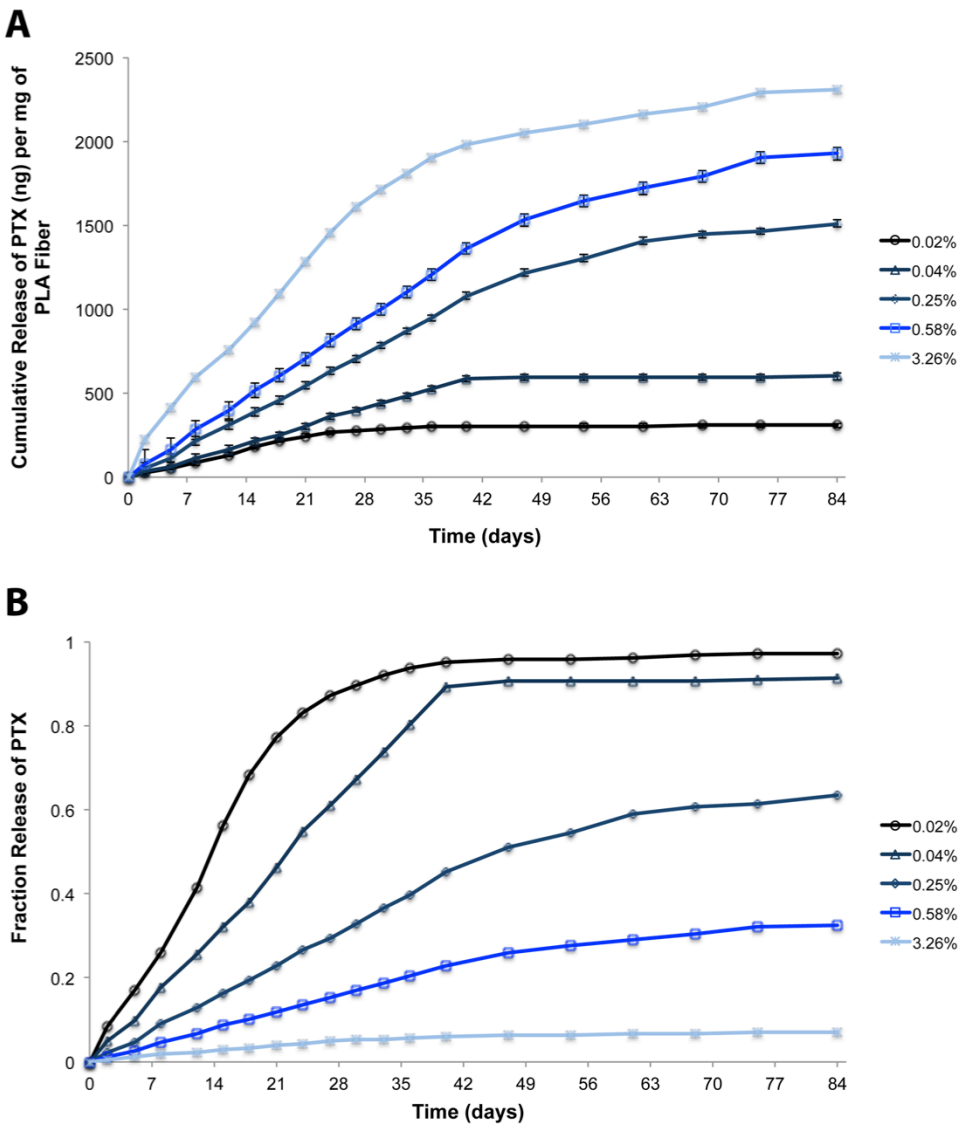

Figure 2-8: Paclitaxel release from electrospun fibers

Paclitaxel release from PLA microfibers can be controlled and tuned based on the original loading level of paclitaxel. PLA microfibers were placed in PBS and aliquots were analyzed by HPLC over 84 days and the cumulative (A) and fraction (B) release were calculated. As the initial loading of paclitaxel increased, the release rate increased, and the fraction released increased at a slower rate than fibers with a lower incorporation of paclitaxel.

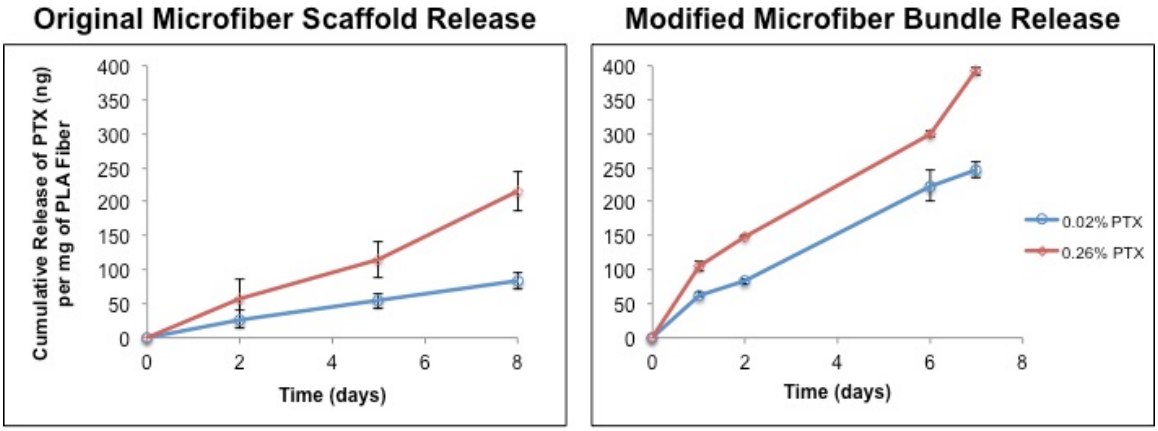

Figure 2-9: Paclitaxel release from microfiber bundles

Larger diameter PLA fibers release paclitaxel faster than smaller diameter fibers. Paclitaxel release from electrospun PLA electrospun fibers (left) releases slower than similar paclitaxel loadings in fiber bundles (right). Both groups show a concentration-dependent effect with a higher loading of paclitaxel resulting in a faster release and larger release of paclitaxel over eight days.

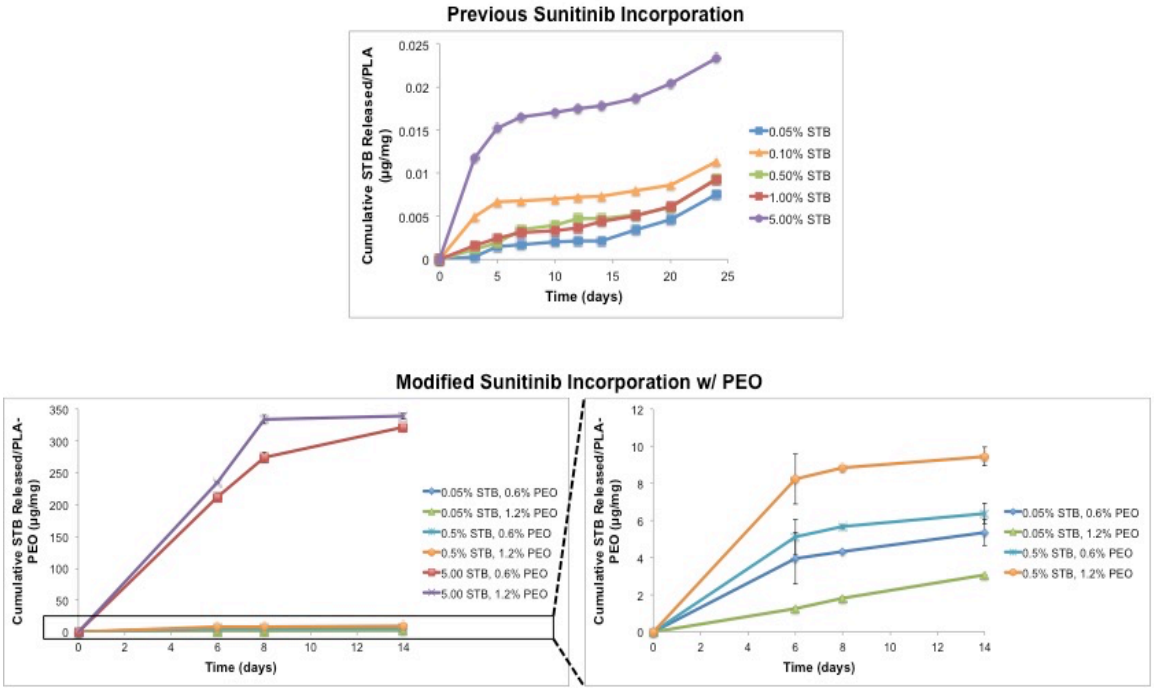

Figure 2-10: Sunitinib release from electrospun fibers

Sunitinib release from PLA microfibers occurs faster with a polyethylene glycol incorporation. Originally, sunitinib was loaded in PLA fibers with the same incorporation technique as paclitaxel. However, minimal sunitinib was released over 25 days of release (top). After incorporation with PEG (0.6% and 1.2%), sunitinib released at a faster rate and amount over 2 weeks in PBS (bottom).

2.6 References

[1] Buddy D. Ratner ASH, Frederick J. Schoen, Jack E. Lemons. Biomaterials Science, Third Edition: An Introduction to Materials in Medicine: Academic Press; 2013.

[2] Arap W, Pasqualini R, Ruoslahti E. Cancer treatment by targeted drug delivery to tumor vasculature in a mouse model. Science. 1998;279:377-80.

[3] Singh R, Lillard JW, Jr. Nanoparticle-based targeted drug delivery. Exp Mol Pathol. 2009;86:215-23.

[4] Patel T, Zhou J, Piepmeier JM, Saltzman WM. Polymeric nanoparticles for drug delivery to the central nervous system. Adv Drug Deliv Rev. 2012;64:701-5.

[5] Davis ME, Hsieh PC, Takahashi T, Song Q, Zhang S, Kamm RD, et al. Local myocardial insulin-like growth factor 1 (IGF-1) delivery with biotinylated peptide nanofibers improves cell therapy for myocardial infarction. Proc Natl Acad Sci U S A. 2006;103:8155-60.

[6] Sterne GD, Brown RA, Green CJ, Terenghi G. Neurotrophin-3 delivered locally via fibronectin mats enhances peripheral nerve regeneration. Eur J Neurosci. 1997;9:1388-96.

[7] Mitra AKK, D.; Vadlapudi, A.D. Drug Delivery: Jones & Bartlett Learning; 2014.

[8] Paclitaxel. Drugs.com 2016.

[9] Wang TH, Popp DM, Wang HS, Saitoh M, Mural JG, Henley DC, et al. Microtubule dysfunction induced by paclitaxel initiates apoptosis through both c-Jun N-terminal kinase (JNK)-dependent and -independent pathways in ovarian cancer cells. J Biol Chem. 1999;274:8208-16.

[10] Smith NF, Acharya MR, Desai N, Figg WD, Sparreboom A. Identification of OATP1B3 as a high-affinity hepatocellular transporter of paclitaxel. Cancer Biol Ther. 2005;4:815-8.

[11] Witte H, Neukirchen D, Bradke F. Microtubule stabilization specifies initial neuronal polarization. J Cell Biol. 2008;180:619-32.

[12] Gelderblom H, Verweij J, Nooter K, Sparreboom A. Cremophor EL: the drawbacks and advantages of vehicle selection for drug formulation. European journal of cancer. 2001;37:1590-8.

[13] Zack DJW, D.S.; Yang, Z. Compounds and methods of use thereof for treating neurodegenerative disorders. USA2013.

[14] Huang D, Ding Y, Li Y, Luo WM, Zhang ZF, Snider J, et al. Sunitinib acts primarily on tumor endothelium rather than tumor cells to inhibit the growth of renal cell carcinoma. Cancer Res. 2010;70:1053-62.

[15] Haggerty AE, Oudega M. Biomaterials for spinal cord repair. Neuroscience bulletin. 2013;29:445-59.

[16] Li D, Xia YN. Electrospinning of nanofibers: Reinventing the wheel? Adv Mater. 2004;16:1151-70.

[17] Li WJ, Laurencin CT, Caterson EJ, Tuan RS, Ko FK. Electrospun nanofibrous structure: a novel scaffold for tissue engineering. Journal of biomedical materials research. 2002;60:613-21.

[18] Xiao LW, B.; Yang, G; Gauthier, M. Poly(Lactic Acid)-Based Biomaterials: Synthesis, Modification and Applications. In: Ghista DN, editor. Biomedical Science, Engineering and Technology 2012.

[19] Pham QP, Sharma U, Mikos AG. Electrospinning of polymeric nanofibers for tissue engineering applications: A review. Tissue Eng. 2006;12:1197-211.

[20] Nair LS, Bhattacharyya S, Laurencin CT. Development of novel tissue engineering scaffolds via electrospinning. Expert opinion on biological therapy. 2004;4:659-68.

[21] Wang HB, Mullins ME, Cregg JM, Hurtado A, Oudega M, Trombley MT, et al. Creation of highly aligned electrospun poly-L-lactic acid fibers for nerve regeneration applications. Journal of neural engineering. 2009;6:016001.

[22] Li YF, Rubert M, Aslan H, Yu Y, Howard KA, Dong M, et al. Ultraporous interweaving electrospun microfibers from PCL-PEO binary blends and their inflammatory responses. Nanoscale. 2014;6:3392-402.

Chapter 3

Local Therapeutic Delivery from Electrospun Fibers for Nerve Regeneration

3.1 Background

Physical trauma occurs and is characterized by an external force impacting the body causing an injury or dysfunction. These medical maladies are unique due to the inability to eliminate them; instead, they can only be treated by mitigating their occurrence through safety measures (seatbelts, helmets, etc.), reducing the complications, and treating the results afterwards [1].

3.1.1 Neuroregeneration

Nervous system tissue degeneration generally occurs after a traumatic injury physically severs an axon or in degenerative disorders such as Alzheimer's or Guillain–Barré syndrome where the neuron slowly degrades over time. Neuroregeneration presents a way for nerves to regrow or repair after issues are initiated to prevent further damage to the surrounding tissue and downstream targets [2]. Neuroregeneration can further be classified into peripheral nervous system regeneration (PNS) and central nervous system (CNS) regeneration. PNS regeneration is localized to the nervous system outside of the brain and spinal cord. Damaged PNS nerves regenerate at a slow rate (~1mm/day), but have a modestly growth conducive environment due to assistance and stimulation from the surrounding glial cells, such as Schwann cells [3]. CNS regeneration, which is

localized to the brain and spinal cord, however, does not readily occur due to the inhibitory environment present after an injury, primarily comprised of glial cell, which can lead axonal degeneration.

3.1.2 Spinal Cord Injury

Spinal cord injuries (SCIs) are traumatic injuries that occur to the spinal cord. SCIs currently affect approximately 282,000 patients with an additional 17,000 new cases each year in the US alone [4]. SCIs typically result in functional deficiencies below the site of injury such as a loss of bladder and locomotor control. Biologically, an SCI is characterized by an initial, physical insult (primary injury) followed by a secondary, deleterious cascade (secondary injury) that culminates in the formation of a cystic cavity lined by a primarily astrocytic scar (reactive gliosis) [5, 6]. Additional inhibitory factors present or upregulated after a spinal cord injury such as myelin debris and the lack of a growth permissive scaffold prevent axonal extension from occurring as shown in Figure 3.1 [7]. Nerves can regenerate across the lesion site but need additional growth-promoting or sustaining factors, such as directional guidance and growth factors, to facilitate this process [8]. For the past ten years, clinical treatments for SCIs have involved the off-label usage of an acute administration of methylprednisolone, a steroid that prevents inflammation [9]. However, due to a lack of clinical efficacy and an increased risk of infections, new treatments for SCI patients must be further developed [10, 11].

3.1.3 Therapeutic Molecules for Nerve Regeneration

Systemic drug delivery approaches have limited access to the spinal cord due to the limited diffusion through the blood spinal cord barrier (BSCB) [12]. Initial solutions to circumvent this issue have involved locally administering biological treatments such as stem cells, peripheral nerves, and Schwann cells although limited cell survival and host tissue regeneration have been observed [13-16]. Due to these limited results, various engineered drug delivery methodologies such as hydrogels [17], nanoparticles [18], and foam scaffolds [19] have been developed. By administering these treatments loaded with hydrophilic neurotrophic growth factors or anti-inflammatory modulators locally at the injury site, issues such as non-specific binding, toxicity, and the need for a second surgery for treatment implantation can be avoided [20, 21]. In order to advance the capability of a local administration to promote spinal cord tissue repair, additional treatments, specifically hydrophobic treatments, must be established.

For axonal formation and extension, microtubule stabilization must occur to prevent the rapid depolymerization of microtubules after axotomy [22-24]. Previous research has been conducted to broaden the knowledge of axonal extension and the role of microtubule stabilization in this process [25, 26]. In the past few years, one of the most promising microtubule-stabilizing agents used for SCI repair has been paclitaxel. In fact, a low concentration administration of paclitaxel has been shown to promote axonal extension *in vitro* [23] as well as mitigate the production of inhibitory molecules by the glial scar *in vivo* [27]. However, previous delivery systems have been limited due to paclitaxel's poor solubility, non-specific binding, and its large size preventing penetration through the BSCB [28]. Additionally, its poor solubility requires that it be administered

in a toxic solvent, Kolliphor EL, that induces neuropathy [29]. One study attenuated these issues by delivering paclitaxel locally via an osmotic mini-pump [27]. However, the mini-pump still requires paclitaxel to be administered in Kolliphor EL and can also be dislodged, induce infections, and has a limited loading capacity.

Another therapeutic that has shown promise in nerve regeneration is sunitinib (STB). Unlike paclitaxel, sunitinib is less hydrophobic than paclitaxel, which means that it can be incorporated at a higher concentration, has a smaller molar mass, and longer half-life, which all can lead to a faster and longer administration. As previously mentioned this anticancer drug stabilizes microtubules, a process necessary for axonal extension. When delivered at low concentrations, sunitinib has previously been shown to induce microtubule stabilization through the nuclear factor-kappa B (NF-κB) signaling pathway, which increases neuronal survival and prevents neuronal cell death in a dose-dependent manner [30, 31]. Based on a patent by the Zack lab at the Johns Hopkins University, the most efficacious doses of STB on retinal ganglion cells for neurite extension *in vitro* were found to be between 0.5 and 1.0 μM [30]. For both paclitaxel and sunitinib, a better delivery mechanism is needed to effectively release the molecules for an extended duration, and control their release to ensure that a minimum effective dosage is administered while preventing toxicity (through high concentration administrations), as well as avoid the use of toxic solvents for administration.

3.1.4 Role of Electrospun Fibers in Nerve Regeneration

As previously mentioned, electrospun fibers have been shown to provide a directional guidance that enhances axonal extension *in vitro* (Figure 1.1) [32] and

decrease the cystic cavity volume *in vivo* [33]. However, these microfibers do not have a direct effect on the inhibitory environment that is present after a traumatic nerve injury occurs. Previous approaches to improve spinal cord tissue repair with aligned microfibers or paclitaxel haven seen limited results by only targeting a subset of the issues associated with an SCI. Therefore, incorporating another system or loading a molecule, such as paclitaxel, in the fibers to attenuate this inhibitory response could promote neuronal regeneration after an SCI occurs.

3.2 Methods

3.2.1 PLA Spin Coating

Glass coverslips were coated with an approximately 50-micron layer of PLA by placing 20 microliters of an 8% w/w PLA solution in chloroform: dimethylformamide (Sigma-Aldrich, 99:1, w/w) on a spin-coater (Laurell, North Wales, PA) for approximately 30 seconds until the surface is evenly-coated.

3.2.2 Retinal Ganglion Cell Isolation and Culture

All of the following animal procedures were conducted in accordance with protocols approved by the Institutional Animal Care and Use Committee (IACUC) at The Johns Hopkins University. Retinal ganglion cells (RGCs) were derived from human embryonic stem cells (hESCs) as described previously [34]. Once these cells were produced, hESCs were incubated in TrypLE (Life Technologies, Carlsbad, CA) for one minute and transferred into DMEM/F12 (Gibco), and centrifuged for six minutes at 150 × g. This cell pellet was then dissociated via gentle pipetting in N2B27 differentiation

media [1:1 mix of DMEM/F12 and Neurobasal media (Life Technologies) with 1x GlutaMAX Supplement (Life Technologies), Antibiotic-Antimycotic (Invitrogen, Carlsbad, CA), N2 Supplement (Life Technologies), and B27 Supplement (Life Technologies)]. The cell clump suspension was then placed onto aligned PLA microfibers with increasing concentrations of paclitaxel (0, 0.02, and 0.58%) coated with 1% Matrigel (Corning Life Sciences, Corning, NY) for 1 hour and cultured for fifteen days in NB27 media.

3.2.3 DRG Explant Extraction

Dorsal root ganglion (DRG) neurons were extracted from P5 Sprague Dawley rat pups (Charles River, Wilmington, MA) and split in half and placed on either poly(L-lysine) (100 mg/ml, Sigma-Aldrich) and laminin-coated (10 μg/mL, Invitrogen) film, random-oriented fibers, or aligned fiber samples. Approximately two explants were placed on each sample for five days in neurobasal medium (Invitrogen) with B-27 supplement, L-glutamine, and penicillin-streptomycin.

3.2.4 DRG Isolation

DRG neurons were isolated from P5 Sprague Dawley rat pups (Charles River, Wilmington, MA) and enzymatically digested in 0.1% collagenase type I (Sigma-Aldrich) for 30 min and then in 0.25% trypsin (Invitrogen) for 45 min at 37ºC. Enzymatic digestion was stopped by adding trypsin neutralizing solution (Invitrogen), and cells were recovered with centrifugation for 8 min at 1000 rpm at 4ºC. Dissociated neurons were filtered through a 40-μm filter onto poly(L-lysine) and laminin-coated film, random-

oriented, or aligned fiber samples for five days in neurobasal medium with B-27 supplement, L-glutamine, and penicillin-streptomycin (P/S). This medium was supplemented with decreasing concentrations of Cytarabine (Sigma-Aldrich) and NGF (Invitrogen). Cells were seeded at a density of 7,500 cells/cm^2.

3.2.5 Transwell Culture with CellCrown™ Inserts

Sheets of random-oriented PLA microfibers (2 mg) with and without paclitaxel were incorporated into CellCrowns™ (Scaffdex Ltd., Tampere, Finland) according to the manufacture's instructions. These CellCrowns™ were then placed over the cultured DRG neurons growing directly on tissue culture polystyrene (TCPS) or aligned PLA microfibers without paclitaxel.

3.2.6 Nocodazole

To assess the mechanism of neurite extension, some of the media for the groups was supplemented with Nocodazole (250 nM, Sigma-Aldrich) at 6 – 24 h after cell seeding. Various concentrations of nocodazole (75 nM – 500nM) were used to determine the concentration that allowed neurite extension to occur but was diminished from the previous control groups.

3.2.7 Neuronal Survival Assay

In order to determine the effect of paclitaxel on neuronal survival, an alamarBlue survival assay was used. Four hundred microliters of a ten percent alamarBlue (Invitrogen) in DRG media solution was added to isolated DRG neurons cultured at

20,000 cells/cm^2 on TCPS or aligned PLA microfibers with 0, 0.02, or 0.58% paclitaxel. After 4 hours of incubation, the plates were exposed to an excitation wavelength of 540 nm, and the emission of 590 nm was recorded in a plate reader (Biotek, Winooski, VT), repeated two times throughout the cell culture, and the results were normalized to TCPS growth.

3.2.8 Immunohistochemistry

In order to visualize the cells, neurons were blocked with antibodies against neuronal specific markers. Cells were fixed for 1 hour with 4% paraformaldehyde (PFA, Electron Microscopy Sciences, Hatfield, PA) and blocked in PBS-5% normal goat serum (Sigma-Aldrich) and 0.1% Triton-X (Sigma-Aldrich). DRG cells were incubated overnight at 4ºC with a chicken anti-neurofilament antibody (NF, 1:1000, Millipore, Temecula, CA). Specimens were subsequently incubated for 1 hour with goat anti-chicken Alexa Fluor® 488-conjugated secondary antibody (1:300, Life Technologies) and cover-slipped with Fluoroshield™ mounting medium (Sigma-Aldrich).

3.2.9 Imaging

Micrographs were acquired after the neurons were cultured for five days using bright field and confocal microscopes (Carl Zeiss, Inc., Oberkochen, Germany). The neurons were imaged using the 5x, 10x, and 20x objectives in the 358 (DAPI), 488, or 550 (CY3) nanometer wavelengths.

3.2.10 Quantitative Analysis

Using the ImageJ software, neurite extension was quantified by outlining the length from the edge of the soma to the end of the neurite for each neurite per neuron. These values were then averaged per well (n = 50 cells/group). Data are shown as mean ± standard error of the mean (SEM), and were analyzed using Matlab® (Mathworks, Natick, MA). The experiments involving a single determination of means between two independent groups were analyzed with the Student's t-test or the one-way analysis of variance (ANOVA). Statistical significance was set at $p < 0.05$ unless otherwise noted.

3.3 Results

3.3.1 Effect of a Local PTX Release on Neuronal Survival

Previous studies have shown that paclitaxel administration can induce neuropathy and neuronal toxicity. Therefore, in order to assess the survival of DRG neurons after five days in culture, an alamarBlue Cell Viability Assay was conducted. Isolated DRG neurons were cultured on either TCPS or PLA microfibers with increasing concentrations of paclitaxel (0, 0.02, 0.58%). Measuring the fluorescence of the samples periodically over five days yielded no significant difference between the normalized activities between the paclitaxel-loaded groups. (Figure 3.2). Therefore, paclitaxel release from PLA microfibers does not inhibit neuronal survival after five days *in vitro* and concerns over future applications with this system preventing neuronal survival is not a concern.

3.3.2 Retinal Ganglion Cell Response to a Local Release of PTX

In order to determine the effect of a local release of paclitaxel has on various central nervous system neuronal extension, retinal ganglion cells (RGCs) derived from human embryonic stem cells (hESCs) were cultured on PLA microfibers with PTX loadings of 0, 0.02, and 0.58% for fifteen days. Although a local release of paclitaxel did not have a stimulatory effect on RGC extension, it did not have a negative effect on RGC extension (Figure 3.3).

3.3.3 Neuronal Extension on Aligned PTX-loaded PLA Fibers

To establish that paclitaxel retains its activity after incorporation into microfibers and the effect of this local release mechanism on neuronal extension, dorsal root ganglion (DRG) neuron explants and isolated neurons were harvested from P5 rat pups and cultured for five days on aligned electrospun microfibers with increasing concentrations of incorporated paclitaxel. Importantly, paclitaxel released from the aligned microfibers modulated neurite extension in both isolated and explanted DRG neurons (Figure 3.4 and Figure 3.5). Furthermore, this extension occurred in a paclitaxel concentration-dependent manner. As the concentration of paclitaxel increased, neurite extension was hindered due to an over-stabilization of microtubules (Figure 3.4D). However, lower concentrations of paclitaxel (0.02% PTX/PLA fiber, w/w) promoted a greater and faster extension of neurites in both isolated and explanted DRGs than PLA fibers alone ($p < 0.01$) as shown in Figure 3.4E and Figure 3.5.

3.3.4 Cell Crowns to Determine Effect of Local PTX Release

In order to determine the necessity of a local release of paclitaxel from electrospun microfibers directly in contact with extending axons, sheets of microfibers loaded with various concentrations of paclitaxel were placed in CellCrown™ inserts in cell culture media approximately 5 mm above isolated DRG neurons (Figure 3.6A). DRGs were simultaneously cultured directly on either TCPS, aligned PLA microfibers, or paclitaxel-loaded aligned microfibers. Released paclitaxel from microfibers placed in the inserts does not significantly promote neurite extension when neurons are cultured on TCPS or aligned PLA microfibers (Figure 3.6D). Additionally, cells cultured directly on paclitaxel-releasing aligned microfibers induced maximum neurite extension, as shown in Figure 3.6D.

3.3.5 PLA Topography Determines Neurite Extension

To examine the importance of the surface topography and alignment of a PLA substrate, DRG neurons were cultured on paclitaxel-incorporated spin-coated thin films and random-oriented microfibers. In order to determine the importance of the fiber alignment, a random microfiber orientation was constructed by electrospinning a PLA solution onto a stationary, grounded surface. As an additional control and to determine the importance of the fiber morphology to neurite extension, a PLA thin film was casted onto glass coverslips with an approximate thickness of 50 microns. Isolated DRG neurons were cultured on paclitaxel-loaded random-oriented microfibers and films (Figure 3.7A-D). This local release of paclitaxel enhanced neurite extension, but not significantly more than films and random-oriented fibers without paclitaxel (Figure 3.7E).

These results confirm that a local release of paclitaxel from aligned PLA microfibers was most effective to promote neurite extension (Figure 3.7E). Thus a local release of paclitaxel coupled with and from an aligned microfiber matrix is necessary to promote neurite extension in a synergistic and concentration-dependent manner.

3.3.6 Nocodazole Administration to Determine Mechanism of Action

Low concentrations of paclitaxel have been shown to induce microtubule stabilization in order to maintain axonal extension. In order to ensure that a local release of paclitaxel does not induce a novel neurite extension mechanism, 250 nM of nocodazole, a molecule that destabilizes microtubule formation, was added to isolated DRG neurons cultured on PLA microfibers with and without paclitaxel. After five days of culture the neurite extension that was previously seen due to a local release of paclitaxel was abolished and there was no significant difference in neurite extension among the groups (Figure 3.8). Because this effect is ablated after the introduction of nocodazole, a local release of paclitaxel has been shown to, at least, stabilize microtubule formation and axonal extension, by activating the DLK pathway.

3.3.7 Effect of a Local Release of Sunitinib on Neuronal Extension

Although the importance of paclitaxel release from aligned microfibers has been shown, sunitinib provides a smaller and less hydrophobic molecule, which could lead to a faster diffusion and better incorporation efficiency as a potential therapeutic for spinal cord injury applications. In order to facilitate this process, PEO was added to promote STB release from the electrospun fibers. In this study, we plated isolated DRG neurons

on top of aligned PLA microfiber with increasing concentrations of STB (0–0.5%) and two concentrations of PEO (0.6% and 1.2% w/w). When 0.6% PEO was incorporated in the fibers, neurite extension increased when STB was included and plateaus at 0.5% STB incorporation (Figure 3.9). However, when 1.2% PEO was added to the fibers, neurite extension significantly increased with the 0.05% STB-loaded group, but decreased (compared to the 0.05% STB group) in the 0.5% STB-loading group (Figure 3.10). Even with this decrease, though, the 0.5% STB-loaded group still had a significant increase in neurite extension compared to the aligned PLA microfiber group (0% STB), suggesting that under these conditions a small concentration of STB is potent enough to promote neurite extension.

3.4 Discussion

Initial testing to determine the effect of paclitaxel on neurite extension involved culturing mature retinal ganglion cells for fifteen days on fibers with increasing concentrations of paclitaxel. Although no significant difference in extension was observed, inhibition of neurite extension was not observed suggesting that that particular concentration of paclitaxel does not have an inhibitory effect on RGC extension. Furthermore, RGC growth may not have occurred due to a mixed culture with glia, because differentiated RGCs may still maintain some glial or proliferating cell morphology, or paclitaxel release could maybe not be effective on RGC nerve growth as other neuronal subtypes [35].

As an additional platform for nerve regeneration applications, SCI axonal extension is limited due to the upregulation and migration of inhibitory factors and cells

to the site of injury [36, 37]. In this study, we demonstrate that a local release of paclitaxel or sunitinib from electrospun fibers, in a concentration-dependent manner, remains active to promote neurite extension after release by stabilizing microtubule formation in neurons. Additionally, this therapeutic release from microfibers can be controlled and tuned for both molecules. Furthermore, incorporated paclitaxel in PLA microfibers can maintain neuronal survival and promote neurite extension under growth-conducive conditions (laminin-coated surfaces).

In addition, paclitaxel incorporated into electrospun microfibers remained active in promoting axonal extension. To establish this, we used a well-characterized model of neurite extension with isolated dorsal root ganglion neurons cultured on approximately 1-milligram of PLA microfibers loaded with various concentrations of paclitaxel. We found that this administration technique retained paclitaxel's axon extension modulation in a concentration-dependent and synergistic effect. By removing this direct release to cells, axons lost their ability to maintain their extensions. We hypothesize that this effect was due to a lack of an efficacious paclitaxel concentration present in the entire well, which can initially be compared to that seen in lower paclitaxel (0.025%) incorporation group (not pictured). Even with the same PLA polymer solution, if the DRG neurons were cultured on this solution (film) or with a similar topography (random fiber), the local release of paclitaxel only slightly increased axonal extension, but not significantly. We hypothesize that this synergistic effect is due to the aligned fibers promoting axonal elongation coupled with the local release of paclitaxel that further maintains these extensions to maximize axonal growth. Only the local release coupled with the directional guidance benefits of aligned microfibers promoted neurite extension under

these conditions showing that this synergistic effect is necessary for maximum neurite extension.

Microtubule stabilization is integral for axonal polarization, extension, and formation during neurite development as well as after an axotomy [22, 23, 38, 39]. Throughout axonal elongation, various intracellular components such as microtubules regulate the direction and formation of growth cones [40, 41]. Paclitaxel prevents the formation of retraction bulbs after a lesion by polymerizing and stabilizing disorganized microtubules into an aligned morphology [42]. However, paclitaxel administration must be controlled to prevent neurite growth inhibition by an over-stabilization of microtubules [39] as well as prevent neuronal toxicity [43]. This study mitigates these concerns by administering paclitaxel at lower concentrations than those used in previous studies [33].

Considering the results seen with paclitaxel, other microtubule-stabilizing molecules, such as sunitinib were incorporated into aligned PLA microfibers. Initial incorporations of STB showed minimal release and effect on neurite extension (Data Not Shown). However, PEO was added at 0.6% and 1.2% w/w in order to facilitate STB release and increase PLA microfiber porosity. When 0.6% PEO was added to the fibers, we hypothesize that a similar amount of STB is released between the same groups so no difference in neurite extension is observed. Therefore, an increase in STB incorporation could potentially lead to longer neurite extensions. In the 1.2% PEO group, we hypothesize that a higher concentration of STB is released from the fibers, which leads to the observed concentration-dependent effect.

3.5 Conclusions

Although preliminary studies have established that paclitaxel can promote neurite extension at low concentrations, we have shown the necessity of paclitaxel release from aligned, electrospun microfibers to promote neurite extension under these conditions. Furthermore, we showed for the first time that sunitinib has an effect on and promotes neuronal extension. Moreover, these studies have demonstrated the requirement of both a growth-promoting scaffold and a microtubule-stabilizing agent to promote a synergistic effect that maximally promotes neurite extension and maintains neuronal survival. Overall, we established that paclitaxel and sunitinib remain active after incorporation into PLA electrospun microfibers. The release of both therapeutic molecules from these fibers is controllable and tunable for a prolonged period of time. The coupling of this release from aligned fibers enhances a greater neurite extension than either component alone under growth-conducive environment. Our findings show that aligned, electrospun microfibers incorporated with a low concentration of paclitaxel can provide a versatile, controllable, and readily tunable administration technique to provide a local, sustained, and tunable delivery mechanism for therapeutic applications after a traumatic spinal cord injury to promote neuronal regrowth. Although this platform had a modest effect on RGC extension, it could be modified with other therapeutic molecules for future studies.

3.6 Figures

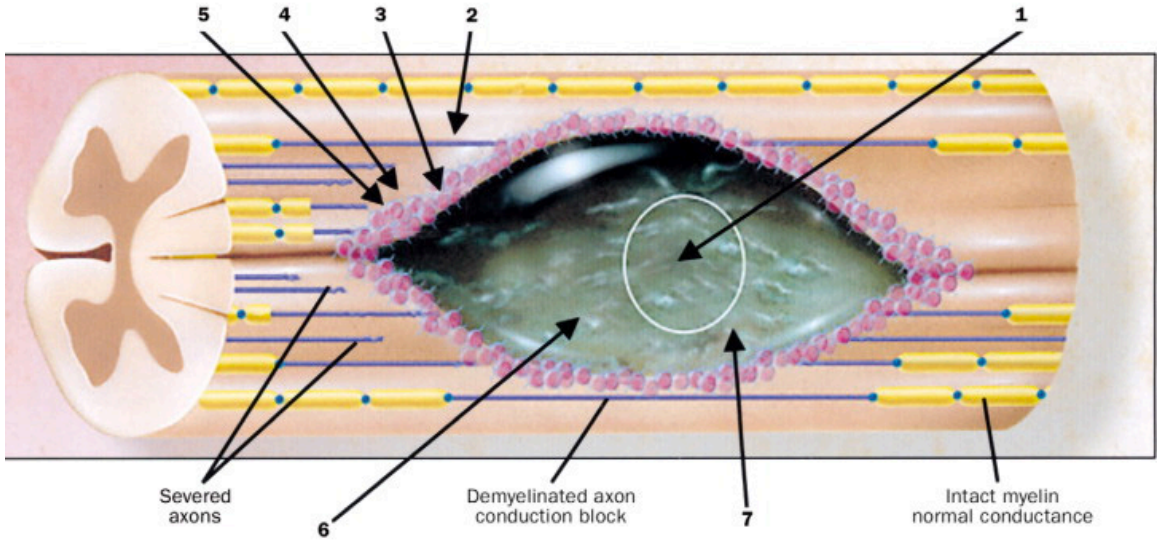

Figure 3-1: Biological response to a spinal cord injury

After a spinal cord injury occurs, axons are severed and multiple factors are induced or upregulated to prevent axonal extension from occurring such as myelin debris (1, 2), reactive astrocytes (3), and the lack of a growth permissive scaffold (1, 6).

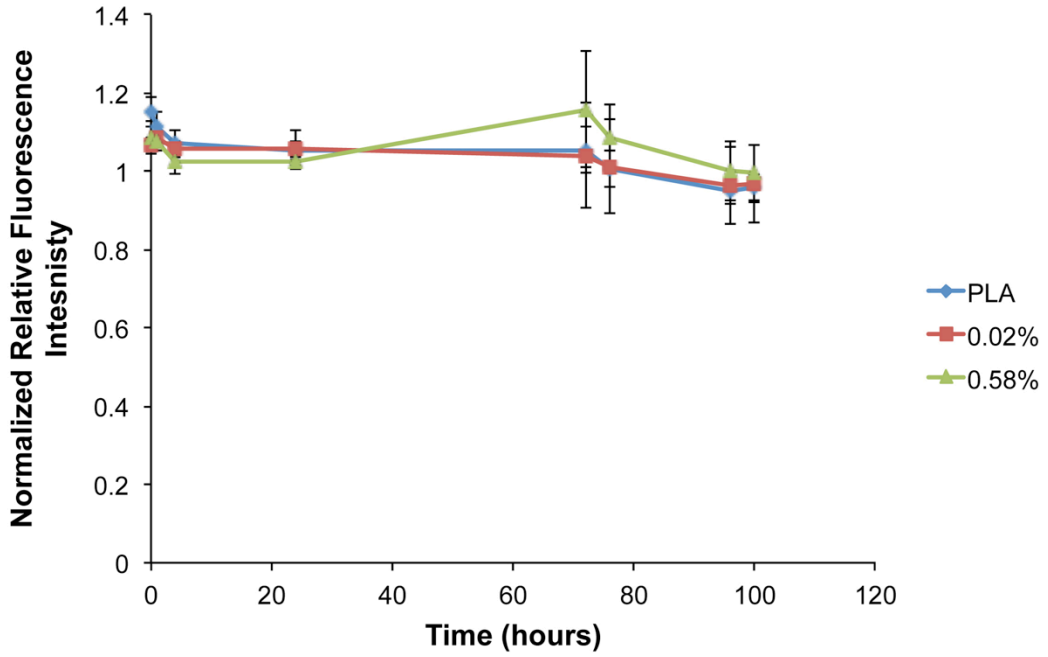

Figure 3-2: Local paclitaxel release effect on neuronal survival

Local paclitaxel administration does not affect neuronal viability. Isolated DRG neurons were cultured on tissue-culture polystyrene or PLA microfibers with various concentration of paclitaxel 0, 0.02%, or 0.58% for five days. Neuronal viability was calculated from an alamarBlue assay (C), normalized against the tissue-culture polystyrene group, and shown to be insignificant between all groups. (n = 5)

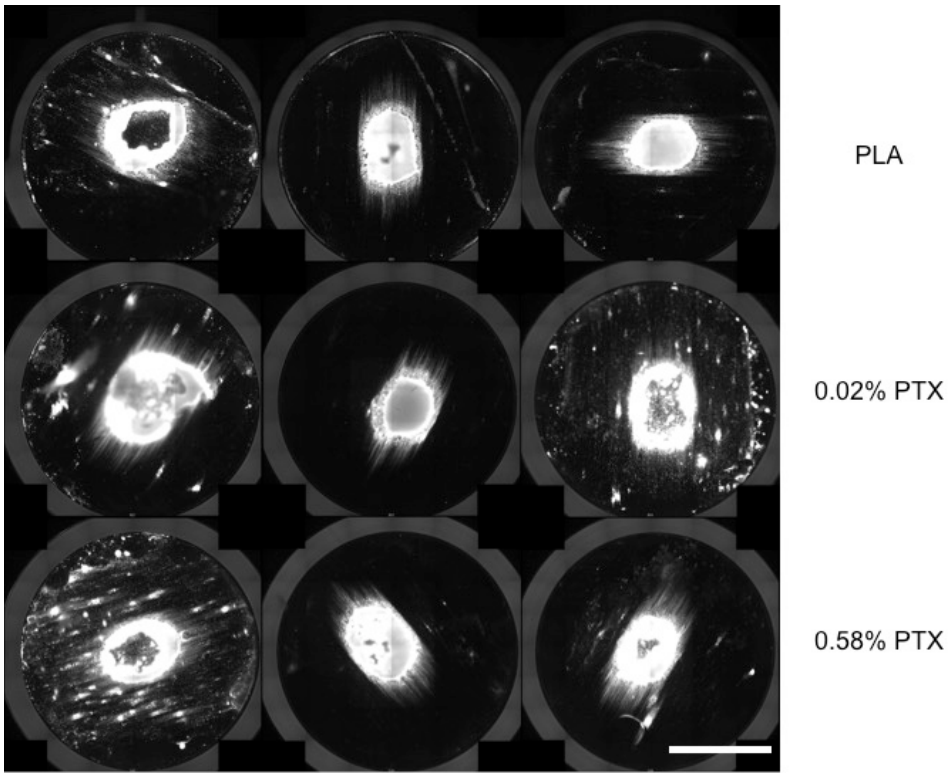

Figure 3-3: Effect of paclitaxel-loaded PLA fibers on RGC Extension

Local release of paclitaxel does not affect RGC neurite extension. Retinal ganglion cells were differentiated from human embryonic stem cells and cultured on electrospun PLA microfibers with increasing concentrations of paclitaxel for 15 days. No significant difference in neurite extension was observed between all of the groups. Scale bar: 5 mm. (n = 3).

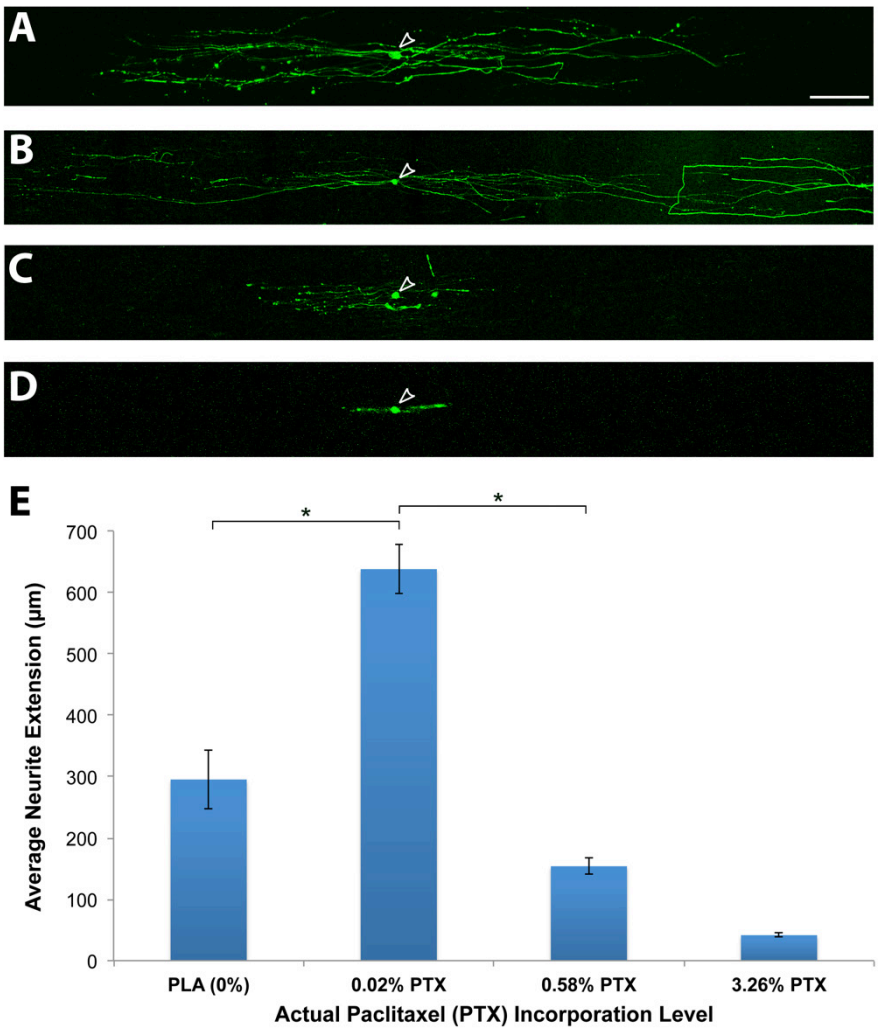

Figure 3-4: Isolated DRGs cultured on PTX-loaded aligned fibers

Paclitaxel release from aligned microfibers modulates neurite extension as visualized by immunostaining for neurofilament. Neurite extension was quantified from isolated DRGs cultured on PLA fibers only (A), 0.02% PTX (B), 0.58% (C), and 3.26% (D). A small incorporation of paclitaxel (0.02%) promoted a significantly greater increase in neurite extension than fibers without paclitaxel and fibers with higher concentrations of paclitaxel (E). Scale bar: 100 µm. ($p < 0.001$, n = 6 – 10).

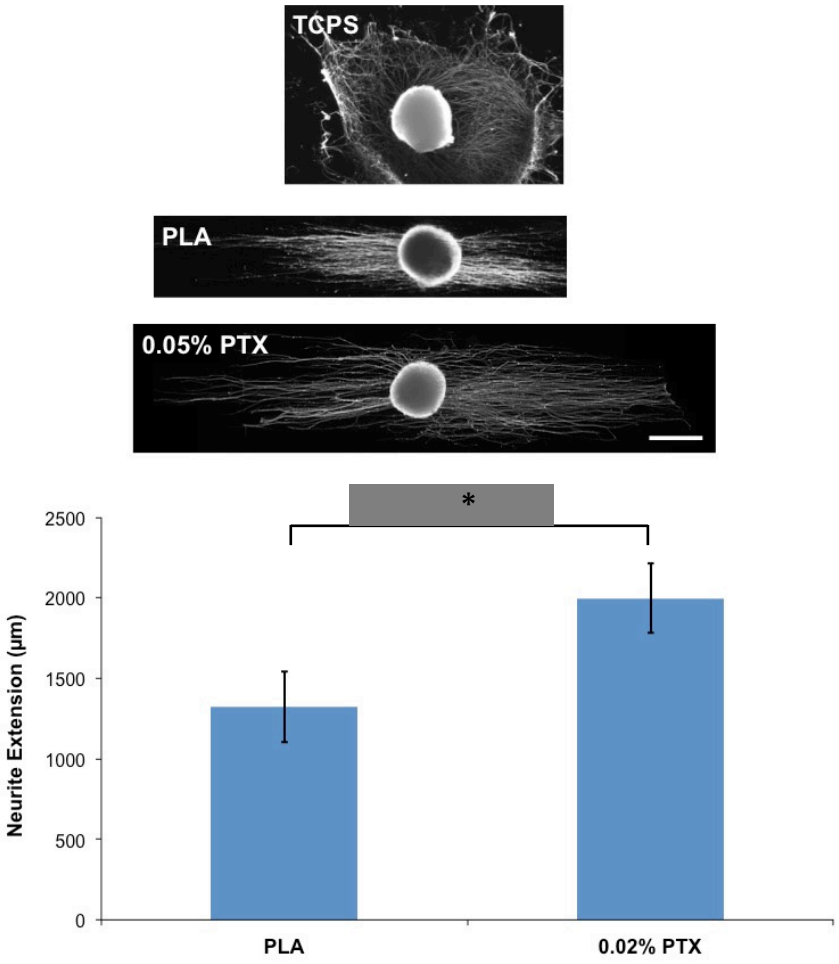

Figure 3-5: Explanted DRGs cultured on PTX-loaded aligned fibers

Local PTX release from aligned fibers promotes DRG explant neurite extension. Neurite extension was quantified from DRG explants cultured on TCPS (top), PLA fibers only (middle image), or 0.02% PTX (bottom image). Paclitaxel incorporation in aligned electrospun microfibers promotes greater neurite extension than the PLA microfibers alone. Scale bar: 500 µm. ($p < 0.05$, n = 4 – 5).

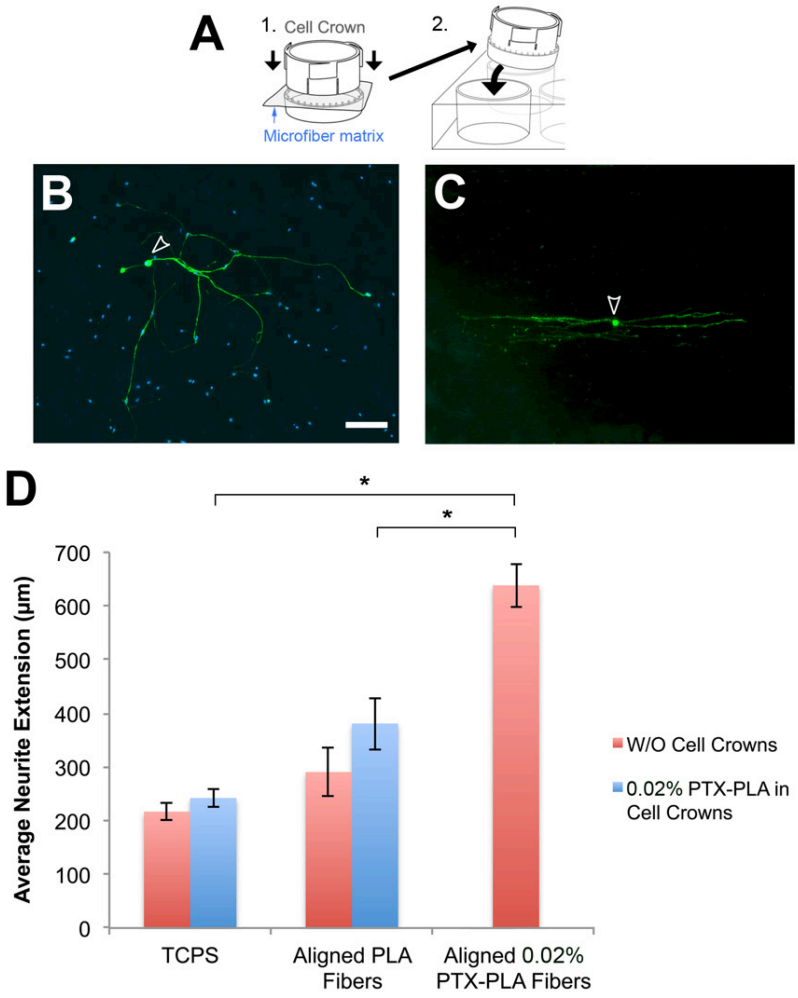

Figure 3-6: Neurite extension due to release of PTX from Cell Crowns

A local delivery of paclitaxel is needed to promote significant DRG neurite extension. Paclitaxel-loaded PLA microfibers were placed in CellCrown™ inserts (A) and suspended above cells cultured on either TCPS (B) or aligned PLA microfibers (C). A modest increase in neurite extension is observed when paclitaxel is released from paclitaxel-loaded microfibers suspended in CellCrowns™ above DRG neurons cultured on TCPS and PLA microfibers alone, but the maximum neurite extension only occurred when the cells were directly in contact with the paclitaxel-loaded microfibers (D). Scale bar: B–C, 40 µm. ($p < 0.001$, n = 7 – 10).

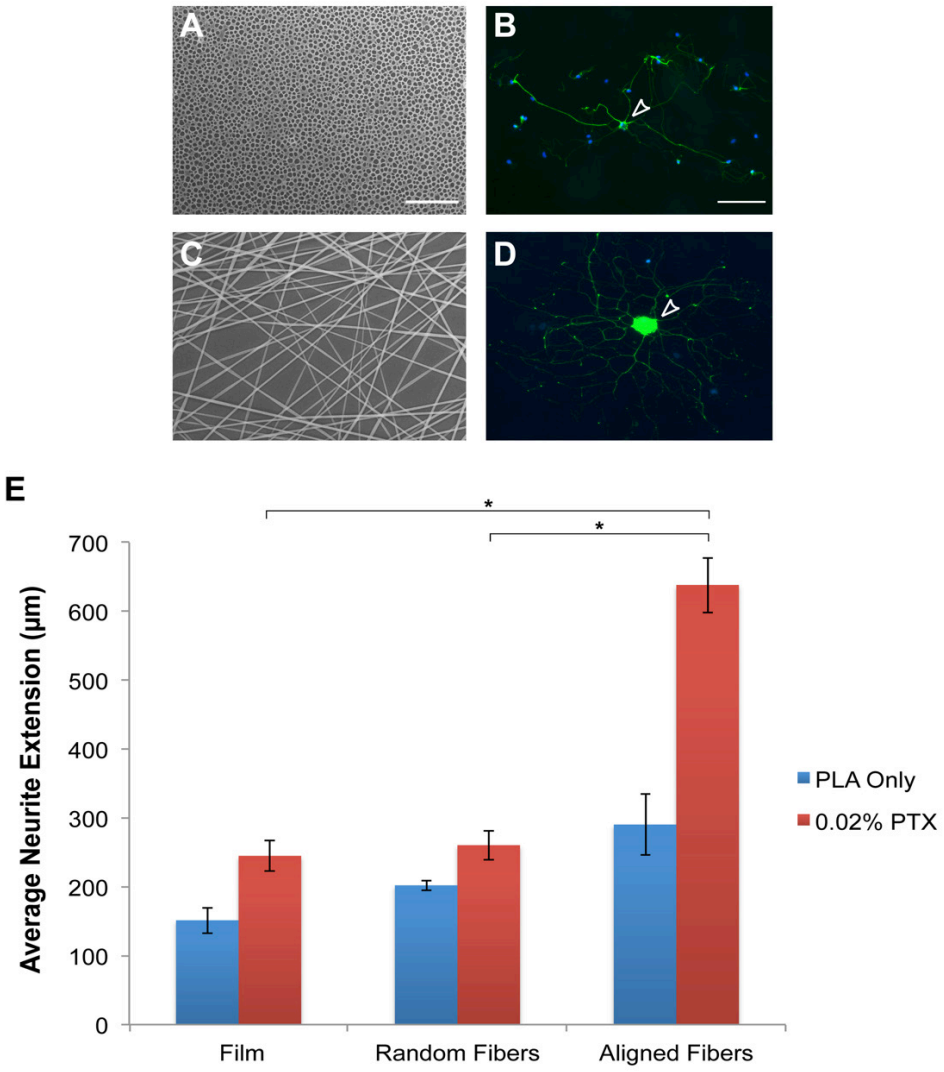

Figure 3-7: Neurite extension on various PLA surface morphologies

The mechanism and surface topography of the local delivery of paclitaxel determines DRG neurite extension. DRG neurons were cultured for five days on PLA films (A) and randomly oriented fibers (C) that were loaded with and without paclitaxel. Although a slight increase in neurite extension was observed among these groups (B, D, E), significant neurite extension only occurred when the microfibers were aligned and coupled with the local release of paclitaxel (E). Scale bars: A, C, 20 µm; B, D, 100 µm. ($p < 0.001$, n = 9 – 10).

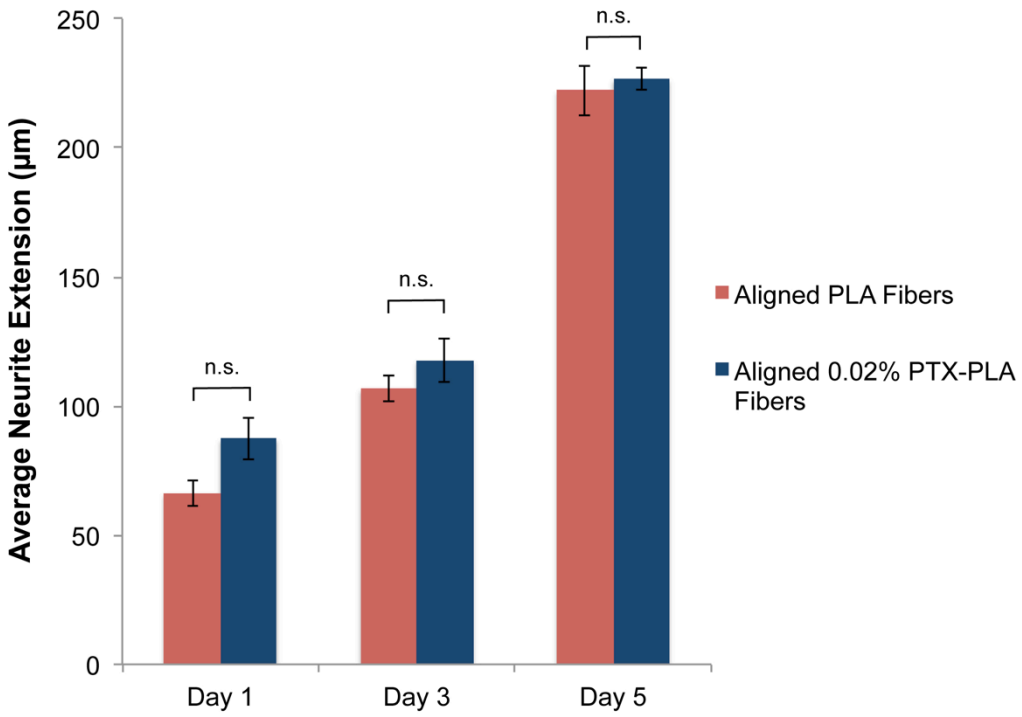

Figure 3-8: Effect of nocodazole administration on neurite extension

A blocking of microtubule stabilization ablates the neurite extension from paclitaxel. To ensure that this paclitaxel delivery mechanism maintains neurite extension via microtubule stabilization nocodazole, a microtubule-destabilizing agent, was added to DRG neurons cultured on PLA microfibers loaded with or without paclitaxel. Once this microtubule stabilization is blocked, the previous axonal extension due to the local release of paclitaxel no longer occurs (n = 3 – 6).

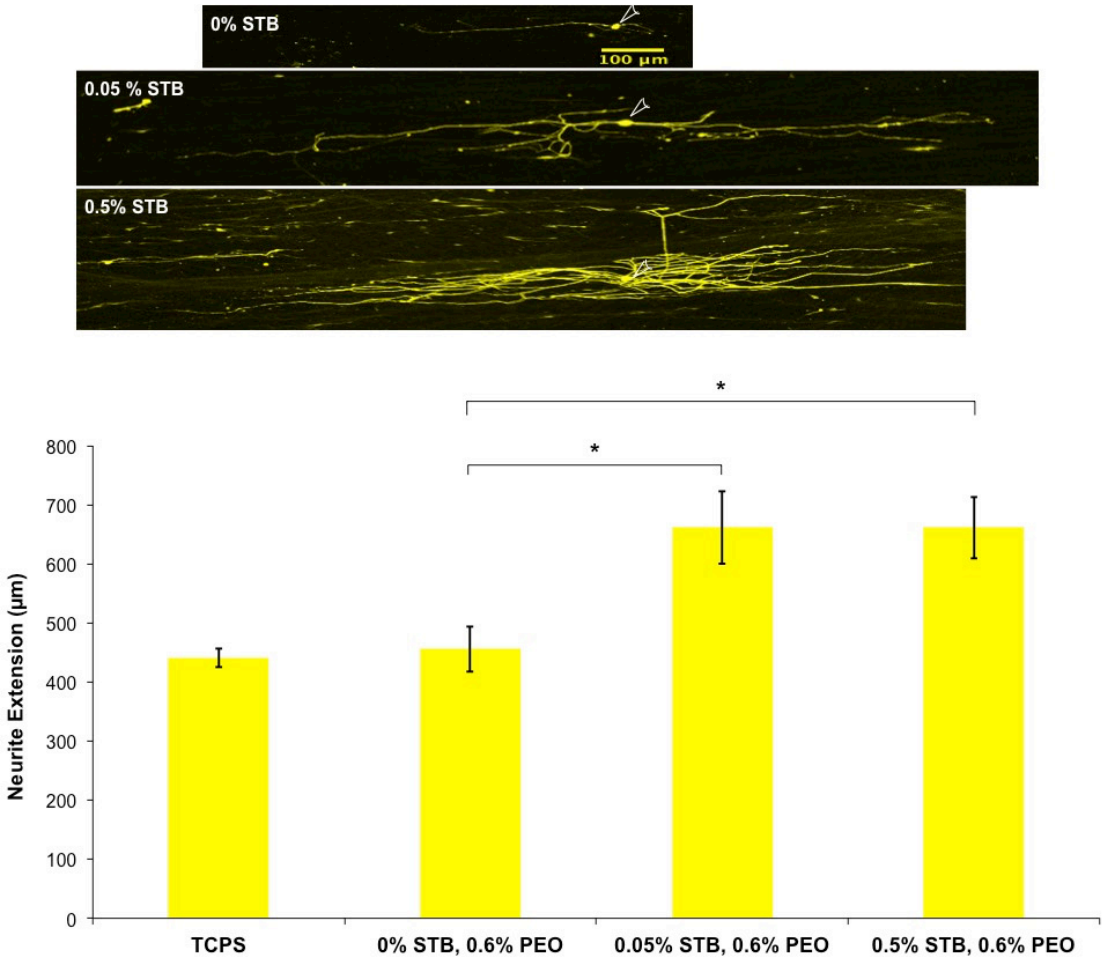

Figure 3-9: Isolated DRGs cultured on STB-loaded aligned fibers with 0.6% PEO

Sunitinib incorporation in aligned PLA microfibers with 0.6% PEO promotes neurite extension. Isolated DRG neurons were cultured on tissue culture polystyrene or PLA fibers with 0.6% PEO (w/w) with increasing concentrations (0 – 0.5%) of sunitinib. As the concentration of sunitinib increased, neurite extension increased. ($p < 0.05$, n = 7).

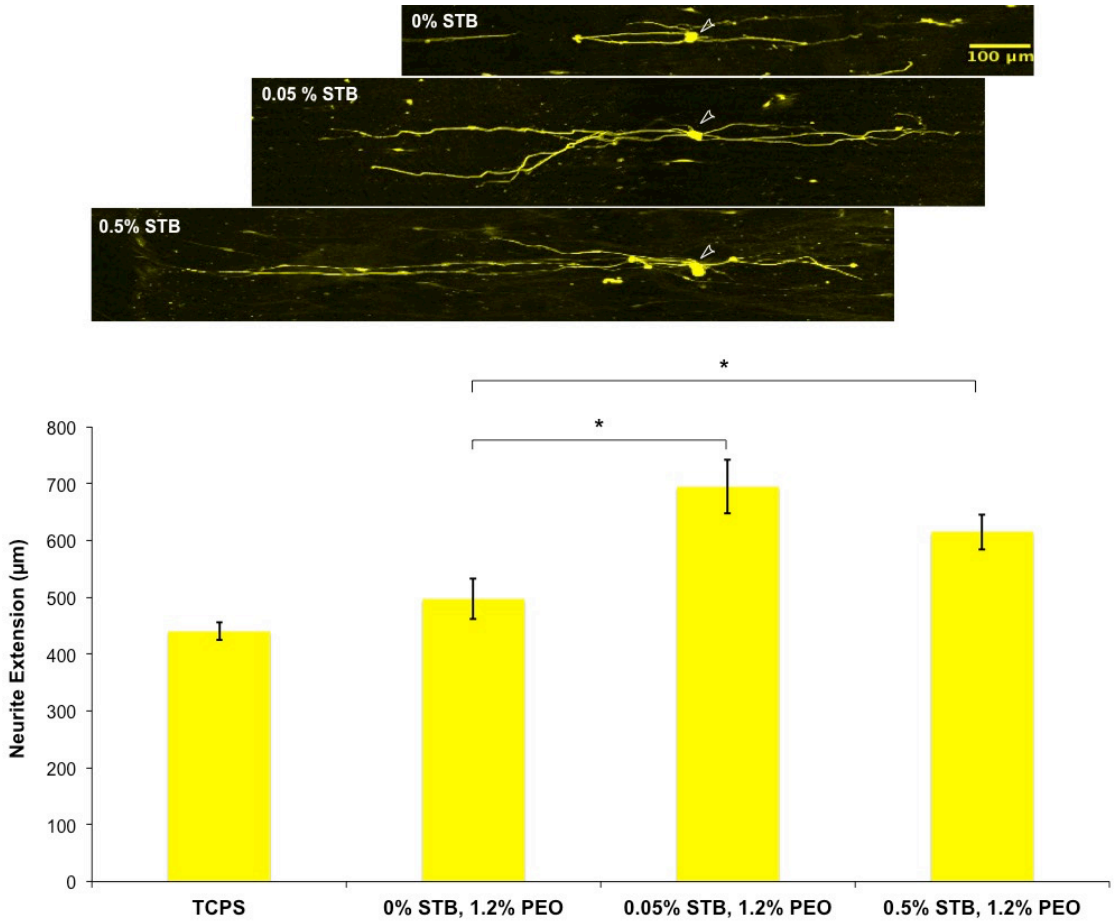

Figure 3-10: Isolated DRGs cultured on STB-loaded aligned fibers with 1.2% PEO

Sunitinib incorporation in aligned PLA microfibers with 1.2% PEO promotes neurite extension in a concentration-dependent manner. Isolated DRG neurons were cultured on tissue culture polystyrene or PLA fibers with 1.2% PEO (w/w) with increasing concentrations (0 – 0.5%) of sunitinib. As the concentration of sunitinib increased, neurite extension increased in a concentration-dependent manner with neurite extension being greater in 0.05% STB-loaded fibers than the fibers alone or 0.5% STB-loaded fibers. ($p < 0.05$, n = 7)

3.7 References

[1] Accidental Death and Disability: The Neglected Disease of Modern Society. Washington (DC): National Academies Press; 1966.

[2] Armstrong RJ, Barker RA. Neurodegeneration: a failure of neuroregeneration? Lancet. 2001;358:1174-6.

[3] Burnett MG, Zager EL. Pathophysiology of peripheral nerve injury: a brief review. Neurosurg Focus. 2004;16:E1.

[4] Annual Statistical Report. National Spinal Cord Injury Statistical Center 2016.

[5] Yiu G, He Z. Glial inhibition of CNS axon regeneration. Nature reviews Neuroscience. 2006;7:617-27.

[6] Burda JE, Sofroniew MV. Reactive gliosis and the multicellular response to CNS damage and disease. Neuron. 2014;81:229-48.

[7] McDonald JW, Sadowsky C. Spinal-cord injury. Lancet. 2002;359:417-25.

[8] Horner PJ, Gage FH. Regenerating the damaged central nervous system. Nature. 2000;407:963-70.

[9] Hugenholtz H, Cass DE, Dvorak MF, Fewer DH, Fox RJ, Izukawa DM, et al. High-dose methylprednisolone for acute closed spinal cord injury--only a treatment option. Can J Neurol Sci. 2002;29:227-35.

[10] Lee HC, Cho DY, Lee WY, Chuang HC. Pitfalls in treatment of acute cervical spinal cord injury using high-dose methylprednisolone: a retrospect audit of 111 patients. Surg Neurol. 2007;68 Suppl 1:S37-41; discussion S-2.

[11] Suberviola B, Gonzalez-Castro A, Llorca J, Ortiz-Melon F, Minambres E. Early complications of high-dose methylprednisolone in acute spinal cord injury patients. Injury. 2008;39:748-52.

[12] Gabathuler R. Approaches to transport therapeutic drugs across the blood-brain barrier to treat brain diseases. Neurobiology of disease. 2010;37:48-57.

[13] McDonald JW, Liu XZ, Qu Y, Liu S, Mickey SK, Turetsky D, et al. Transplanted embryonic stem cells survive, differentiate and promote recovery in injured rat spinal cord. Nature medicine. 1999;5:1410-2.

[14] Cheng H, Cao Y, Olson L. Spinal cord repair in adult paraplegic rats: partial restoration of hind limb function. Science. 1996;273:510-3.

[15] Kuhlengel KR, Bunge MB, Bunge RP. Implantation of cultured sensory neurons and Schwann cells into lesioned neonatal rat spinal cord. I. Methods for preparing implants from dissociated cells. The Journal of comparative neurology. 1990;293:63-73.

[16] Kuhlengel KR, Bunge MB, Bunge RP, Burton H. Implantation of cultured sensory neurons and Schwann cells into lesioned neonatal rat spinal cord. II. Implant characteristics and examination of corticospinal tract growth. The Journal of comparative neurology. 1990;293:74-91.

[17] Jain A, Kim YT, McKeon RJ, Bellamkonda RV. In situ gelling hydrogels for conformal repair of spinal cord defects, and local delivery of BDNF after spinal cord injury. Biomaterials. 2006;27:497-504.

[18] Wang YC, Wu YT, Huang HY, Lin HI, Lo LW, Tzeng SF, et al. Sustained intraspinal delivery of neurotrophic factor encapsulated in biodegradable nanoparticles following contusive spinal cord injury. Biomaterials. 2008;29:4546-53.

[19] Patist CM, Mulder MB, Gautier SE, Maquet V, Jerome R, Oudega M. Freeze-dried poly(D,L-lactic acid) macroporous guidance scaffolds impregnated with brain-derived neurotrophic factor in the transected adult rat thoracic spinal cord. Biomaterials. 2004;25:1569-82.

[20] Colello RJ, Chow WN, Bigbee JW, Lin C, Dalton D, Brown D, et al. The incorporation of growth factor and chondroitinase ABC into an electrospun scaffold to promote axon regrowth following spinal cord injury. Journal of tissue engineering and regenerative medicine. 2013.

[21] Lavin DM, Stefani RM, Zhang L, Furtado S, Hopkins RA, Mathiowitz E. Multifunctional polymeric microfibers with prolonged drug delivery and structural support capabilities. Acta biomaterialia. 2012;8:1891-900.

[22] Bradke F, Fawcett JW, Spira ME. Assembly of a new growth cone after axotomy: the precursor to axon regeneration. Nature reviews Neuroscience. 2012;13:183-93.

[23] Erturk A, Hellal F, Enes J, Bradke F. Disorganized microtubules underlie the formation of retraction bulbs and the failure of axonal regeneration. The Journal of neuroscience : the official journal of the Society for Neuroscience. 2007;27:9169-80.

[24] Xia C, Nguyen M, Garrison AK, Zhao Z, Wang Z, Sutherland C, et al. CNP/cGMP signaling regulates axon branching and growth by modulating microtubule polymerization. Developmental neurobiology. 2013;73:673-87.

[25] Park KK, Liu K, Hu Y, Smith PD, Wang C, Cai B, et al. Promoting axon regeneration in the adult CNS by modulation of the PTEN/mTOR pathway. Science. 2008;322:963-6.

[26] Tedeschi AD, S.; Laskowski, C.; Xue, J.; Ulas, T.; Beyer, M.; Schultze, J.; Bradke, F. The Calcium Channel Subunit Alpha2delta2 Suppresses Axon Regeneration in the Adult CNS. Neuron. 2016.

[27] Hellal F, Hurtado A, Ruschel J, Flynn KC, Laskowski CJ, Umlauf M, et al. Microtubule stabilization reduces scarring and causes axon regeneration after spinal cord injury. Science. 2011;331:928-31.

[28] Zhang Z, Mei L, Feng SS. Paclitaxel drug delivery systems. Expert opinion on drug delivery. 2013;10:325-40.

[29] Gelderblom H, Verweij J, Nooter K, Sparreboom A. Cremophor EL: the drawbacks and advantages of vehicle selection for drug formulation. European journal of cancer. 2001;37:1590-8.

[30] Zack DJW, D.S.; Yang, Z. Compounds and methods of use thereof for treating neurodegenerative disorders. USA2013.

[31] Sanchez A, Tripathy D, Yin X, Luo J, Martinez JM, Grammas P. Sunitinib enhances neuronal survival in vitro via NF-kappaB-mediated signaling and expression of cyclooxygenase-2 and inducible nitric oxide synthase. J Neuroinflammation. 2013;10:93.

[32] Wang HB, Mullins ME, Cregg JM, Hurtado A, Oudega M, Trombley MT, et al. Creation of highly aligned electrospun poly-L-lactic acid fibers for nerve regeneration applications. Journal of neural engineering. 2009;6:016001.

[33] Hurtado A, Cregg JM, Wang HB, Wendell DF, Oudega M, Gilbert RJ, et al. Robust CNS regeneration after complete spinal cord transection using aligned poly-L-lactic acid microfibers. Biomaterials. 2011;32:6068-79.

[34] Sluch VM, Davis CH, Ranganathan V, Kerr JM, Krick K, Martin R, et al. Differentiation of human ESCs to retinal ganglion cells using a CRISPR engineered reporter cell line. Sci Rep. 2015;5:16595.

[35] Zheng H, Xiao WH, Bennett GJ. Functional deficits in peripheral nerve mitochondria in rats with paclitaxel- and oxaliplatin-evoked painful peripheral neuropathy. Exp Neurol. 2011;232:154-61.

[36] Silver J, Miller JH. Regeneration beyond the glial scar. Nature reviews Neuroscience. 2004;5:146-56.

[37] Davies SJ, Fitch MT, Memberg SP, Hall AK, Raisman G, Silver J. Regeneration of adult axons in white matter tracts of the central nervous system. Nature. 1997;390:680-3.

[38] Tedeschi A, Bradke F. The DLK signalling pathway--a double-edged sword in neural development and regeneration. EMBO Rep. 2013;14:605-14.

[39] Witte H, Neukirchen D, Bradke F. Microtubule stabilization specifies initial neuronal polarization. J Cell Biol. 2008;180:619-32.

[40] Gordon-Weeks PR. Microtubules and growth cone function. J Neurobiol. 2004;58:70-83.

[41] Conde C, Caceres A. Microtubule assembly, organization and dynamics in axons and dendrites. Nature reviews Neuroscience. 2009;10:319-32.

[42] Chuckowree JA, Vickers JC. Cytoskeletal and morphological alterations underlying axonal sprouting after localized transection of cortical neuron axons in vitro. The Journal of neuroscience : the official journal of the Society for Neuroscience. 2003;23:3715-25.

[43] Figueroa-Masot XA, Hetman M, Higgins MJ, Kokot N, Xia Z. Taxol induces apoptosis in cortical neurons by a mechanism independent of Bcl-2 phosphorylation. The Journal of neuroscience : the official journal of the Society for Neuroscience. 2001;21:4657-67.

Chapter 4

Local Paclitaxel Release from Electrospun Fibers to Attenuate the Inhibitory Response Present After a Spinal Cord Injury

4.1 Background

Under ideal growth conditions, mature central nervous system neurons can extend; however, after a traumatic injury occurs they cannot due to the presence of inhibitory components or a paucity of growth-promoting substrates [1, 2]. Therefore, an ideal therapeutic platform would simultaneously promote axonal extension while attenuating the inhibitory response present after a traumatic injury occurs.

4.1.1 Glial Response to a Spinal Cord Injury

After a spinal cord injury occurs, astrocytes are recruited to and modestly proliferate at the injury site and form a hallmark effect from an SCI – an astrocyte-lined (glial scar) cystic cavity [3, 4]. Previous research has further shown this astrocytic response to be inhibitory due to its prevention of axonal extension and blood vessel formation [5]. But recent research has shown the importance and necessity of this scar due to its attenuation of the inflammatory response present after the injury and stabilization of the injury to prevent further damage, suggesting that a balance between the inhibitory and growth-promoting aspect of the injury site must be balanced to promote maximum regeneration [6]. In fact, if these inhibitory factors are selectively attenuated/removed [7] or the growth-promoting factors are upregulated [8], then

neuronal extension can occur.

Once astrocytes become reactive, they physically inhibit neuronal extension [9, 10] as well as upregulate inhibitory molecules such as chondroitin-sulfate proteoglycans (CSPGs) that inhibit axonal extension and tissue repair [11]. CSPG upregulation is sustained for about eight weeks after the initial SCI with most deposition occurring in the first two weeks [11]. Therefore, an ideal treatment delivery system to improve spinal cord tissue repair should have a targeted and sustained therapeutic release for eight weeks at a minimum.

Previous methods to promote spinal cord tissue repair have focused on attenuating the glial and inflammatory response through cleaving the CSPGs to make them inactive [12], blocking the receptors on the myelin debris present after the injury [13], or attenuating the inflammatory response [14]. Although most treatments focus on one of these aspects, some of the more promising therapeutic molecules have targeted both the glial response and lack of neuronal extension into the injury site rather than each component individually [6, 15]. Paclitaxel, for instance, both promotes neurite extension and inhibits CSPG upregulation after an SCI [15]. However, as previously discussed, current paclitaxel delivery systems are limited. Aligned, electrospun PLA microfibers have been shown to promote neurite extension and decrease the cystic cavity volume after an SCI, but do not directly affect the secondary injury response [16]. As a combinatorial therapeutic system, paclitaxel-loaded PLA microfibers could provide a multifaceted platform to not only promote neurite extension (as previously shown) but also attenuate the secondary response after an SCI.

4.2 Methods

4.2.1 Aggrecan Surface Coating

A solution of aggrecan (200 μg/mL, Sigma-Aldrich), a type of CSPG, with laminin (10 μg/mL) was used to coat tissue culture polystyrene or PLA microfibers alone or with paclitaxel (0.02%). These protein coating concentrations were determined by observing neurite extension of DRG neurites after varying the concentration of aggrecan (50–700 μg/mL) and picking a concentration that prevented neurite extension but did not inhibit it. Dissociated DRG neurons were then plated at 30,000 cells/well on these coated and uncoated (negative control) surfaces for five days in DRG media (neurobasal media, 5% FBS, 1% P/S, 1x GlutaMax) and then fixed with 4% paraformaldehyde (EMS).

4.2.2 CSPG Spot Assay

DRG neurons were cultured on either a laminin-coated surface, next to a CSPG (EMD Millipore, Billerica, MA) spot (somas present outside of the spot but neurites entering into the spot), or in a CSPG spots per well (somas and neurites contained within the spot). Prior to plating, 24-well tissue culture plates were coated with poly-L-lysine (PLL, Sigma-Aldrich) for one hour at 37ºC, and then washed 5 times with phosphate buffer solution (PBS, pH 7.4), and dried overnight. Once dried, three 1-μL spots of CSPGs (10 μg/mL) and Rhodamine B (1 μg/mL, Sigma) in PBS were placed onto the PLL-coated wells and allowed to dry overnight. Dissociated DRG neurons were then plated and cultured under the same conditions previously described in the Aggrecan Surface Coating conditions.

4.2.3 Astrocyte Isolation

All astrocyte culture procedures using animals were conducted in accordance with protocols approved by the Institutional Animal Care and Use Committee (IACUC) at The Johns Hopkins University. As previously described, astrocytes were harvested and isolated from P0 Sprague-Dawley rat pups [17]. Cerebral cortices were isolated, meninges removed, separated into 4-8 pieces, and placed in Hanks' Balanced Salt Solution (HBSS, Gibco). The tissue was then treated with 0.25% trypsin in HBSS for 30 minutes at 37ºC and mechanically dissociated by trituration through a Pasteur pipette. Cells were then placed on poly-D-lysine (PDL, 50 μg/mL, Sigma-Aldrich) coated flasks and cultured for a week. Astrocytes were further isolated from other glia by vigorously shaking the flasks to remove non-adherent cells and further isolated for an additional two weeks in culture in DMEM with 10% FBS. These cells were then plated onto PDL-coated tissue-culture polystyrene (TCPS) or random-oriented fibers with increasing concentrations of paclitaxel (0 – 0.25%) and maintained for 5 days in culture in DMEM with 10% FBS.

4.2.4 Astrocyte Proliferation Assay

Isolated astrocytes were plated at 4,000 cells/cm^2 and allowed to proliferate for five days on TCPS, random-oriented PLA microfibers only (n = 4), PLA microfibers with a low concentration of paclitaxel (0.02% PTX, n = 4) or a high concentration of paclitaxel (0.25% PTX, n = 4) in DMEM and 10% FBS. After three days in culture, 10% alamarBlue® (Invitrogen, Eugene, OR) was added to each well and the fluorescence was quantified daily for 2 days in a Plate Reader (Biotek, Winooski, VT) at an excitation

wavelength of 540 nm and an emission wavelength of 590 nm. These values were normalized to the astrocytes grown on TCPS.

4.2.5 Astrocyte CSPG Upregulation Assay

CSPG upregulation by astrocytes was determined by plating isolated astrocytes at 4,000 cells/cm^2 and allowing them to proliferate on TCPS, random-oriented PLA microfibers only (n = 6), PLA microfibers with a low concentration of paclitaxel (0.02% PTX, n = 6) or a high concentration of paclitaxel (0.25% PTX, n = 6) in DMEM and 10% FBS. After five days, the cells were fixed and fluorescently labeled with an antibody against CSPGs (Sigma). The fluorescence of the samples was quantified in a Plate Reader at an excitation wavelength of 600 nm and an emission wavelength of 640 nm.

4.2.6 Astrocyte Spheroid Formation and Culture

A 3-D mold for spheroid formation was made by placing 1-milligram of sterile agarose in 50-milliliters of sterile saline and heated until the agarose completely dissolves. Once the solution cools to approximately 65ºC, 330-microliters of this solution was then placed in a 24-series mold (Microtissues®, Providence, RI) until the solution gels, cools, and separated from the molds. To form astrocyte spheroids of approximately 50 microns, 100-µL of 2,000 cells/µL was added to each mold with 1-milliliter of astrocyte media (DMEM and 10% FBS) added to the outside of the molds per well in a 24-well plate. After these molds were placed on a shaker overnight at 200 rpm, the spheroids were removed by slowly pipetting media into the wells and then plating the spheroids on tissue-culture polystyrene, random-oriented PLA microfiber, or PLA microfibers with

paclitaxel (0.02% or 0.25%).

4.2.7 Astrocyte Migration Assay

Approximately five 50-µm astrocyte spheroids were placed on TCPS, random-oriented PLA microfibers only, PLA microfibers with a low concentration of paclitaxel (0.02% PTX) or a high concentration of paclitaxel (0.25% PTX) in DMEM and 10% FBS (n = 8/group). After four days in culture, 10% alamarBlue® (Invitrogen, Eugene, OR) was added to each well and the fluorescence was quantified periodically for the next 24 hours in a Plate Reader at an excitation wavelength of 540 nm and an emission wavelength of 590 nm.

4.2.8 Immunohistochemistry

In order to visualize the neurons, fixed cells with 4% paraformaldehyde were blocked in PBS-5% normal goat serum (Sigma-Aldrich) and 0.1% Triton-X (Sigma-Aldrich) and fluorescently labeled with a chicken anti-neurofilament antibody (NF, 1:1000, Millipore) overnight at 4ºC. Specimens were subsequently incubated for 1 h with goat anti-chicken Alexa Fluor® 488-conjugated secondary antibody (1:300, Life Technologies) and cover-slipped with Fluoroshield™ mounting medium (Sigma-Aldrich).

For astrocytes, cells were again fixed with 4% paraformaldehyde and blocked in PBS-5% normal goat serum (Sigma-Aldrich) and 0.1% Triton-X (Sigma-Aldrich). They were subsequently fluorescently labeled with a rabbit anti-glial fibrillary acidic protein antibody (GFAP, 1:1000, Dako, Carpinteria, CA) overnight at 4ºC. Specimens were subsequently incubated for 1 h with goat anti-rabbit Alexa Fluor® 488-conjugated

secondary antibody (1:300, Life Technologies) and again cover-slipped with Fluoroshield™ mounting medium (Sigma-Aldrich).

For visualizing CSPG upregulation, astrocytes were again fixed with 4% paraformaldehyde and blocked in PBS-5% normal goat serum (Sigma-Aldrich) and 0.1% Triton-X (Sigma-Aldrich). They were subsequently fluorescently labeled with a mouse anti-CSPG (1:200, Sigma) overnight at 4ºC. Specimens were subsequently incubated for 1 h with goat anti-mouse Cy3-conjugated secondary antibody (1:300, Jackson ImmunoResearch, West Grove, PA) and again cover-slipped with Fluoroshield™ mounting medium (Sigma-Aldrich).

4.2.9 Quantitative Analysis

Neurite extension was quantified as previously described. Additionally, neurite extension onto an inhibitory CSPG substrate was quantified by drawing a circle around the perimeter of the CSPG substrate and quantifying the neurite length inside, into, and outside of the CSPG spot of approximately 100 neurites/group.

Astrocyte spheroid diameter was quantified by measuring the diameter of approximately 50 astrocyte spheroids by placing a circle around the spheroid perimeter and quantifying the diameter using ImageJ. Furthermore, astrocyte migration was determined by determining the diameter of these spheres five days after initial plating on a TCPS surface, PLA fibers alone, or PLA fibers with low paclitaxel (0.02%) or high paclitaxel (0.25%) loading.

Data are shown as mean ± standard error of the mean (SEM), and were analyzed using Matlab®. The experiments involving a single determination of means between two

independent groups were analyzed with the Student's t-test or the one-way analysis of variance (ANOVA). Statistical significance was set at $p < 0.05$ unless otherwise noted.

4.3 Results

4.3.1 Neuronal Growth and Extension on Inhibitory Substrates

After an SCI occurs, inhibitory factors such as chondroitin sulfate proteoglycans are upregulated at the site of injury and inhibit axonal extension across the site of injury. Aggrecan is a CSPG that has been shown to inhibit axonal extension *in vitro*. Five hundred micrograms of aggrecan was coated on surfaces containing aligned PLA microfibers alone and PLA microfibers incorporated with 0.02% PTX. As expected, aggrecan diminished neurite extension between all DRG culture conditions tested compared to just laminin-coating the surface alone (Figure 3.1). However, a local release of paclitaxel promoted a significant increase in neurite extension than PLA microfibers alone under these inhibitory conditions ($p < 0.001$, Figure 4.1). Consequently, paclitaxel release from aligned microfibers promotes neurite extension in an inhibitory environment similar to that seen after an SCI ($p < 0.005$).

Although culturing neurons on an evenly covered surface of aggrecan provides an initial platform to assess the effect of a local release of paclitaxel has on neuronal extension on an inhibitory substrate, it does not represent the conditions present after an SCI. Therefore, a CSPG spot assay was produced in which neurons were cultured on, near, or around three 1-microliter 10-µg/mL spots of CSPGs coating a surface of TCPS, PLA fibers alone, or paclitaxel-loaded PLA fibers (0.02%). Under these conditions, a local release of paclitaxel was shown to promote axonal extension into the inhibitory

CSPG spot compared to fibers alone or TCPS (Figure 4.2) as well as in the inhibitory environment as well as shown previously.

4.3.2 Astrocyte Isolation and Spheroid Formation

In order to determine the effect of a local release of paclitaxel on the glial cell response after a spinal cord injury, an *in vitro* assay of the inhibitory environment present after a spinal cord injury was developed by first determining the effect of this system on astrocyte function. To first do this, astrocytes were effectively isolated from rat cortices and cultured for approximately two weeks (Figure 4.3).

Isolated astrocytes provided a platform to determine proliferation and viability, but are not as effective at quantifying astrocyte migration. Therefore a platform that temporarily confines the astrocytes must be established. Approximately 15-30 isolated astrocytes were cultured in agarose molds overnight to effectively bind together and form astrocyte spheroids of approximately 50 microns (Figure 4.4).

4.3.3 Astrocyte Proliferation

Once a traumatic spinal cord injury occurs, astrocytes migrate, surround the site of injury, and increase in activity, which results in a primarily inhibitory environment. Isolated astrocytes were cultured on TCPS, PLA, 0.02% PTX, or 0.25% PTX for five days. Using an alamarBlue® assay, astrocyte proliferation and viability were quantified. After three days in culture, astrocytes showed no difference in activity among the different groups; however, by day 4 astrocytes cultured on PLA fibers alone showed a significant increase in activity compared to the fibers loaded with a high concentration of

paclitaxel (Figure 4.5). Furthermore, after five days in culture, a local paclitaxel release from the PLA fibers maintained the same rate of astrocyte proliferation than the PLA fibers alone ($p < 0.001$).

4.3.4 CSPG Upregulation

Once astrocytes are recruited to the site of injury, they upregulate both growth-promoting as well as inhibitory factors such as CSPGs that prevent axonal extension from occurring. Isolated astrocytes were again cultured on TCPS, PLA fibers alone, or fibers loaded with a low concentration (0.02%) or a high concentration of paclitaxel (0.25%). By fluorescently labeling the CSPGs, their upregulation was quantified and measured by determining the fluorescence of the CSPGs five days after initial plating of the astrocytes (Figure 4.6A-D). Although astrocyte reactivity remained about the same among all groups (Figure 4.6E), CSPG production decreased in the group with the highest incorporation of paclitaxel (Figure 4.6F).

4.3.5 Astrocyte Migration

As previously discussed, after a spinal cord injury occurs astrocytes migrate to the site of injury physically and chemically inhibiting axonal extension from occurring. An *in vitro* assay for astrocyte migration was established by plating 50-µm diameter astrocyte spheroids on top of TCPS, PLA fibers alone, or fibers loaded with a low concentration (0.02%) or high concentration of paclitaxel (0.25%). Astrocyte diameter and migration rate were quantified and compared among the groups. There were no observable difference in the astrocyte spheroid diameter or astrocyte migration rate from the

astrocytes cultured on TCPS or PLA fibers alone (Figure 4.7). However, a concentration-dependent effect was seen in that as the concentration of paclitaxel increased, astrocyte migration significantly decreased in the astrocytes cultured on fibers loaded with paclitaxel.

4.4 Discussion

Although neurite extension under a growth-conducive environment is essential for understanding this mechanism, it is not the environment present after an SCI. Once an SCI occurs, various inhibitory factors are present or upregulated that prevent axonal extension from occurring such as chondroitin-sulfate proteoglycans [3, 4, 11, 18]. To properly mimic the inhibitory effects present after a spinal cord injury, dorsal root ganglion neurons were cultured on an inhibitory substrate of aggrecan or CSPGs. To ensure that the laminin itself was also not inhibitory, we cultured the cells on an uncoated surface as well and observed a slight decrease in neurite extension compared to the laminin only group (not shown). By culturing the neurons either directly on the inhibitory surface (aggrecan and CSPGs) or next to the inhibitory surface (CSPGs only), we established that not only can a local release of paclitaxel promote neurite extension under an entirely inhibitory condition (aggrecan), but it can also promote neurite extension into the inhibitory environment as well (CSPGs). As a negative control, spots of just the fluorescent dye were prepared and neurons were cultured on these spots under the same conditions as described previously. As expected, the dye did not have an inhibitory effect on neurite extension (not pictured). This control group also established that the CSPGs were the inhibitory component in this system. We established that this platform of a local

release of paclitaxel can overcome an inhibitory environment and promote neurite extension under conditions similar to those seen after an SCI occurs. Additional testing that induced reactive astrocytes (i.e. through the addition of TGF-ß) could be used to further determine if a local release of paclitaxel attenuates astrocytes that have already undergone a reactive phenotype.

As another consideration, recent studies have shown that CSPGs are not solely inhibitory for axonal extension in a spinal cord injury, but can also promote neuronal growth as well [6, 19]. Therefore further elucidating whether the growth-promoting or inhibitory CSPG upregulation is decreased under the conditions presented in Figure 4.6 will need to be determined to understand the translation of this system from an *in vitro* model to an *in vivo* model of spinal cord tissue repair. In this study, we only performed one assay (immunohistochemistry) to determine if CSPG upregulation changed in reactive astrocytes, but future studies that quantify CSPG upregulation using rtPCR or Western blot assays should also be conducted.

Because the reactive gliosis produced after an SCI not only physically inhibits axonal extension, but also is necessary for axonal extension to occur, decreasing but not ablating astrocyte reactivity could end up promoting spinal cord tissue repair after a traumatic injury. Once the biological cascade is initiated after the initial physical injury, astrocytes migrate and proliferate forming the glial scar around the injury site. We showed that a local release of paclitaxel significantly attenuated astrocyte proliferation, migration, and inhibitory molecule production when compared to the fibers alone or cells cultured on TCPS. These findings further elucidate the importance of a local release of paclitaxel on astrocyte function. That being said, studies by Anderson et al. have shown

that astrocytes are essential to promoting axonal extension after an SCI [6]. Therefore, the inhibitory components of astrocyte reactivity must be attenuated while simultaneously promoting the growth-promoting aspects to optimize SCI tissue repair. Future studies will be needed to further understand how to initiate this system and determine the optimum astrocytic response for SCI tissue repair.

4.5 Conclusions

When neurons are cultured on fibers that administer a local release of paclitaxel under inhibitory conditions similar to those seen after a SCI, neurite extension is promoted on and into an inhibitory substrate of aggrecan and CSPGs. In addition, astrocytes were successfully isolated from rat cortices and formed into 50-μm diameter spheroids to produce an *in vitro* model of the reactive gliosis present after an SCI. A local release of paclitaxel inhibited astrocytic activity (proliferation, migration, and CSPG upregulation). Overall, the same local release of paclitaxel from electrospun microfibers not only promoted neurite extension but also reduced some of the inhibitory aspects present after an SCI.

4.6 Figures

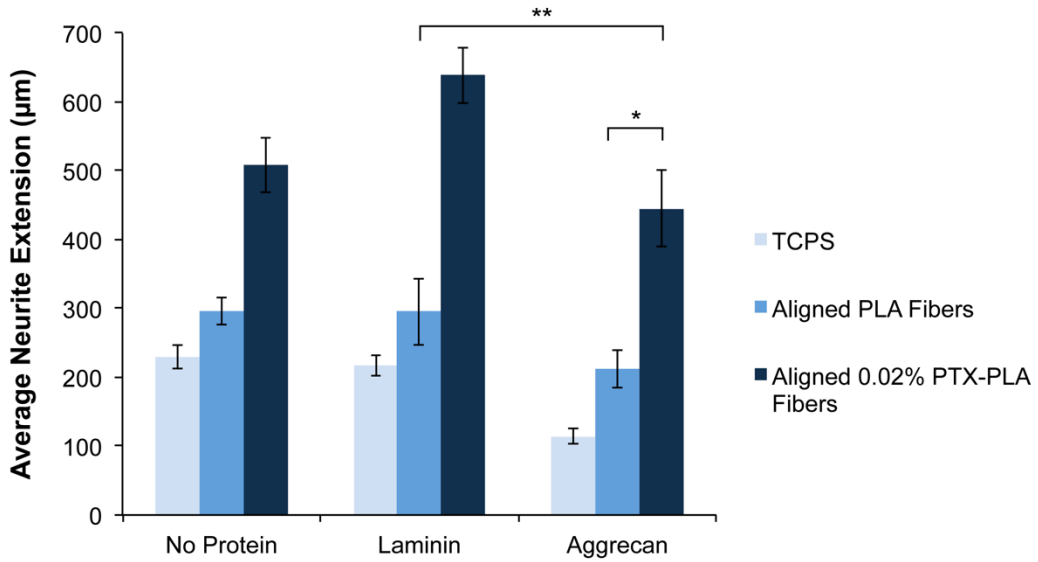

Figure 4-1: Neurite extension on an aggrecan surface

A local release of paclitaxel from aligned PLA microfibers significantly promotes neurite extension under inhibitory conditions similar to those seen after a spinal cord injury. Isolated DRG neurons were cultured on an uncoated surface, laminin only, or laminin/aggrecan-coated tissue culture polystyrene, aligned PLA microfibers only, or aligned paclitaxel-loaded PLA microfibers. Paclitaxel-loaded microfibers significantly promoted neurite extension than PLA microfibers under both a growth-conducive environment and inhibitory environment (*$p < 0.001$, **$p < 0.005$, n = 5 – 10).

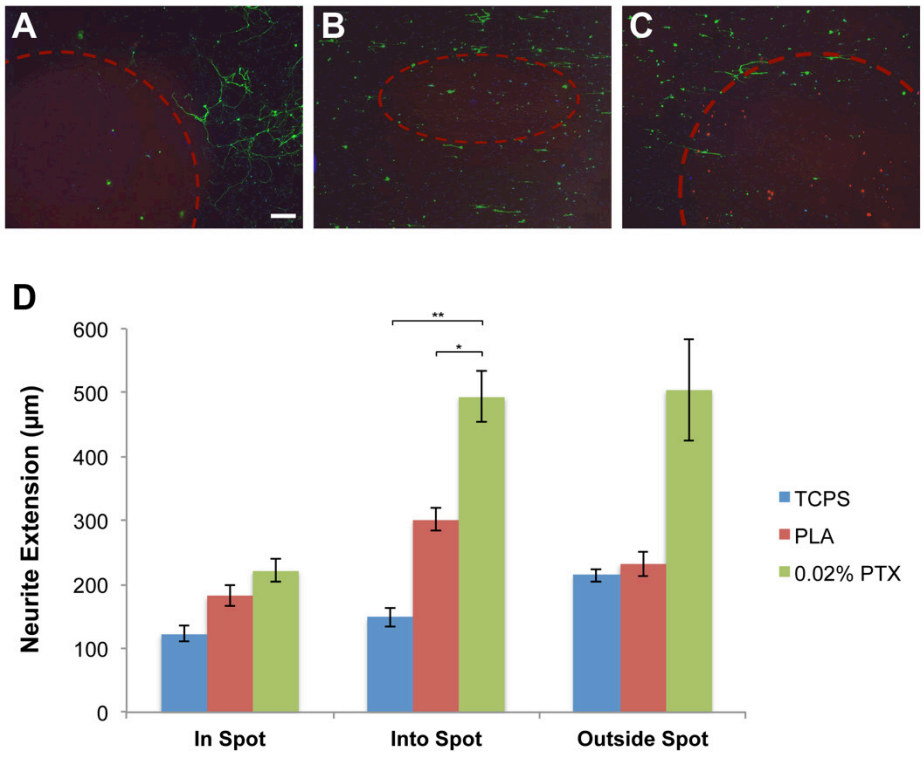

Figure 4-2: Neurite extension onto a CSPG spot

Local release of paclitaxel promotes neurite extension into an inhibitory substrate. Isolated neurons were cultured either in, near, or outside of CSPG (10 µg/mL) spots. These spots were placed on either TCPS (A), PLA fibers (B), or 0.02% PTX-PLA fibers (C). Neurite extension was significantly increased into the CSPG spot when a local release of paclitaxel from aligned PLA microfibers was present (D) than the fibers alone or TCPS. Scale bar: 100 µm. (n = 3, $*p < 0.05$, $**p < 0.005$).

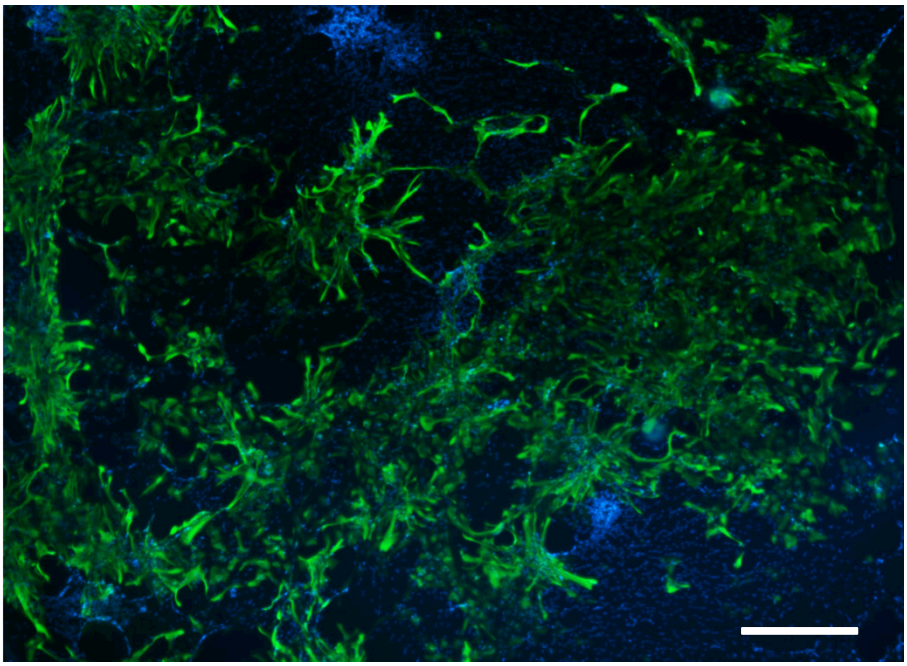

Figure 4-3: Astrocyte isolation

Astrocytes were effectively isolated and cultured. Astrocytes were removed from P0 rat cortices and isolated after shaking and culture for 2 weeks on TCPS. Scale bar: 500 µm.

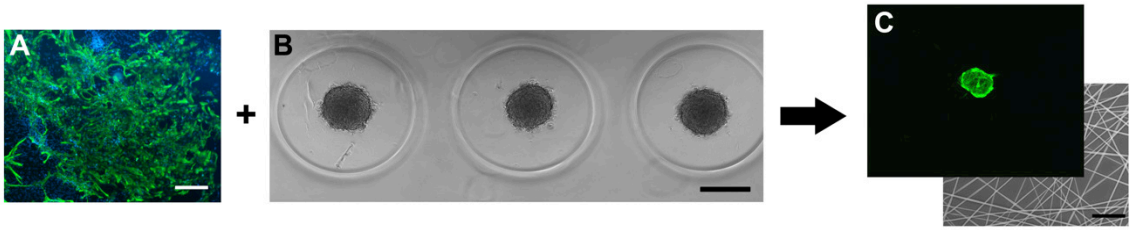

Figure 4-4: Astrocyte spheroid formation

Fifty-micron astrocyte spheroids were effectively formed and cultured. After astrocytes were isolated from rat cortices (A), approximately 15 were placed in agarose molds to promote self-adhesion overnight on a shaker at 200 rpm (B). The cell spheroids were then plated on top of random-oriented PLA microfibers for 5 days (C). Scale bars: A: 500 µm, B and C (front): 50 µm, C (back): 10 µm.

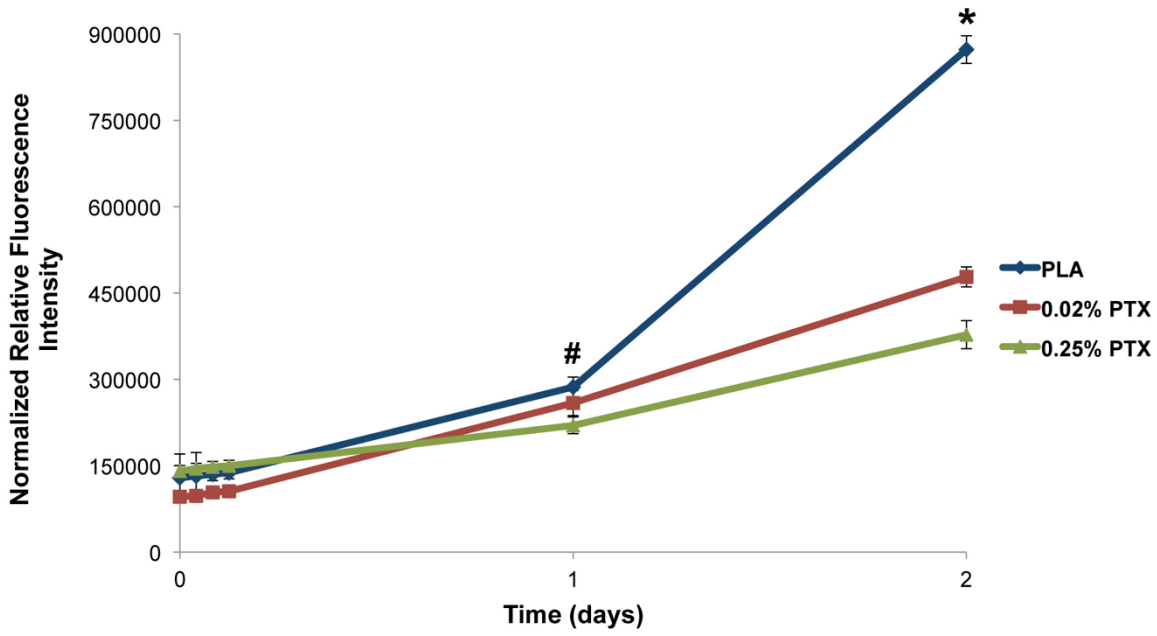

Figure 4-5: Astrocyte proliferation and survival

Local release of paclitaxel inhibits astrocyte proliferation. Isolated astrocytes were cultured on TCPS, random-oriented PLA fibers, or PTX-loaded PLA fibers (0.02% or 0.25% PTX) for five days. After three days in culture, no difference in astrocyte proliferation was observed among all of the groups. However by days 4 and 5 (shown as days 1 and 2 above), astrocyte proliferation significantly decreased in the fibers loaded with a low concentration of paclitaxel or both paclitaxel-loading levels, respectively. ($^{\#}p < 0.05$, $^{*}p < 0.001$, n = 4).

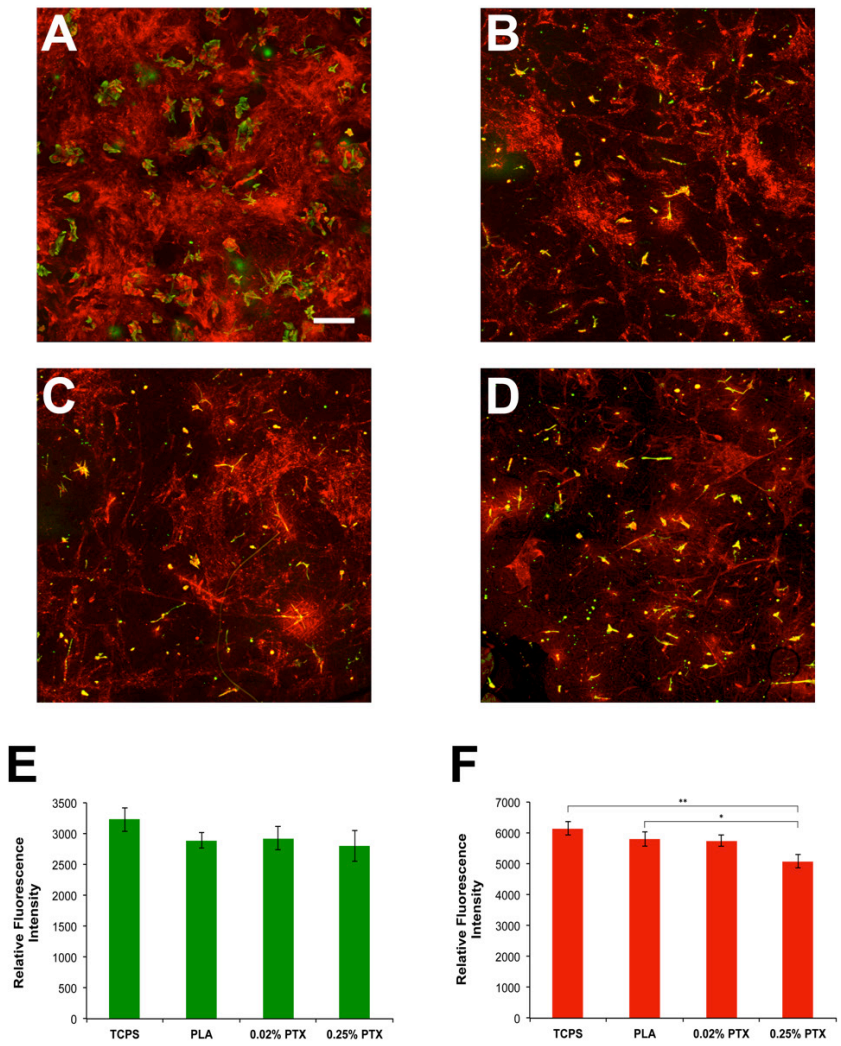

Figure 4-6: CSPG upregulation from astrocytes

Paclitaxel release from PLA microfibers inhibits CSPG upregulation. Isolated astrocytes were cultured on TCPS, PLA fibers, or paclitaxel-loaded PLA fibers (0.02% or 0.25% PTX) for five days (A-D). After fluorescently labeling astrocytes (green) and CSPGs (red), relative fluorescence intensity was quantified for each sample using a Plate Reader. Astrocyte reactivity slightly decreased among the groups loaded with paclitaxel (E), but most noticeably CSPG production decreased if paclitaxel was released from PLA fibers (F). Scale bar: 200 μm. (*$p < 0.05$, **$p < 0.01$, n = 6).

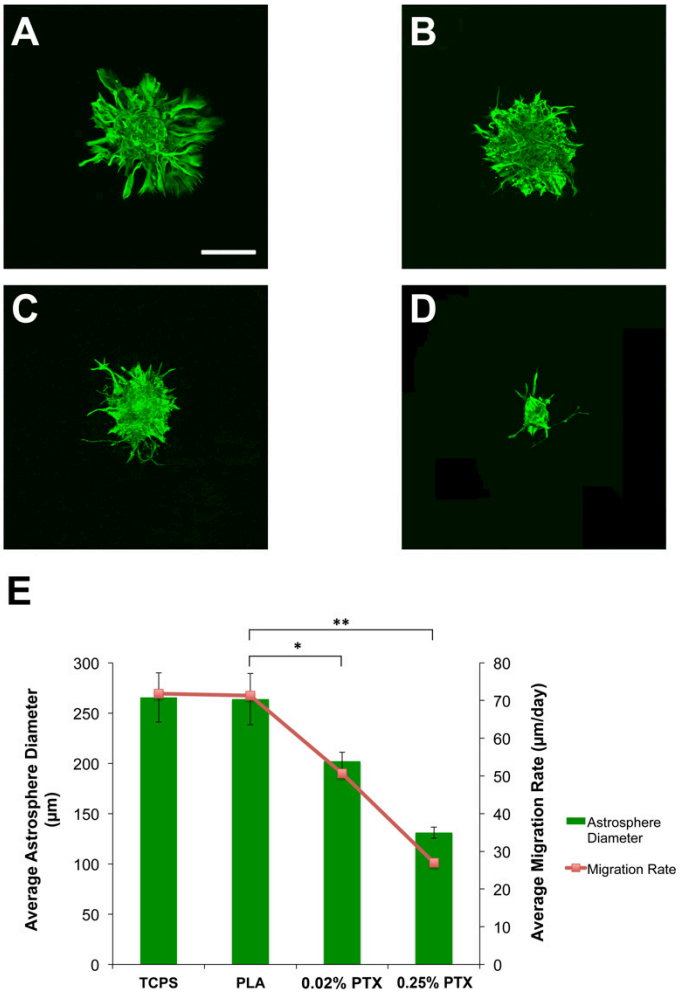

Figure 4-7: Astrocyte migration

Local release of paclitaxel inhibits astrocyte migration. Fifty-micron astrocyte spheroids were cultured on TCPS, PLA fibers, or paclitaxel-loaded PLA fibers (0.02% or 0.25%, A-D). After five days in culture, spheroid diameter was quantified for each group. By incorporating paclitaxel in PLA fibers, astrocyte migration speed significantly decreased than TCPS or PLA fibers alone (E). Scale bar: 100 µm. (*$p < 0.05$, **$p < 0.001$, n = 8).

4.7 References

[1] Ye JH, Houle JD. Treatment of the chronically injured spinal cord with neurotrophic factors can promote axonal regeneration from supraspinal neurons. Exp Neurol. 1997;143:70-81.

[2] Snow DM, Steindler DA, Silver J. Molecular and cellular characterization of the glial roof plate of the spinal cord and optic tectum: a possible role for a proteoglycan in the development of an axon barrier. Dev Biol. 1990;138:359-76.

[3] Yiu G, He Z. Glial inhibition of CNS axon regeneration. Nature reviews Neuroscience. 2006;7:617-27.

[4] Burda JE, Sofroniew MV. Reactive gliosis and the multicellular response to CNS damage and disease. Neuron. 2014;81:229-48.

[5] Cregg JM, DePaul MA, Filous AR, Lang BT, Tran A, Silver J. Functional regeneration beyond the glial scar. Experimental Neurology. 2014;253:197-207.

[6] Anderson MA, Burda JE, Ren YL, Ao Y, O'Shea TM, Kawaguchi R, et al. Astrocyte scar formation aids central nervous system axon regeneration. Nature. 2016;532:195-+.

[7] Wilems TS, Sakiyama-Elbert SE. Sustained dual drug delivery of anti-inhibitory molecules for treatment of spinal cord injury. Journal of controlled release : official journal of the Controlled Release Society. 2015;213:103-11.

[8] Jones LL, Sajed D, Tuszynski MH. Axonal regeneration through regions of chondroitin sulfate proteoglycan deposition after spinal cord injury: a balance of permissiveness and inhibition. The Journal of neuroscience : the official journal of the Society for Neuroscience. 2003;23:9276-88.

[9] Windle WF, Clemente CD, Chambers WW. Inhibition of formation of a glial barrier as a means of permitting a peripheral nerve to grow into the brain. The Journal of comparative neurology. 1952;96:359-69.

[10] Liuzzi FJ, Lasek RJ. Astrocytes block axonal regeneration in mammals by activating the physiological stop pathway. Science. 1987;237:642-5.

[11] Jones LL, Margolis RU, Tuszynski MH. The chondroitin sulfate proteoglycans neurocan, brevican, phosphacan, and versican are differentially regulated following spinal cord injury. Exp Neurol. 2003;182:399-411.

[12] Bradbury EJ, Moon LD, Popat RJ, King VR, Bennett GS, Patel PN, et al. Chondroitinase ABC promotes functional recovery after spinal cord injury. Nature. 2002;416:636-40.

[13] Simonen M, Pedersen V, Weinmann O, Schnell L, Buss A, Ledermann B, et al. Systemic deletion of the myelin-associated outgrowth inhibitor Nogo-A improves regenerative and plastic responses after spinal cord injury. Neuron. 2003;38:201-11.

[14] Hausmann ON. Post-traumatic inflammation following spinal cord injury. Spinal Cord. 2003;41:369-78.

[15] Hellal F, Hurtado A, Ruschel J, Flynn KC, Laskowski CJ, Umlauf M, et al. Microtubule stabilization reduces scarring and causes axon regeneration after spinal cord injury. Science. 2011;331:928-31.

[16] Hurtado A, Cregg JM, Wang HB, Wendell DF, Oudega M, Gilbert RJ, et al. Robust CNS regeneration after complete spinal cord transection using aligned poly-L-lactic acid microfibers. Biomaterials. 2011;32:6068-79.

[17] Schildge S, Bohrer C, Beck K, Schachtrup C. Isolation and culture of mouse cortical astrocytes. J Vis Exp. 2013.

[18] Silver J, Miller JH. Regeneration beyond the glial scar. Nature reviews Neuroscience. 2004;5:146-56.

[19] Rolls A, Shechter R, London A, Segev Y, Jacob-Hirsch J, Amariglio N, et al. Two faces of chondroitin sulfate proteoglycan in spinal cord repair: a role in microglia/macrophage activation. PLoS Med. 2008;5:e171.

Chapter 5

The *In Vivo* Response to Paclitaxel Administration from Electrospun PLA Microfibers

5.1 Background

Although *in vitro* studies are necessary to further elucidate the processes and pathways present after a spinal cord injury is induced, this controlled environment does not accurately portray the entire injury and repair system present after an SCI. Most notably, the inflammatory response after an SCI is extremely complex and still not completely understood, which makes it hard to model *in vitro* [1]. In fact, multiple potential therapies for spinal cord injury applications showed promising results *in vitro*, but when tested *in vivo* saw limited functional recovery improvements [2, 3]. Consequently, *in vivo* animal models are necessary to advance therapeutic interventions to potential human clinical applications.

5.1.1 SCI Injury Models

Although ideally clinical testing in humans would be preferred to optimize therapeutic interventions, due to FDA safety and efficacy regulations animal models must be initially developed and used. For spinal cord injury animal models specifically, many animal models have been used from mice to non-human primates, but a majority of the studies in the past ten years (88%) have involved rodents [4]. Rats, specifically, are more advantageous to use in SCI models than mice due to their larger size (advantageous for

treatment implantation and observing behavioral recovery) and more similar scar formation to humans than mice [5].

In addition, there are multiple injury models of a spinal cord injury that are commonly used, such as contusion, compression, and transection models [6]. For a contusion injury, a transient or acute injury impacts the spinal cord. A contusion is a clinically-relevant model and can be induced through an impactor or weight-drop apparatus. Some of the primary issues with the contusion model are that there can be a large variability per injury and some of the impactors have issues with supporting the animal [6, 7].

Unlike a contusion injury, in a compression injury a device squeezes the spinal cord with a specific force for a more extended duration to induce an SCI [8]. Clinically this type of injury occurs due to a fracture dislocation in which a bone constantly impacts the spinal cord until it is removed. This injury model can be induced via clips, forceps, or even balloons and is advantageous in understanding the effect of a loss of blood flow while keeping the surrounding tissue intact. However, some of these models don't induce the acute injury commonly present in a spinal cord injury and have some issues with repetition as well [6].

In a transection spinal cord injury, the spinal cord is either partially or completely severed at a particular level by severing the tissue with a scalpel. Although this model does not represent the injuries most common after a spinal cord injury, they do present the opportune model to determine the axonal extension and tissue repair due to a therapeutic intervention [6, 9]. That being said, a complete transection injury model is much more severe to the animal and makes behavioral recovery hard to measure and

track. In a partial transection model (also referred to a hemisection in some cases), the behavioral improvements are easier to assess, but it can be more difficult to induce a consistent injury over time. One example of a partial transection injury is the dorsal column transection model in which a section of the dorsal column is surgically removed from the spinal cord, resulting primarily in loss of sensory function (severing of the ascending tracts and inadvertently some descending tracts as well) below the site of injury (Figure 5.1).

Even though each injury system has its advantages and disadvantages, the partial transection system is ideal for an initial assessment of biomaterials efficacy due to its similarities to clinically induced injuries, ease of determining novel axonal growth and extension at the injury site, and ability to monitor animal behavioral or functional recovery.

5.2 Methods

5.2.1 Conduit Assembly

Aligned PLA fibers were produced as mentioned previously onto a PLA film-covered 20-µm x 20-µm coverslip. Two sheets of these fibers were then peeled from the coverslips and placed back-to-back and rolled into conduits (Figure 5.1). By folding the conduit in an S-shape, a middle insert was created within the conduit lumen to increase the surface area for cell-substrate interactions and to decrease the probability of tube collapse. Prior to usage in animal models, samples were sterilized using an ethylene oxide sterilizer for a 12-hour cycle.

5.2.2 Dorsal Column Transection Spinal Cord Injury Model

Animals

Ten-week old Female Sprague-Dawley rats (strain 400, 180-200 g, Charles River) were housed according to NIH and USDA guidelines within the double-barrier facility of the Miami Project to Cure Paralysis.

Pre-Surgery Preparation

Before surgery, rats were anesthetized with an intraperitoneal injection of Ketaset® (ketamine, 75 mg/kg, i.p.) and Dexdomitor® (dexmedetomidine, 0.5 mg/kg, i.p.) which is consistent with recommendations of the Panel on Euthanasia of the American Veterinary Medical Association [10, 11]. An adequate level of anesthesia was determined by monitoring the absence of corneal reflexes and hindlimb withdrawal to an otherwise painful stimulus. Then, the back of the rats was shaved and aseptically prepared using Betadine. Lacri-Lube ointment was applied to the eyes to prevent drying while under anesthesia. Rats were kept on a regulatable heating pad set at 37 ± 0.5ºC during surgical procedures to maintain their body temperature constant.

Injury Paradigm

From anaesthetized rats, the back over the mid/low thoracic (T) level of the spinal column was incised, the back muscles retracted to expose the spinal column, and the dorsal aspect of the T8 vertebra was removed without damaging the dura mater to expose the underlying T9 spinal cord [10, 11]. Next, with surgical microscissors, the dura was opened without damaging the exposed spinal cord and a longitudinal rectangular shaped

gap (2 mm long and 1 mm wide) was created in the dorsal column [12, 13]. If needed, gelfoam was gently applied to stop bleedings within the lesion gap. After bleeding had stopped, the lesion gap was dried and the material (either PLA fiber bundle or PLA fiber scaffold) implanted. The material was kept in saline during the surgical procedures and cut in the appropriate length to cross the lesion gap and oppose the rostral and caudal spinal cord. Then, the exposed area was rinsed with 0.1 % gentamicin in PBS (0.1 M, pH 7.4), the back muscles were closed in layers with 4.0 Ethicon sutures, and the skin was closed with metal wound clips.

Pilot Study

For the short-term pilot study, rats (n = 18) were randomly divided into 4 groups and implanted with gel foam (n = 3), aligned PLA fibers (n = 5), a low concentration paclitaxel-loaded PLA fibers (0.02% PTX, n = 5), or a high concentration of paclitaxel-loaded PLA fibers (0.25% PTX, n = 5). The rats were then euthanized 2 weeks after this surgery.

Long-Term Study

Two experimental groups (n = 60) received PLA microfiber bundles (that were prepared as described previously) with or without (control) PTX. Each of the two groups consisted of 15 rats that were used for anatomical assessments only (survival 2, 4, and 8 weeks, n = 5/group) and 15 rats that were used for functional assessments at 2, 4, 6, and 8 (n = 5/group) weeks.

Post-Surgery

Rats receive Antisedan® (1 mg/kg; intramuscular) to reverse the anesthesia and lactated Ringers' solution (10 ml, subcutaneous) to replenish electrolytes/fluids [10, 11, 14]. Rats were kept in an incubator at 37°C and monitored continuously until awake before they were returned to their cages. To prevent possible infections rats were treated subcutaneously with gentamicin (6 mg/kg body weight) daily during the first week post-surgery [10, 11, 14]. Rats received buprenorphine (0.03 mg/kg body weight; Sigma) subcutaneously twice a day (every 12 h) for 3 days post-injury/implantation [10, 11]. The general health of the rats was evaluated by direct observations by professional caretakers twice daily during the first week and once daily thereafter. Rats were kept clean on a daily basis if needed and monitored for urine scalding. If necessary they were treated with anti-scalding ointment. Water and food were available *ad libitum* throughout survival. The bladder was manually emptied manually twice a day until no longer needed. The metal skin wound clips were removed after 7 days. If pain or distress occurred during survival, we treated the rats subcutaneously with buprenorphine (0.03 mg/kg body weight; Sigma).

5.2.3 Behavioral Response and Observation

Rats were tested for changes in hind limb motor/sensorimotor and sensory function for up to 8 weeks after lesion/implantation [10, 11]. With our lesion paradigm, rats perform the proposed functional tests without problems other than the inflicted impairment. For overground walking, we used the 21-point BBB open field locomotor test specifically designed to evaluate automated hind limb function after spinal cord

contusion [15, 16]. This test distinguishes between movements of individual joints of the hind limbs. Complete paralysis scores a '1' and normal walking scores a '21'. All rats that needed to perform the BBB test were in the open field and their performance scored twice a week for 2 weeks before being subjected to injury and implantation. This provided baseline values and allowed the rats to adapt to the testing environment. During survival, 2 examiners oblivious of the treatments were located at a constant position relevant to the open field and performed the tests over a period of 4 min weekly until termination of the experiment. For higher motor functions we used the BBB subscore [10, 11, 17]. In the predominant paw, weekly the position [internal/external at initial contact (IC) and liftoff (0 points), parallel at IC and internal/external at liftoff or vice versa (1), parallel at IC and liftoff (2)], toe clearance [none (0), occasional (1), frequent (2), consistent (3)], tail position [down (0), up (1)), and trunk stability (no (0), yes (1)] were determined. Scores are summed for a maximum score of 7.

Sensorimotor function was evaluated using the horizontal ladder-walking test [10, 11, 18]. Walking over the horizontal ladder requires integration of sensory and descending information to control proper (hind) paw placement and weight support. We tested the rats on the ladder at 2, 4, 6, and 8 weeks post-injury/implantation. A 100 cm long custom-made (horizontal) ladder was used which the rats walked across 3 times each test. Every passage was videotaped to enable accurate evaluation of the performances. Only the middle 60 cm of the ladder was used for measurements. Small (foot or part of foot), medium (foot and part of lower leg), and large (full leg) slips were counted and were expressed as a percentage of the total number of steps. The test was

performed before injury to determine normal baseline values, just before injury/implantation and at 4 and 6 weeks post-treatment.

Sensory function was assessed using mechanical allodynia (i.e., a pain-related response to a normally innocuous stimulus), which was measured at 3 and 6 post-injury/implantation by assessing the force to the hind paw resulting in limb withdrawal [19]. Rats were acclimated for 5 min before measurements in a Plexiglas test box with an elevated mesh floor. An electronic von Frey anesthesiometer was applied perpendicularly to the mid-plantar area of each hind paw and the pressure increased until limb withdrawal. The force (in g) at withdrawal was recorded. Three middle measurements out of five of each paw were averaged. Baseline values were determined before injury/implantation.

5.2.4 Tissue Processing

Rats were anaesthetized with Ketaset® (100 mg/kg, i.p.), injected with 0.5 mL heparin (heparin sodium, 1000 units/mL) in the heart, and perfused transcardially with 300 ml saline (room temperature) to rinse out the blood and 500 ml of 4 % paraformaldehyde in PBS (0.1M, pH 7.4) [10, 11]. This procedure fixes the spinal cord for harvesting and processing for histology. The spinal cord was dissected out and post-fixed in the same fixative overnight at 4ºC before being transferred to 30% sucrose in PBS (0.1M, pH 7.4) for at least 24 hours. Then, a 2 cm long segment of the spinal cord centered at the dorsal column lesion was cut on a cryostat in 10 series of 20 µm thick sagittal sections, which were mounted on positively charged microscope slides. For immunostaining, non-specific binding sites were blocked using 0.01M PBS (pH 7.4) with 5% Normal Goat Serum (NGS) and 0.03% Triton blocking solution at room temperature

for 1 hour. Sections were immunostained with antibodies against neurofilament to recognize axons, GFAP to recognize astrocytes, and NeuN to recognize neurons. All incubations with primary antibodies were overnight at 4ºC. Then, sections were rinsed, incubated at room temperature for 2 hours with secondary antibodies conjugated with fluorescent markers, rinsed, DAPI counterstained, and finally covering with a glass slip using anti-fade fluorescent mounting media (Dako, #S3023). One series of sections was stained with cresyl violet to identify neurons.

5.2.5 Quantification and Data Analysis

Tissue sample metrics were completed using the StereoInvestigator software (MicroBrightField Inc., Colchester, VT). For neurofilament, the counting frame was started at a randomized first section and then the inclusion criteria included a NF of minimum length of 5 μm, inclusion in the boundaries set by StereoInvestigator, and in order to minimize error due to irregular slicing NF location within 1 μm of the set z-axis. Outlining of the serial sections was conducted by a single investigator naïve to the treatment group. The total approximation by optical fractionator and the second coefficient of error were calculated as estimates and a value of 0.1 for the second coefficient of error was accepted. Using StereoInvestigator, relative fluorescence intensity and tissue volume were also calculated with tissue labeled with antibodies against GFAP or processed with the cresyl violet stain for Cavalieri tissue volume analyses, respectively.

5.3 Results

5.3.1 Microfiber Conduit Assembly

PLA microfiber conduits were assembled by wrapping two electrospun of PLA microfiber sheets (20 mm x 20 mm) into an S-shaped conduit (Figure 5.2) similar to previous methods by *Hurtado et al.* [20]. This conduit was approximately 1.7 mm in diameter and ranged in length based on the size of the injury for implantation (1-2 mm). Previous studies have show that the formation of the conduit did not affect fiber alignment and provided an adequate platform to promote spinal cord tissue repair after an SCI [20].

5.3.2 Pilot Study (Conduit)

Shortly after production, PLA S-shaped conduits with increasing concentrations of paclitaxel (0, 0.02, 0.25%, or 3.26%) were disinfected by ethylene oxide sterilization and implanted into a dorsal column transection spinal cord injury. Two weeks after implantation, the animals were euthanized, tissue fixed, and samples labeled for astrocyte markers and neuronal markers.

After an SCI occurs, a large, complex inflammatory response is induced that prevents axonal and blood vessel infiltration into the site of injury [1]. Two weeks after implantation of paclitaxel-loaded fibers, tissue cavitation and sparing was quantified by staining the samples with the cresyl violet stain and processing them with the Cavalieri method of segmentation with point-counting from spinal cord cross-sections in StereoInvestigator. By quantifying the tissue present around the injury, we determined

that a local release of paclitaxel did not promote or exacerbate tissue cavitation after an SCI (Figure 5.3).

In a second set of serial sections, immunohistochemistry analysis with an antibody against glial fibrillary acidic protein (GFAP) was conducted. Figure 5.4 shows some representative micrographs depicting a cross-section of rat spinal cord at the epicenter of the lesion stained for GFAP (Figure 5.4A and B). Quantification of GFAP-reactivity with relative fluorescence intensity showed that the administration of a local release of paclitaxel from aligned PLA fibers significantly inhibited reactive gliosis starting two weeks after conduit implantation (Figure 5.4C).

Once we determined that reactive gliosis was attenuated, we wanted to determine the effect of a local release of paclitaxel on neurite extension into the conduit. Cross-sections of the conduit in the epicenter of the lesion were removed and fluorescently labeled against the Neurofilament (NF) antibody (Figure 5.5A and B). The number of axons within each conduit was determined by counting the number of axons within the section. By completing this quantification, we determined that a local release of paclitaxel does not have a direct effect on axonal extension under these conditions (Figure 5.5C).

5.3.3 Long-Term Study (Bundles)

After determining that administering a local release of paclitaxel from aligned PLA microfibers promote spinal cord tissue repair, PLA fiber bundles were produced as previously mentioned with a diameter of approximately 1 mm – twisting the fiber bundles tighter or looser to modify the diameter – and length based on the size of the

injury (0.5-1 mm). Shortly after production, these bundles were then implanted for six weeks in animals that received a dorsal column transection. After six weeks *in* situ, these bundles were successfully implanted in the injury site, integrated with the host tissue, and modestly aligned with the direction of the spinal cord as well (Figure 5.6).

Six weeks after injury and implantation of gel foam, PLA microfiber bundles only, or PLA microfiber bundles loaded with 0.25% PTX, locomotor and sensory behavioral analysis was conducted. To determine locomotor recovery, the BBB test was performed and quantified six weeks after injury (Figure 5.7A). As shown in Figure 5.7B, a local release of paclitaxel did not improve locomotor function than PLA fibers alone.

Additionally, after a spinal cord injury occurs, sensory deprivation and an increase in pain sensation occur at targets below the site of injury. In order to quantify this *in vivo*, mechanical allodynia was evaluated using an electronic von Frey anesthesiometer – Figure 5.8A shows the mechanical von Frey filaments. No decrease in mechanical threshold was observed between the groups with or without paclitaxel-loaded fiber bundles suggesting no allodynia was induced (Figure 5.8B).

5.4 Discussion

Even though the original S-shaped conduit design showed preliminary promise in spinal cord injury tissue repair, the diameter of the conduit was not ideal for the injury model used. For a rat dorsal column injury, the diameter of the injury can range from 0.5–1 mm, whereas the smallest diameter capable of being produced in this conduit is approximately 1.5 mm– in our case it was approximately 1.7 mm. Previous research using this material conduit involved a complete transection injury, which required a

conduit with a much larger diameter (1.5 mm–3 mm). Therefore, a smaller diameter conduit design was necessary to continue using the dorsal column transection model for spinal cord injury. Although axonal extension into the scaffold remained the same for all paclitaxel-loading levels, this could be attributed to not enough time for the neurons to extend into the middle of the scaffold or insufficient adherence of the neurons to the fibers, which would prevent the previous effect seen *in vitro* that a local release of paclitaxel is necessary to promote neurite extension from occurring. For the pilot study, no control group of PLA fibers only was used solely to determine which paclitaxel loading level should be used in subsequent long-term studies. From the promising results seen in the pilot study with regards to the effects of a local release of paclitaxel decreasing reactive gliosis and not inhibiting axonal extension, the middle concentration loading of paclitaxel (0.25%) was chosen for subsequent long-term *in vivo* studies.

Following a spinal cord injury, a loss of motor function and sensory sensation occurs below the site of injury. After a six-week implantation of PLA microfiber bundles loaded without or with 0.25% paclitaxel, behavioral recovery and pain stimulation were monitored and quantified. Due to the complexity and long-term recovery after a spinal cord injury, these functions were monitored under the longer durations and varying conditions of this study. Although no locomotor recovery was observed after six weeks of implantation, further analysis of axonal extension into the fibers and a longer duration of implantation (8+ weeks) may be necessary to further determine the effects of this treatment on spinal cord tissue repair. Although no locomotor recovery was observed, limited locomotor was expected due to the severity and location of the injury in the dorsal column of the rat spinal cord.

Furthermore, paclitaxel administration has been shown to induce peripheral neuropathic pain [21]. Because axonal sprouting has been shown to induce neuropathic pain and paclitaxel modulates neuronal sprouting, an effect of a paclitaxel administration on pain induction in a rat model of spinal cord injury was quantified [22, 23]. Specifically, mechanical allodynia was quantified six weeks after injury. After this duration it was determined that a local release of paclitaxel did not induce allodynia compared to the control group of just PLA microfibers alone.

5.5 Conclusions

In these studies, we successfully produced two varieties of growth-promoting scaffolds for spinal cord injury repair, an S-shaped conduit and a PLA fiber bundle that were then implanted into a dorsal column transection injury for 2 or 6 weeks, respectively. The paclitaxel-loaded S-shaped conduit provided an opportune platform to maintain tissue sparing, inhibit reactive gliosis, and support axonal extension. Furthermore, the PLA fiber bundle loaded with paclitaxel had a limited effect on locomotor recovery, but did not induce neuropathic pain.

5.6 Figures

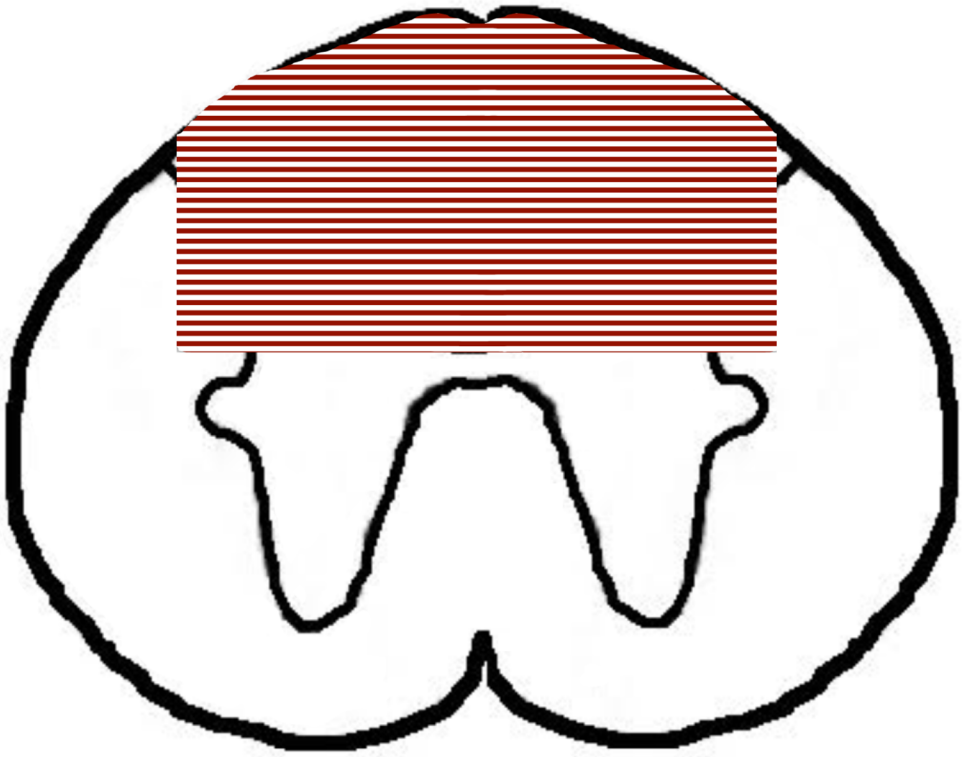

Figure 5-1: Dorsal column transection model injury

The dorsal column transection injury primarily involves slicing or removing an approximately 1-millimeter section of the dorsal column of the spinal cord.

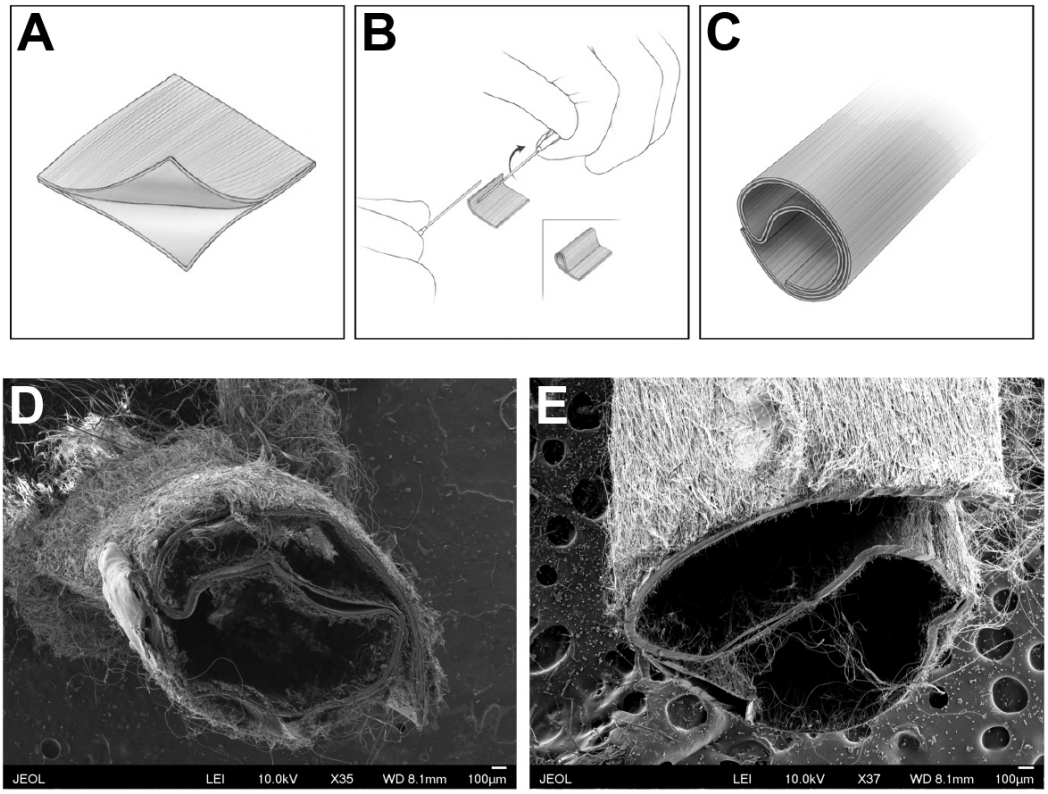

Figure 5-2: PLA microfiber scaffold and preparation

Electrospun PLA microfiber conduits were successfully constructed and assembled. A fiber square (20 mm x 20 mm) mesh (A) was wrapped (B) and glued together with a PLA solution to form an S-shaped conduit (C). Fiber conduits of approximately 1.7 mm diameters were developed and coated with an exterior random fiber mesh (D, E). Scale bar: 100 µm.

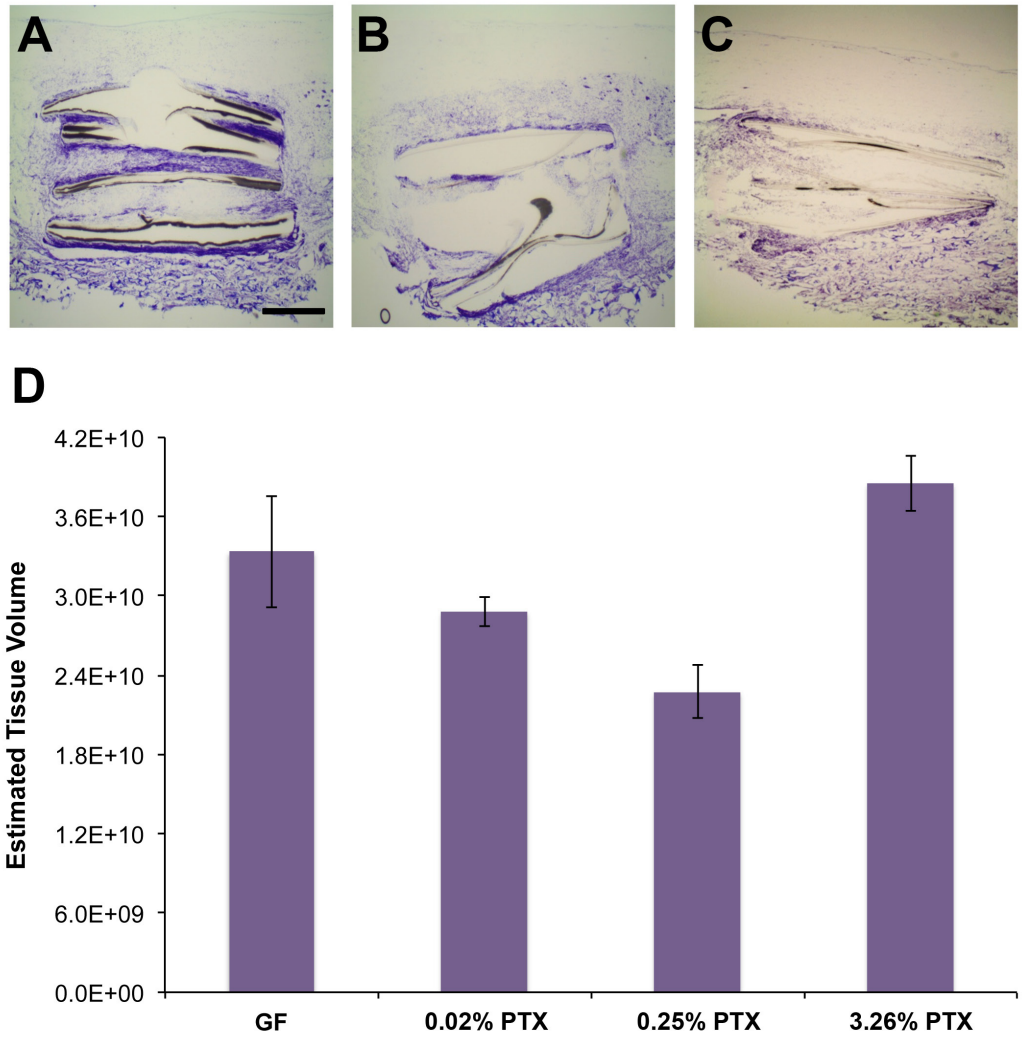

Figure 5-3: Pilot study – Tissue sparing

Local release of paclitaxel does not promote tissue cavitation. Rats were given a dorsal column transection injury and implanted with either gel foam or PLA fibers loaded with 0.02% (A), 0.25% (B), or 3.26% (C) paclitaxel. Spinal cord cross-sections were fixed and labeled with a cresyl violet stain. After two weeks of implantation, no significant difference was observed in tissue sparing when the paclitaxel-loaded fibers were implanted after an SCI. Scale bar: 1 mm. (n = 3 – 5).

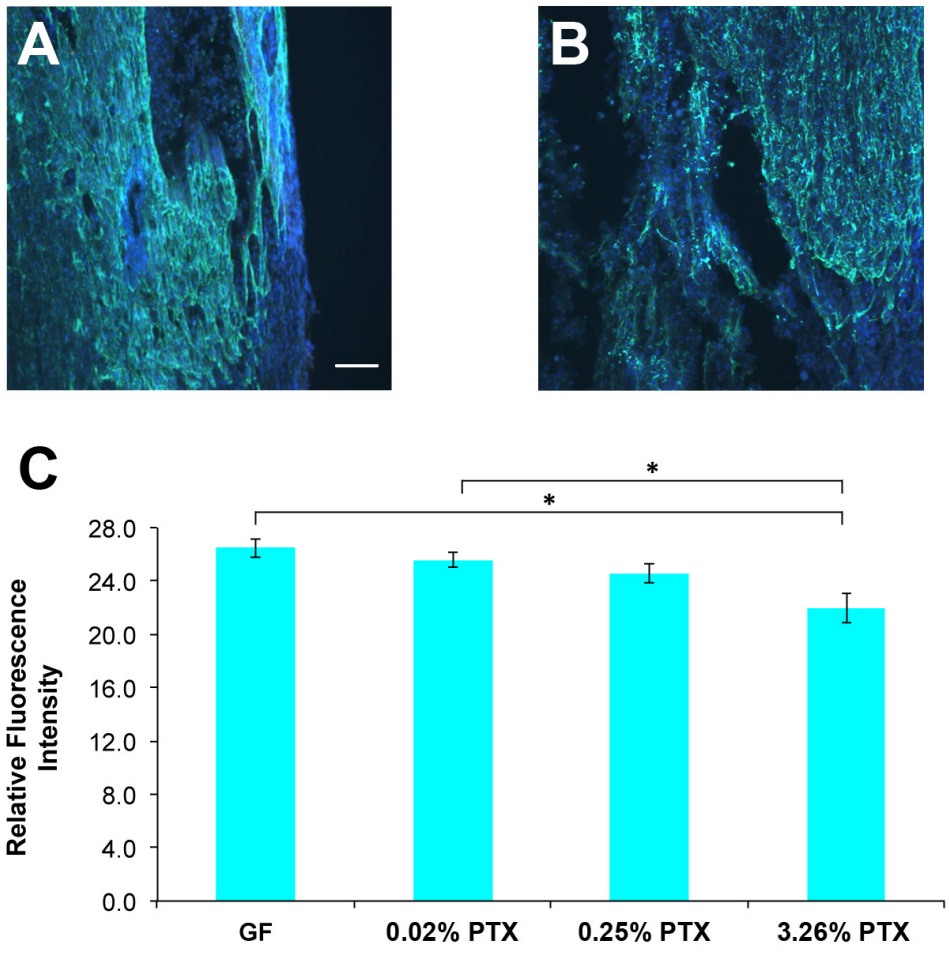

Figure 5-4: Pilot study – Glial response

Local release of paclitaxel inhibits reactive gliosis. Rats were given a dorsal column transection injury and implanted with either gel foam (A) or PLA fibers loaded with 0.02%, 0.25%, or 3.26% (B) paclitaxel. Spinal cord cross-sections were fixed and fluorescently labeled for astrocytes with a GFAP antibody. After two weeks of implantation, a local release of paclitaxel from aligned PLA microfibers promoted a concentration-dependent decrease in reactive gliosis production (C). Scale bar: 500 µm. ($p < 0.05$, n = 3 – 5).

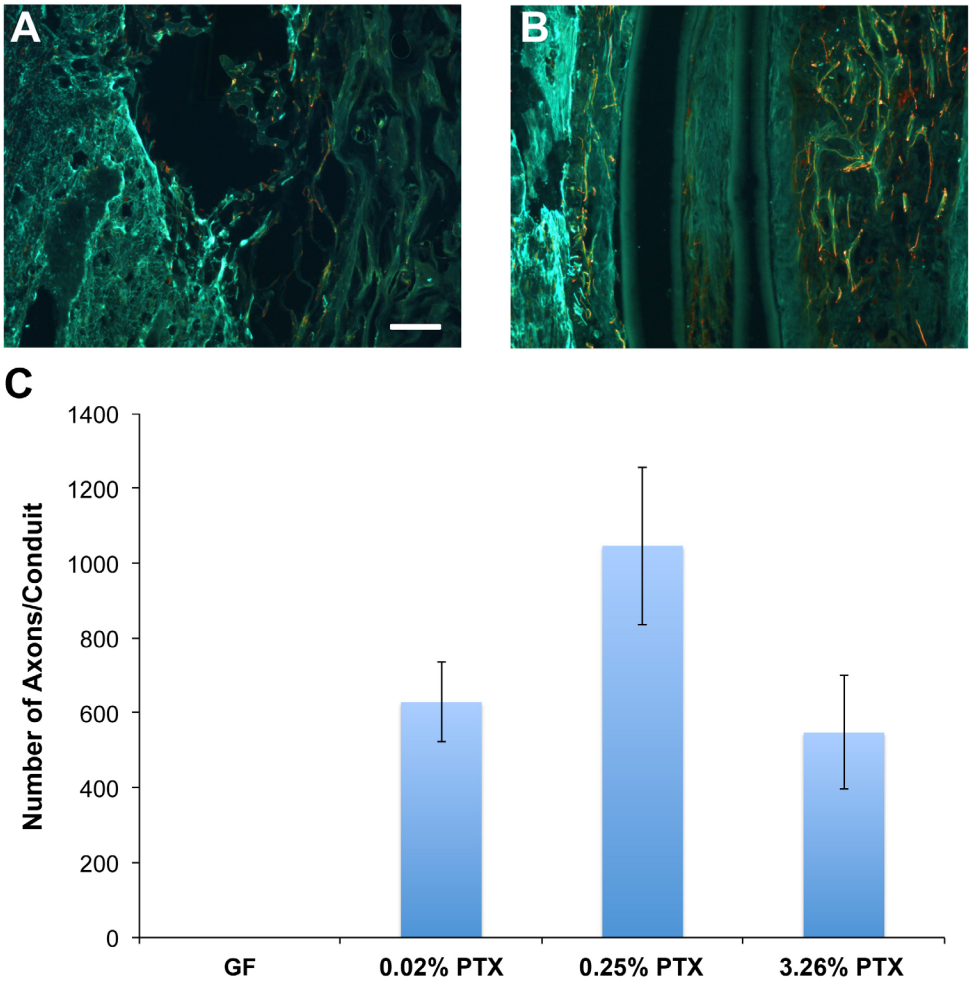

Figure 5-5: Pilot study – Axonal extension

Local release of paclitaxel does not affect axonal extension. Rats were given a dorsal column transection injury and implanted with either gel foam (A) or PLA fibers loaded with 0.02%, 0.25%, or 3.26% (B) paclitaxel. Spinal cord cross-sections were fixed and fluorescently labeled for neurons with a neurofilament antibody. After two weeks of implantation, a local release of paclitaxel from aligned PLA microfibers had no effect on axonal extension (C). Scale bar: 500 µm. (n = 3 – 5).

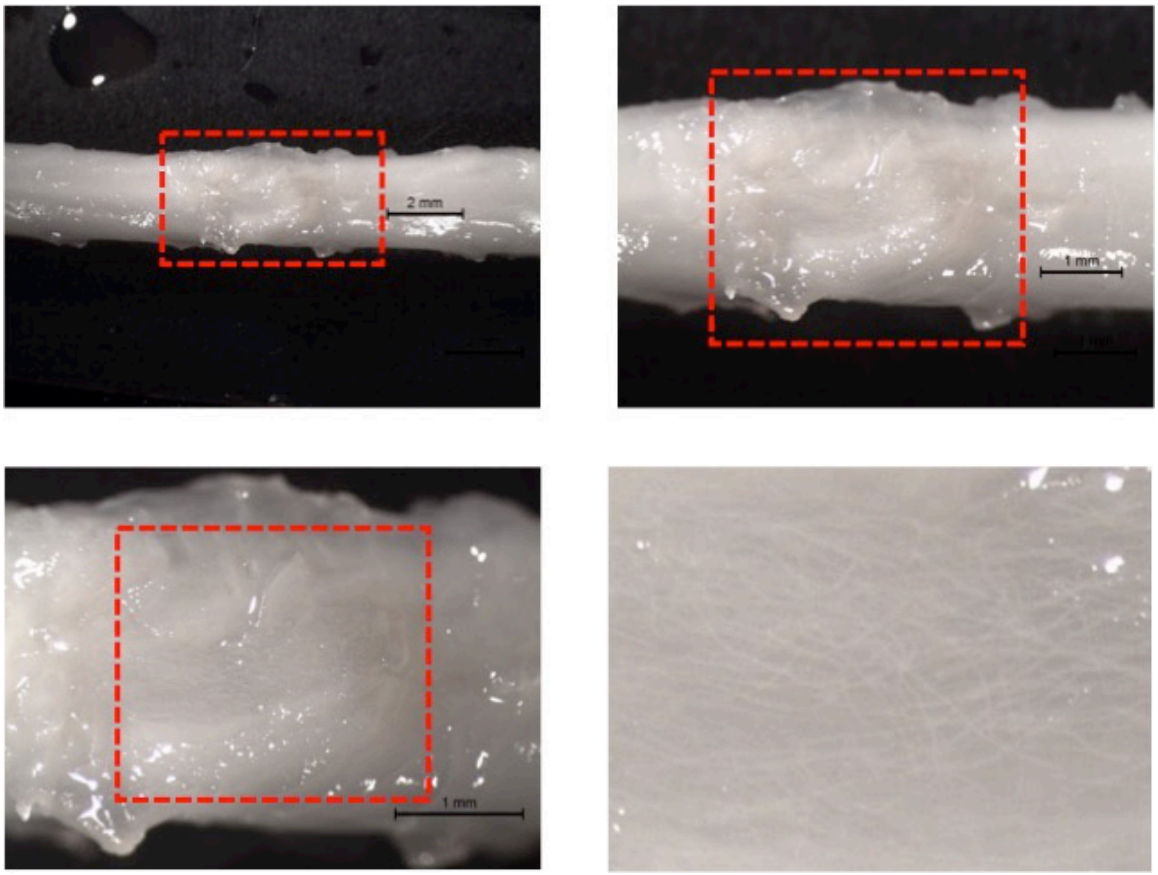

Figure 5-6: Long-term study – Fiber incorporation 6 wpi

Fibers incorporate with spinal cord tissue. Rats were given a dorsal column transection injury and implanted with PLA bundles loaded with or without paclitaxel. Implanted fibers successfully integrated with native tissue and moderately maintained their alignment 6 weeks after implantation (wpi).

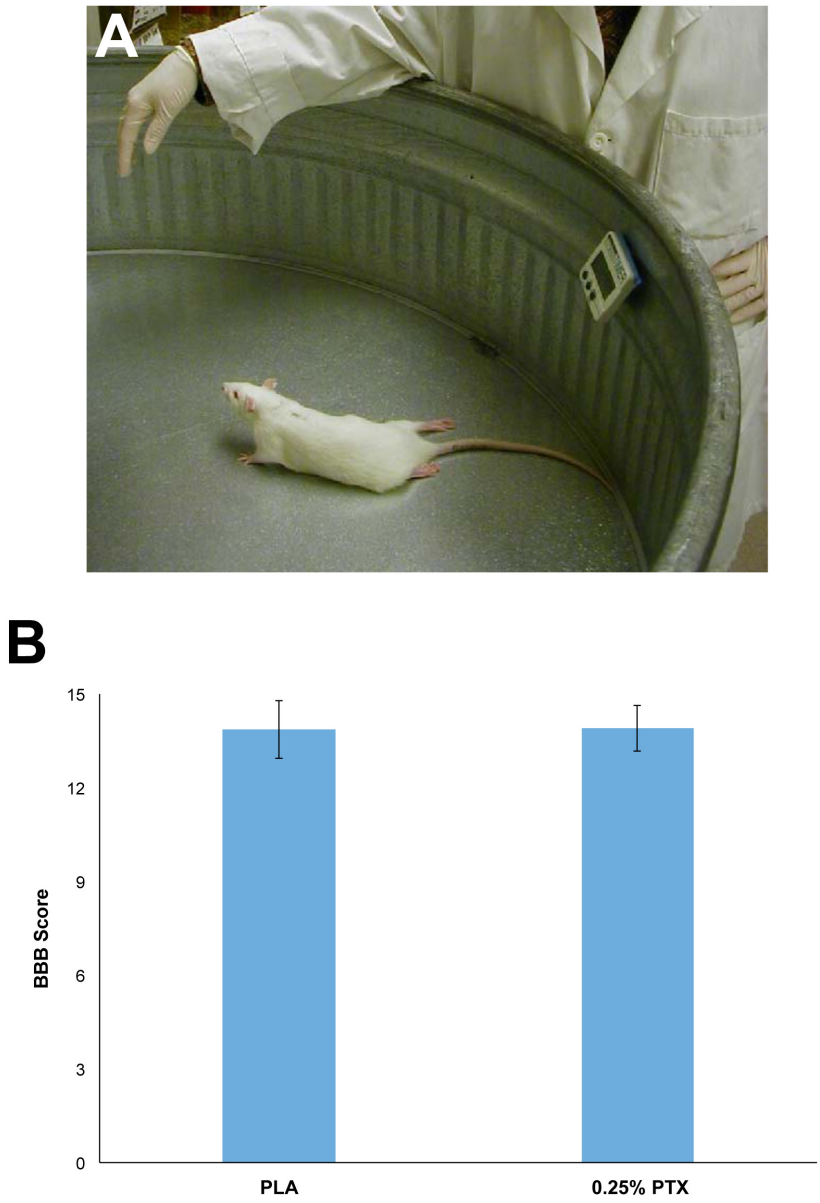

Figure 5-7: Long-term study – Locomotor recovery

Local release of paclitaxel from aligned PLA fibers does not effect locomotor recovery. Hind limb locomotor function was evaluated in the open field and scored using the BBB test (A). Post-SCI evaluation was quantified 6 weeks post-injury. There was no difference in locomotor recovery in animals receiving a local release of paclitaxel than animals with only the PLA microfiber bundles (B). (n = 14 – 15).

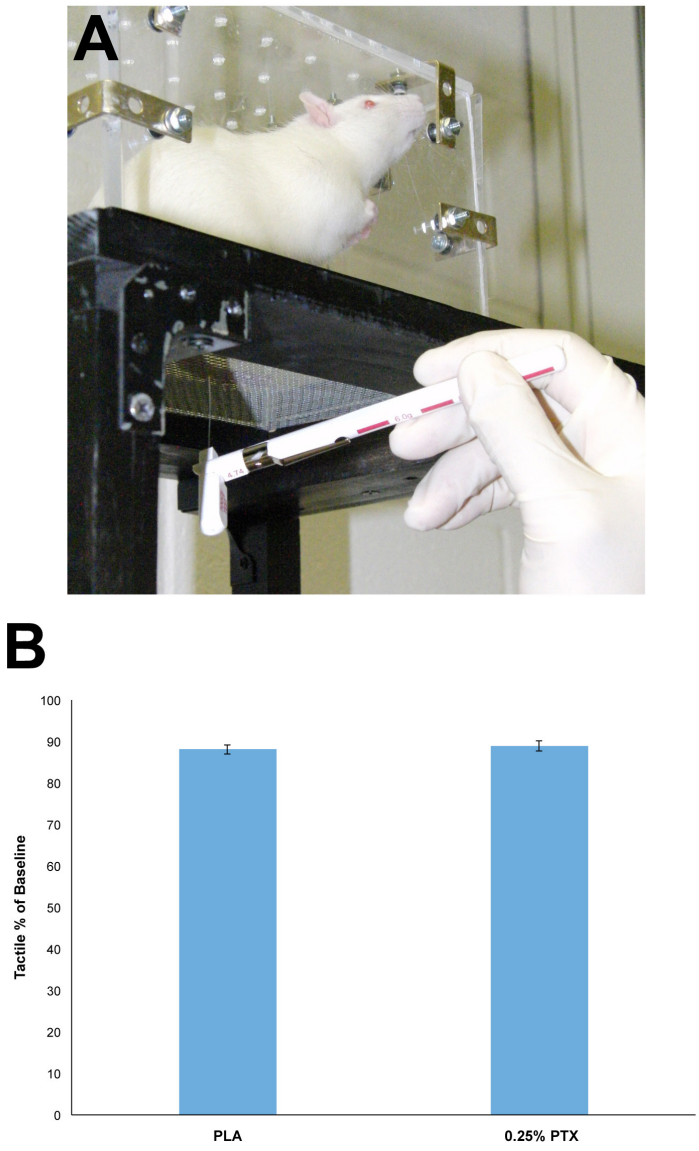

Figure 5-8: Long-term study – Sensory response

Local release of paclitaxel from aligned PLA fibers does not induce mechanical allodynia. A non-noxious light touch of the plantar surface of the paw with von Frey filaments was used to assess hind limb sensation and mechanical allodynia (A). The withdrawal threshold in response to mechanical stimulation was quantified. Post-SCI evaluation was quantified 6 weeks post-injury. A local release of paclitaxel did not exacerbate the mechanical allodynia present from the PLA microfiber bundles alone (B). (n = 14 – 15).

5.7 References

[1] Hausmann ON. Post-traumatic inflammation following spinal cord injury. Spinal Cord. 2003;41:369-78.

[2] Tysseling-Mattiace VM, Sahni V, Niece KL, Birch D, Czeisler C, Fehlings MG, et al. Self-assembling nanofibers inhibit glial scar formation and promote axon elongation after spinal cord injury. The Journal of neuroscience : the official journal of the Society for Neuroscience. 2008;28:3814-23.

[3] Roman JA, Niedzielko TL, Haddon RC, Parpura V, Floyd CL. Single-walled carbon nanotubes chemically functionalized with polyethylene glycol promote tissue repair in a rat model of spinal cord injury. Journal of neurotrauma. 2011;28:2349-62.

[4] Zhang N, Fang M, Chen H, Gou F, Ding M. Evaluation of spinal cord injury animal models. Neural Regen Res. 2014;9:2008-12.

[5] Onifer SM, Rabchevsky AG, Scheff SW. Rat models of traumatic spinal cord injury to assess motor recovery. ILAR J. 2007;48:385-95.

[6] Cheriyan T, Ryan DJ, Weinreb JH, Cheriyan J, Paul JC, Lafage V, et al. Spinal cord injury models: a review. Spinal Cord. 2014;52:588-95.

[7] Krishna V, Andrews H, Jin X, Yu J, Varma A, Wen X, et al. A contusion model of severe spinal cord injury in rats. J Vis Exp. 2013.

[8] Rivlin AS, Tator CH. Effect of duration of acute spinal cord compression in a new acute cord injury model in the rat. Surg Neurol. 1978;10:38-43.

[9] Bradbury EJ, Moon LD, Popat RJ, King VR, Bennett GS, Patel PN, et al. Chondroitinase ABC promotes functional recovery after spinal cord injury. Nature. 2002;416:636-40.

[10] Ritfeld GJ, Nandoe Tewarie RD, Vajn K, Rahiem ST, Hurtado A, Wendell DF, et al. Bone marrow stromal cell-mediated tissue sparing enhances functional repair after spinal cord contusion in adult rats. Cell Transplant. 2012;21:1561-75.

[11] Ritfeld GJ, Rauck BM, Novosat TL, Park D, Patel P, Roos RA, et al. The effect of a polyurethane-based reverse thermal gel on bone marrow stromal cell transplant survival and spinal cord repair. Biomaterials. 2014;35:1924-31.

[12] Oudega M, Varon S, Hagg T. Regeneration of adult rat sensory axons into intraspinal nerve grafts: promoting effects of conditioning lesion and graft predegeneration. Exp Neurol. 1994;129:194-206.

[13] Oudega M, Hagg T. Nerve growth factor promotes regeneration of sensory axons into adult rat spinal cord. Exp Neurol. 1996;140:218-29.

[14] Nandoe Tewarie RD, Hurtado A, Levi AD, Grotenhuis JA, Oudega M. Bone marrow stromal cells for repair of the spinal cord: towards clinical application. Cell Transplant. 2006;15:563-77.

[15] Basso DM, Beattie MS, Bresnahan JC. A sensitive and reliable locomotor rating scale for open field testing in rats. Journal of neurotrauma. 1995;12:1-21.

[16] Basso DM, Beattie MS, Bresnahan JC. Graded histological and locomotor outcomes after spinal cord contusion using the NYU weight-drop device versus transection. Exp Neurol. 1996;139:244-56.

[17] Lankhorst AJRV, M.; Hamers, F.P.T. Experimental spinal cord contusion injury: Comparison of different outcome parameters. Neuroscience Research Communications. 1999;24:135-48.

[18] Kunkel-Bagden E, Dai HN, Bregman BS. Recovery of function after spinal cord hemisection in newborn and adult rats: differential effects on reflex and locomotor function. Exp Neurol. 1992;116:40-51.

[19] Chaplan SR, Bach FW, Pogrel JW, Chung JM, Yaksh TL. Quantitative assessment of tactile allodynia in the rat paw. J Neurosci Methods. 1994;53:55-63.

[20] Hurtado A, Cregg JM, Wang HB, Wendell DF, Oudega M, Gilbert RJ, et al. Robust CNS regeneration after complete spinal cord transection using aligned poly-L-lactic acid microfibers. Biomaterials. 2011;32:6068-79.

[21] Scripture CD, Figg WD, Sparreboom A. Peripheral neuropathy induced by paclitaxel: recent insights and future perspectives. Curr Neuropharmacol. 2006;4:165-72.

[22] Woolf CJ, Mannion RJ. Neuropathic pain: aetiology, symptoms, mechanisms, and management. Lancet. 1999;353:1959-64.

[23] Chuckowree JA, Vickers JC. Cytoskeletal and morphological alterations underlying axonal sprouting after localized transection of cortical neuron axons in vitro. The Journal of neuroscience : the official journal of the Society for Neuroscience. 2003;23:3715-25.

Chapter 6

Discussion and Conclusions

6.1 Novelty and Significance

Throughout this study, we have demonstrated that microtubule-stabilizing agents (such as paclitaxel) can be successfully incorporated into electrospun PLA microfibers. Furthermore, this incorporation method releases these molecules constantly over a 12-week period, promotes axonal extension *in vitro*, and inhibits reactive gliosis *in vivo*.

Although our study is not the first to incorporate paclitaxel in electrospun fibers, it is the first to use this platform to be developed for spinal cord tissue repair. In this system, we controlled the continuous release of paclitaxel for up to 4 weeks longer than previous studies have already shown [1]. In animal studies, this delivery mechanism does not induce neuropathic pain, which could be a concern with paclitaxel delivery. Interestingly, this study is not only the first to incorporate sunitinib in electrospun fibers, but also discovered that sunitinib has an effect on neuronal extension.

6.2 Implications

There are currently no FDA-approved treatments to promote spinal cord tissue repair after a traumatic SCI. This study advanced the understanding of how a local drug delivery system coupled with an aligned contact guidance can affect axonal growth and ultimately spinal cord tissue repair. One main advantage of this system is that it is not limited to one drug or treatment, which broadens its possible treatment indications

outside of traumatic nerve regeneration alone. Other aligned tissue engineering applications, such as muscle regeneration, could also benefit from this study's findings.

In order to establish this system, we first wanted to determine if the release of paclitaxel from electrospun microfibers could be modified and controlled. To do this, we varied the amount of paclitaxel that we loaded into the PLA polymer solution and measured paclitaxel release from these fibers over 12 weeks and found that due to the slow diffusion of paclitaxel from these microfibers, larger incorporations of paclitaxel in the fibers promoted a faster and larger release. This timeline is ideal for spinal cord tissue therapeutic applications due to the scar formation occurring within the first few weeks/months after the injury occurs [2]. In addition, modifying the fiber density can also modify the amount of released paclitaxel as well as provide a more uniform growth conduit for axons to grow on as well. These findings are necessary to modify this platform for future animal models of SCI and translational applications.

Previous approaches of paclitaxel administration for anti-cancer treatments have involved osmotic mini-pumps, hydrogels, and nanoparticles [3-5], which can be difficult to administer for a long duration in humans. However, electrospun microfibers provide a unique platform for spinal cord injury applications due to their lack of necessity to incorporate paclitaxel in a neuropathic solvent, directed growth-permissive scaffold to promote axonal extension across the injury site, biodegradable platform, and long-term treatment release. A low concentration administration of paclitaxel has previously been shown to promote neurite extension [3, 6]. By incorporating paclitaxel into aligned microfibers, neurons receive a controlled, low concentration dosage of paclitaxel that, when coupled with a growth-permissive scaffold, promoted axonal extension by

stabilizing microtubule formation. Furthermore, other therapeutic applications that require a localized treatment delivery, such as anticancer or antibiotic delivery, could leverage the advantages of this platform to maximize potency and limit the adverse effects [1, 7].

6.3 Limitations

6.3.1 Translation

One of the most pertinent issues of this novel platform with regards to translatability is that incorporating paclitaxel in aligned fibers for spinal cord injury applications can no longer be patented. Due to this issue, it is very unlikely that a pharmaceutical company will be willing to invest the time and money to scale this platform for patient usage. That being said, other novel microtubule-stabilizing therapeutics such as sunitinib and epothilone B [8] could instead be incorporated.

As another consideration for translation, this platform will require a surgical intervention for implantation –likely days-weeks after the initial injury to assess and characterize the injury severity. This platform has only been tested in an acute injury and will need to be further tested to determine its effects on a chronic (months-years after the initial injury) spinal cord injury, which make up greater than 90% of current patients with a spinal cord injury.

Finally, the injury paradigm tested requires a spinal cord injury that severs or removes a large portion of the spinal cord to be effective, whereas in most real-world SCIs a contusion is more prevalent [9]. Therefore, this platform will need to be adapted for these systems, which it can easily be modified by simply placing a sheet of the

paclitaxel-loaded fibers on top of the spinal cord rather than implanting them directly into the spinal cord similar to previous treatment applications [10].

6.3.2 Material

One of the biggest concerns of using PLA for medical applications is the toxicity of its degradation byproducts [11]. Due to previous *in vivo* testing with PLA products, we do not believe that this platform should develop a high enough concentration of PLA to produce a toxic environment for spinal cord tissue repair, but subsequent testing will monitor these degradation products to prevent this from becoming an issue.

As previously mentioned a surgical intervention would be necessary to introduce this platform, which could expose the patient to unnecessary infections and complications. Therefore, this system would need to be adapted to mitigate these issues, potentially by incorporating the paclitaxel in self-assembling PLA block copolymers [12] that could then be injected into the injury site rather than implanted.

As an additional consideration, NatureWorks LLC has recently determined that their commercially available polylactic acid can no longer be used in medical device testing due to safety concerns. Therefore, a new supply of FDA-approved PLA would need to eventually be sourced for future safety and efficacy testing applications.

Under *in vitro* conditions, paclitaxel release was quantified through a diffusion-based system. However, in the *in vivo* studies, this release was not quantified. Due to the complex biological response that occurs after a spinal cord injury, the paclitaxel may not have released at the same rate as previously determined, which could explain some of the

limited results observed. The remaining paclitaxel in the fibers, and in turn the concentration of paclitaxel released, could be quantified in future tests similar to the UV-Vis Spectroscopy methods mentioned previously.

6.3.3 Cellular

Although we preliminarily looked at the mechanism driving axonal extension in this system, with nocodazole administration, more than likely there are multiple pathways acting on microtubule formation in this system. For instance, paclitaxel, like most other lipophilic drugs, is uptaken by cells through a passive diffusion process via transcellular transport across the cellular membrane. Because of the potency effect that we observed from a local paclitaxel administration on axonal extension, we hypothesize that different uptake mechanisms could be driving this system. For instance, paclitaxel may not fully incorporate in the media and instead be directly uptaken by the cell, which would require a smaller, local concentration to be effective. Considering the strong synergistic effect seen in this system from the local release of paclitaxel and the aligned fibers, there is probably a convergence of multiple pathways that drives the axonal extension that future studies would need to further elucidate.

Despite the fact that neuronal survival assays were conducted *in vitro*, limited axonal extension occurred *in vivo*. Future studies will further clarify whether apoptosis is also being affected in this *in vitro* assay and if any of this could explain the limited axonal extension into the conduit two weeks after implantation. One of the most likely reasons is that there was not enough time for the axons to grow into the center of the conduit. Another reason could be what is known as the “candy store effect” in which an

ideal environment (the scaffold itself) does not incentivize the axons to leave and reinnervate with other target, downstream axons. Introducing a paclitaxel concentration gradient in subsequent studies could help alleviate these issues.

6.4 Future Directions

Recent tissue engineering applications have utilized the necessity of cellular incorporations, especially pluripotent stem cells, with materials to better simulate a 3-dimensional environment as well as better promote autologous tissue regeneration after implantation [13]. That being said, this system will need to undergo a long regulatory process once cells are incorporated, especially considering that stem cell differentiation has not been fully optimized.

There have been a large amount of therapies and materials used for spinal cord tissue regeneration applications [10, 14, 15], but most have had limited functional improvements after administration. Some of the most promising in the past have involved combinational therapeutics that target multiple inhibitory components of a spinal cord injury to promote axonal regeneration [16]. As previously mentioned, self-assembling molecules other than PLA could also be used to incorporate and deliver paclitaxel for spinal cord injury applications to prevent the need for a surgery and potential for additional complications [17].

Incorporating drugs that block other inhibitory substrates present at the site of injury, such as NEP1-40 for myelin fragments, with paclitaxel in the fibers could further promote autologous cellular regeneration and ultimately spinal cord tissue repair. As more pathways associated with axonal growth continue to be discovered, new therapeutic

applications, such as inhibiting the phosphatase and tensin homolog (PTEN) pathway, could be also be targeted [18].

6.5 Conclusions

These studies have established the necessity of a local release of a therapeutic molecule that must be delivered within a narrow concentration range to prevent adverse effects while also promoting tissue regeneration. Furthermore, these therapeutic molecules can be incorporated into electrospun PLA microfibers and released at a controlled rate over an extended period of time (12 weeks+). Most important for spinal cord tissue repair, this system effectively promoted neurite extension while also inhibiting astrocyte function in an *in vitro* and *in vivo* model of SCI. Even after a long-term administration of paclitaxel *in vivo*, neuropathic pain is not stimulated. Most importantly, this system provides a platform that could promote tissue engineering among multiple systems (e.g. muscle regeneration) throughout the body and has implications in the development and production of other controlled drug delivery systems as well.

6.6 References

[1] Xie J, Wang CH. Electrospun micro- and nanofibers for sustained delivery of paclitaxel to treat C6 glioma in vitro. Pharm Res. 2006;23:1817-26.

[2] Silver J, Miller JH. Regeneration beyond the glial scar. Nature reviews Neuroscience. 2004;5:146-56.

[3] Hellal F, Hurtado A, Ruschel J, Flynn KC, Laskowski CJ, Umlauf M, et al. Microtubule stabilization reduces scarring and causes axon regeneration after spinal cord injury. Science. 2011;331:928-31.

[4] Ruel-Gariepy E, Shive M, Bichara A, Berrada M, Le Garrec D, Chenite A, et al. A thermosensitive chitosan-based hydrogel for the local delivery of paclitaxel. Eur J Pharm Biopharm. 2004;57:53-63.

[5] Danhier F, Lecouturier N, Vroman B, Jerome C, Marchand-Brynaert J, Feron O, et al. Paclitaxel-loaded PEGylated PLGA-based nanoparticles: in vitro and in vivo evaluation. Journal of controlled release : official journal of the Controlled Release Society. 2009;133:11-7.

[6] Erturk A, Hellal F, Enes J, Bradke F. Disorganized microtubules underlie the formation of retraction bulbs and the failure of axonal regeneration. The Journal of neuroscience : the official journal of the Society for Neuroscience. 2007;27:9169-80.

[7] Xue J, Niu Y, Gong M, Shi R, Chen D, Zhang L, et al. Electrospun microfiber membranes embedded with drug-loaded clay nanotubes for sustained antimicrobial protection. ACS Nano. 2015;9:1600-12.

[8] Ruschel J, Hellal F, Flynn KC, Dupraz S, Elliott DA, Tedeschi A, et al. Axonal regeneration. Systemic administration of epothilone B promotes axon regeneration after spinal cord injury. Science. 2015;348:347-52.

[9] Sekhon LH, Fehlings MG. Epidemiology, demographics, and pathophysiology of acute spinal cord injury. Spine (Phila Pa 1976). 2001;26:S2-12.

[10] Hurtado A, Cregg JM, Wang HB, Wendell DF, Oudega M, Gilbert RJ, et al. Robust CNS regeneration after complete spinal cord transection using aligned poly-L-lactic acid microfibers. Biomaterials. 2011;32:6068-79.

[11] Taylor MS, Daniels AU, Andriano KP, Heller J. Six bioabsorbable polymers: in vitro acute toxicity of accumulated degradation products. J Appl Biomater. 1994;5:151-7.

[12] Oh JK. Polylactide (PLA)-based amphiphilic block copolymers: synthesis, self-assembly, and biomedical applications. Soft Matter. 2011;7:5096-108.

[13] Wobma H, Vunjak-Novakovic G. Tissue Engineering and Regenerative Medicine 2015: A Year in Review. Tissue Eng Part B Rev. 2016;22:101-13.

[14] Bradbury EJ, Moon LD, Popat RJ, King VR, Bennett GS, Patel PN, et al. Chondroitinase ABC promotes functional recovery after spinal cord injury. Nature. 2002;416:636-40.

[15] Roman JA, Niedzielko TL, Haddon RC, Parpura V, Floyd CL. Single-walled carbon nanotubes chemically functionalized with polyethylene glycol promote tissue repair in a rat model of spinal cord injury. Journal of neurotrauma. 2011;28:2349-62.

[16] Wilems TS, Sakiyama-Elbert SE. Sustained dual drug delivery of anti-inhibitory molecules for treatment of spinal cord injury. Journal of controlled release : official journal of the Controlled Release Society. 2015;213:103-11.

[17] Holmes TC, de Lacalle S, Su X, Liu G, Rich A, Zhang S. Extensive neurite outgrowth and active synapse formation on self-assembling peptide scaffolds. Proc Natl Acad Sci U S A. 2000;97:6728-33.

[18] Park KK, Liu K, Hu Y, Smith PD, Wang C, Cai B, et al. Promoting axon regeneration in the adult CNS by modulation of the PTEN/mTOR pathway. Science. 2008;322:963-6.

CURRICULUM VITAE

José Andrés Román **30 September 2016**

Office Address: Translational Tissue Engineering Center
Whitaker Biomedical Engineering Institute
Johns Hopkins School of Medicine
5001 Smith Building, Desk I
400 North Broadway
Baltimore, Maryland 21287
Office: (410) 502-1297
FAX: (443) 287-6951
Email: jroman9@jhmi.edu

Educational History

Ph.D. expected	2016	Biomedical Engineering	Johns Hopkins School of Medicine Mentor: Hai-Quan Mao, PhD
B.S.	2011	Biomedical Engineering	University of Alabama at Birmingham University Honors in Science and Technology Biomedical Engineering Honors *Cum Laude*

Professional Experience

Research Rotation	Aug – Oct 2011	Lab of Andres Hurtado, MD, International Center for Spinal Cord Injury, Kennedy Krieger Institute
Summer Research	May – July 2010	Lab of Robert Anderson, PhD, Centre for Automotive Safety Research, University of Adelaide
Honors Research	2008 – 2011	Lab of Candace Floyd, PhD, Dept. of Physical Medicine and Rehabilitation, University of Alabama at Birmingham
Research Rotation	Jan – Mar 2008	Lab of Kevin Roth, MD, PhD, Dept. of Neuropathology, University of Alabama at Birmingham
Summer Research	June – July 2005	Lab of Howard Gibson, Dept. of Tribology, National Aeronautics and Space Administration

Scholarship and Funding Support

2015 Scientist Mentoring & Diversity Program Fellow (Conference Award)

2013 National Science Foundation Graduate Research Fellowship Recipient (Stipend support)

2011 NIH Neuroengineering Training Initiative Fellowship (Stipend support)

2010 HENAAC/Cardinal Health Scholar (Conference Award)

2010 Foundation for Asia Pacific Education Scholarship (Travel Award)

2009 Ronald E. McNair Post-Baccalaureate Achievement Scholar (Research Award)

2007 Wells Fargo Foundation Scholars Award (Tuition Support)

2007 Francis J. Dupuis Engineering Scholarship (Tuition Support)

2007 University Scholars Award (Tuition Support)

Honors Distinctions

2011 Graduation with University Honors
University of Alabama at Birmingham

2011 Graduation with Honors in Biomedical Engineering
University of Alabama at Birmingham

2011 Department of Biomedical Engineering Outstanding Undergraduate Thesis Award
University of Alabama at Birmingham

2010 Department of Biomedical Engineering Outstanding Undergraduate Student of the Year University of Alabama at Birmingham

Peer-Reviewed Publications

Roman JA, Haddon R, Parpura V, Floyd, CL (2009). "Single-Walled Carbon Nanotubes as a Regenerative Substrate in Spinal Cord Injury." *Inquiro.* **3:** 70-76.

Roman JA, Niedzielko T, Haddon R, Parpura V, Floyd, CL (2011). "Single-Walled Carbon Nanotubes Chemically-Functionalized with Polyethylene Glycol Promote Tissue Repair in a Rat Model of Spinal Cord Injury." *J Neurotrauma.* **28 (11):** 2349-62.

Roman JA, Reucroft I, Martin R, Hurtado A, Mao HQ (2016). "Local Release of Paclitaxel from Aligned, Electrospun Microfibers Promotes Axonal Extension." *Advanced Healthcare Materials.*

Wang X, Maruotti J, Majumdar S, Zack DJ, **Roman JA**, Mao HQ, Elisseeff J (2016). "Low-Fibril Density Collagen Vitrigels Enhance Human Embryonic Stem Cell-Derived Retinal Pigment Epithelial Cell Maturation." *Under Review.*

Roman JA, Haggerty A, Oudega M, Mao HQ (2016). "Local Release of Paclitaxel from Aligned, Electrospun Microfibers Promotes Spinal Cord Tissue Repair." *In Preparation.*

Tsou B, **Roman JA**, Reucroft I, Mao HQ (2016). "Local Release of Sunitinib from Aligned, Electrospun Microfibers Promotes Axonal Extension." *In Preparation.*

Chapter Publications

Li X, **Roman JA**, Mao HQ (2016). "Chapter 30: Biomimetic Nanofibers as an Artificial Stem Cell Niche." *Stem Cell Niche*: *Biology & Engineering.*

Poster Presentations

- **Roman JA**, Niedzielko T, Haddon R, Parpura V, Floyd, CL (2008) Single Walled Carbon Nanotubes Promote Axonal Regrowth After Spinal Cord Injury. Bevill Conference on Glial Biology in Medicine, Birmingham, AL, December 2008.

- **Roman JA**, Niedzielko T, Haddon R, Parpura V, Floyd, CL (2009) Immediate Administration of Single Walled Carbon Nanotubes Promotes Axonal Growth After Spinal Cord Injury. American Society for Neurochemistry Meeting, Charleston, SC, March 2009.

- **Roman JA**, Niedzielko T, Haddon R, Parpura V, Floyd, CL (2009) Immediate Administration of Single Walled Carbon Nanotubes Does Not Exacerbate Reactive Gliosis After Spinal Cord Injury. UAB Undergraduate Research Expo, Birmingham, AL, April 2009.

- **Roman JA**, Niedzielko T, Haddon R, Parpura V, Floyd, CL (2009) The Delayed Administration of Single Walled Carbon Nanotubes Promotes Functional Recovery after Spinal Cord Injury. UAB Summer Undergraduate Research Expo, Birmingham, AL, July 2009.
    - Won First Place in the Engineering/Technology Division

- **Roman JA**, Niedzielko T, Haddon R, Parpura V, Floyd, CL (2009) Axonal Growth is Facilitated by an Administration of Single Walled Carbon Nanotubes after Spinal Cord Injury. National/International Neurotrauma Society Conference, Santa Barbara, CA, September 2009.

- **Roman JA**, Niedzielko T, Haddon R, Parpura V, Floyd, CL (2010) The Effects of Single Walled Carbon Nanotubes as a Regenerative Substrate in Spinal Cord Injury. University of Alabama System Honors Research Conference, Huntsville, AL, April 2010.
    - Won First Place in the Business and Engineering Division

- **Roman JA**, Niedzielko T, Haddon R, Parpura V, Floyd, CL (2010) The Effects of Single Walled Carbon Nanotubes as a Regenerative Substrate in Spinal Cord Injury. UAB Undergraduate Research Expo, Birmingham, AL, April 2010.

- **Roman JA**, Anderson R (2010). The Characterization of an Ovine Model of Shaken Baby Syndrome. UAB Summer Undergraduate Research Expo, Birmingham, AL July 2010.
    - Won Second Place in the Engineering/Technology Division

- **Roman JA**, Niedzielko T, Haddon R, Parpura V, Floyd, CL (2010) The Delayed Administration of Chemically Functionalized Single Walled Carbon Nanotubes Promotes Tissue Repair After Spinal Cord Injury in a Rat Model. HENAAC/Great Minds in Stem Conference, Orlando, FL, October 2010.
    - Won First Place in the Science/Math Undergraduate Division

- **Roman JA**, Niedzielko T, Haddon R, Parpura V, Floyd, CL (2011) The Delayed Administration of Chemically Functionalized Single Walled Carbon Nanotubes After Spinal Cord Injury Improves Functional Recovery. American Association for the Advancement of Science (AAAS) Annual Meeting, Washington, D.C., February 2011.

- **Roman JA**, Niedzielko T, Haddon R, Parpura V, Floyd, CL (2011) The Delayed Administration of Chemically Functionalized Single Walled Carbon Nanotubes After Spinal Cord Injury Improves Functional Recovery. Council for Undergraduate Research's Poster on the Hill Seminar, Washington, D.C., February 2011.

- Chuang JC, Hadley N, **Roman JA**, Threet A, Floyd, CL (2011) A Device to Simulate Primary Blast Injury in an Animal Model. UAB Undergraduate Research Expo, Birmingham, AL, April 2011.
    - Won Second Place in the Engineering Division

- **Roman JA**, Hurtado A, Mao HQ (2013) An Aligned Electrospun Fiber Matrix with Local Release of Paclitaxel for Spinal Cord Injury Repair. Biomedical Engineering Society Meeting, Seattle, WA, September 2013.

- **Roman JA**, Hurtado A, Mao HQ (2014) Local Delivery of Paclitaxel from Aligned Electrospun Microfibers Promotes Neurite Extension *In Vitro*. Biomedical Engineering Society Meeting, San Antonio, TX, October 2014.

- **Roman JA**, Mao HQ (2015) Aligned Taxol-Eluting Microfibers Promote Axonal Extension Over an Inhibitory Substrate From a Spinal Cord Injury. Biomedical Engineering Society Meeting, Tampa, FL, October 2015.

- **Roman JA**, Mao HQ (2015) Aligned Taxol-Eluting Microfibers Inhibit Astrocyte Migration. Society of Hispanic Professional Engineers, Baltimore, MD, November 2015.

Oral Presentations

- **Roman JA**, Hurtado A, Mao HQ (2014) Local Release of Paclitaxel from Aligned, Electrospun Poly(lactic-acid) Microfibers Promotes Directed Axonal Extension. Society for Neuroscience, Washington, D.C., November 2014.

- **Roman JA**, Hurtado A, Mao HQ Sustained Local Delivery Of Paclitaxel From Aligned, Electrospun Poly(lactic-acid) Microfibers Promotes Axonal Extension *In Vitro*. Tissue Engineering and Regenerative Medicine International Society – Americas, Washington, D.C., December 2014.

Service and Leadership Experience

2014 – 2015	Teaching Assistant for two undergraduate core courses
2012 – 2013	Vice President of the Johns Hopkins University Biomedical Scholars Association
2009 – 2011	President of the University of Alabama at Birmingham Chapter of the Biomedical Engineering Society
2010	Teaching Assistant for an Honors innovation project course
2004	Eagle Scout Award